

## Extractive distillation with ionic liquids as solvents : selection and conceptual process design

**Citation for published version (APA):**

Gutierrez Hernandez, J. P. (2013). *Extractive distillation with ionic liquids as solvents : selection and conceptual process design*. [Phd Thesis 1 (Research TU/e / Graduation TU/e), Chemical Engineering and Chemistry]. Technische Universiteit Eindhoven. <https://doi.org/10.6100/IR751728>

**DOI:**

[10.6100/IR751728](https://doi.org/10.6100/IR751728)

**Document status and date:**

Published: 01/01/2013

**Document Version:**

Publisher's PDF, also known as Version of Record (includes final page, issue and volume numbers)

**Please check the document version of this publication:**

- A submitted manuscript is the version of the article upon submission and before peer-review. There can be important differences between the submitted version and the official published version of record. People interested in the research are advised to contact the author for the final version of the publication, or visit the DOI to the publisher's website.
- The final author version and the galley proof are versions of the publication after peer review.
- The final published version features the final layout of the paper including the volume, issue and page numbers.

[Link to publication](#)

**General rights**

Copyright and moral rights for the publications made accessible in the public portal are retained by the authors and/or other copyright owners and it is a condition of accessing publications that users recognise and abide by the legal requirements associated with these rights.

- Users may download and print one copy of any publication from the public portal for the purpose of private study or research.
- You may not further distribute the material or use it for any profit-making activity or commercial gain
- You may freely distribute the URL identifying the publication in the public portal.

If the publication is distributed under the terms of Article 25fa of the Dutch Copyright Act, indicated by the "Taverne" license above, please follow below link for the End User Agreement:

[www.tue.nl/taverne](http://www.tue.nl/taverne)

**Take down policy**

If you believe that this document breaches copyright please contact us at:

[openaccess@tue.nl](mailto:openaccess@tue.nl)

providing details and we will investigate your claim.

**Extractive distillation with ionic liquids as  
solvents: selection and conceptual process  
design**

**Juan P. Gutiérrez H.**

### Doctoral committee

Chairman	Prof.dr.ir. Hans Kuipers	Eindhoven University of Technology
Promoter	Prof.dr.ir. André B. de Haan	Eindhoven University of Technology
Co-promoter	Dr.ir. G. Wytze Meindersma	Eindhoven University of Technology
Examiners	Prof.dr. Geert-Jan Witkamp	Delft University of Technology
	Prof.dr. Henk van den Berg	University of Twente
	Prof.dr. Dieter Vogt	Eindhoven University of Technology
	Prof.dr. Kai Leonhard	RWTH Aachen University
	Dr. ir. Anton A. Kiss	AkzoNobel B.V. RD&I.

This project was financially supported by AgentschapNL, formerly SenterNovem, project number EOSLT06016 (Energie Onderzoek Subsidie, Lange Termijn).

A catalogue record is available from the Eindhoven University of Technology Library.  
Extractive distillation with ionic liquids as solvents: selection and conceptual process design  
Gutiérrez H., J.P.  
ISBN: 978-90-386-3356-5

Cover designed by Juan P. Gutiérrez H.

Printed by Gildeprint, Enschede, The Netherlands.

Copyright © Gutierrez, J.P. The Netherlands, 2013.  
All rights reserved.

# **Extractive distillation with ionic liquids as solvents: selection and conceptual process design**

PROEFSCHRIFT

ter verkrijging van de graad van doctor aan de Technische Universiteit Eindhoven, op gezag van de rector magnificus, prof.dr.ir. C.J. van Duijn, voor een commissie aangewezen door het College voor Promoties in het openbaar te verdedigen op dinsdag 2 april 2013 om 16.00 uur

door

Juan Pablo Gutiérrez Hernández

geboren te Manizales, Colombia

Dit proefschrift is goedgekeurd door de promotor:

prof.dr.ir. A.B. de Haan

Copromotor:

dr.ir. G.W. Meindersma

## Summary

Extractive distillation technology is widely used in the chemical and petrochemical industries for separating azeotropic, close-boiling and low relative volatility mixtures. It uses an additional solvent in order to interact with the components of different chemical structure within the mixture. The activity coefficients are modified in such a way that the relative volatility is increased. Therefore, the choice of the solvent determines the effectiveness of this process. Several solvent selection methodologies had been developed in the literature. They are based on one-way interaction parameters, meaning interactions of the components to be separated with the solvent. It has been widely accepted to consider as a promising solvent the one which is able to increase the relative volatility the most. However, the total annual cost (TAC) and the energy demand influence the final selection.

Ionic liquids (ILs) are promising replacements of existing volatile solvents in extractive distillation. However, at this moment insufficient knowledge exists on the optimal properties for ionic liquids to be employed and their implementation in actual process systems.

The main goal of this research was to analyze the selection and performance of ionic liquids in extractive distillation processes for three separation cases which differ from each other in polarity and chemical structures: 1-hexene/*n*-hexane, methylcyclohexane/toluene and water/ethanol. Theoretical ionic liquid design and selection for each mixture is done using *COSMOtherm* software (version C2.1, release 01.11a) by predicting activity coefficients at infinite dilution. Experimental selectivities and relative volatilities of real solutions were measured in order to choose the most suitable ionic liquids. At last, different extractive distillation processes using ionic liquids were proposed and analyzed.

### 1-Hexene/*n*-hexane separation

Olefins are important base chemicals used for the manufacture of poly(olefins), plasticizers, etc. and according to Sasol, the projected demand for 2012 of C<sub>6</sub>-C<sub>8</sub> olefins is around 0.85x10<sup>6</sup> ton. Due to the small differences in boiling temperatures and to the low relative volatility of the system, the separation of olefins and paraffins is energy intensive, meaning that all the commercially available processes for the production of olefins use several fractional distillation columns. In this work, 1-hexene and *n*-hexane were chosen as representative olefin and paraffin components. Extractive distillation using N-methyl-2-pyrrolidone (NMP) has been used to separate this mixture.

*COSMOtherm* activity coefficients at infinite dilution were used to select suitable ionic liquids for this case study. Non-cyclic, cyclic and aromatic-like cations were tested in this software in combination with 27 different anions. According to the

activity coefficients predicted with *COSMOtherm*, the solubility and selectivity of ionic liquids in 1-hexene and *n*-hexane is very low. This was confirmed experimentally for the selected ionic liquids using vapor – liquid equilibrium data.

None of the ILs studied in this work is able to significantly increase the relative volatility in comparison with the conventional solvent NMP. Only the ionic liquid 1-hexyl-3-methyl-imidazolium tetracyanoborate [HMIM][TCB] reached a slightly higher relative volatility (1.63) than the conventional solvent NMP (1.55). However, the increase is not large enough to consider this solvent as a suitable replacement. Besides this, the ionic liquids have solubility constraints which force the use of large solvent to feed ratios to avoid the formation of two liquid phases.

### Methylcyclohexane/toluene separation

Aromatics are among the most important chemical raw materials for the manufacture of plastics, synthetic rubber and synthetic fiber. The total production in 2009 in Western Europe of benzene, toluene and *p*-xylene was about  $7.2 \times 10^6$ ,  $1.6 \times 10^6$  and  $1.7 \times 10^6$  tons, respectively. Because of the low relative volatility, external agents are used to increase the economic feasibility of the distillation units, e.g. N-methyl-2-pyrrolidone, sulfolane.

The activity coefficients at infinite dilution for the mixture methylcyclohexane (MCH) and toluene with ionic liquids predicted with *COSMOtherm* showed a clear compromise between selectivity (easiness of separation) and solubility. Aromatic-like cations in combination with bis((trifluoromethyl)sulfonyl)imide (BTI) and tetracyanoborate (TCB) anions were selected and experimentally investigated. The relative volatility of the mixture MCH + toluene increased when any of the selected solvents (including the conventional solvent NMP) was added. The results showed that the TCB anion performed better than BTI. Therefore, the ILs 1-hexyl-3-methyl imidazolium tetracyanoborate [HMIM][TCB] and 1-butyl-3-methyl imidazolium tetracyanoborate [BMIM][TCB] seem to be the most promising replacements of NMP in the extractive distillation of methylcyclohexane and toluene.

Binary and ternary liquid-liquid experimental data for the systems methylcyclohexane + toluene + [HMIM][TCB] and [BMIM][TCB] were collected and correlated with the NRTL and UNIQUAC thermodynamic models. The binary correlations were less satisfactory than ternary correlations. The results showed that UNIQUAC represented the experimental data better than the NRTL model, with a root mean square error below 0.02. The parameters obtained from the regressions of liquid-liquid equilibrium data were used to predict the vapor-liquid equilibrium (VLE). These were compared with experimental data taken by a headspace technique which showed that UNIQUAC and its parameters are able to predict the VLE of the ternary systems with a maximum error of 0.2. The non-

aromatic/aromatic selectivities and relative volatilities of the ionic liquids make them suitable solvents to be used in extractive distillation processes.

After obtaining the parameters for the thermodynamic model, process simulations for the extractive distillation technology using the IL [HMIM][TCB] were performed and compared with the benchmark solvent NMP. The process variables (reflux, solvent flow and number of stages) are obtained such that the energy requirements of the process are minimized. Just in the extractive distillation column, the process using the ionic liquid requires 43% less energy than the conventional solvent. Several recovery technologies were analyzed (e.g. flash evaporation, stripping with hot nitrogen, supercritical CO<sub>2</sub>, and stripping with hot MCH). The most energy efficient process (using [HMIM][TCB]) saves up to 50% of the energy requirements compared to the conventional solvent. This optimized process requires an extractive distillation column of 22 equilibrium stages, using a molar reflux ratio of 0.2 and a solvent to feed mass ratio of 2.03. The recovery of [HMIM][TCB] is done in a stripping column using part of the distillate product of the extractive distillation column as the stripping agent.

### Ethanol/water separation

Ethanol is an important base chemical which is produced from petrochemical streams or bioprocesses. It has been used as solvent, in cosmetic and food industry, among others. However, ethanol as a (partial) replacement of gasoline has influenced its worldwide demand. Just in USA,  $42 \times 10^6 \text{ m}^3$  ( $33 \times 10^6$  tons) of ethanol were added to gasoline in 2009 accounting for about 8% of gasoline consumption by volume. Water is involved in the ethanol production chain. This mixture forms an azeotrope with an ethanol mass composition of 0.956 and its challenging energy-efficient separation has been widely reported. Extractive distillation using ethylene glycol (EG) is commonly used to separate this mixture.

Selectivities and activity coefficients at infinite dilution were predicted using *COSMOtherm*. In this case, the activity coefficients showed high attractive forces among the most promising ionic liquids and water, meaning that these ionic liquids are highly hydrophilic. The experimental relative volatility can be increased up to 23% when the conventional solvent is replaced by 1-ethyl-3-methyl-imidazolium acetate [EMIM][OAc] or 1-ethyl-3-methyl-imidazolium dicyanamide [EMIM][DCA]. These ionic liquids seem to be promising solvents for the extractive distillation of water and ethanol.

Ternary VLE data were collected for the systems ethanol + water + [EMIM][OAc] and [EMIM][DCA]. In this case, the NRTL model correlates the data better than UNIQUAC, with a value for the root mean square error below 0.02. The ionic liquids are able to increase the relative volatility of the mixture ethanol – water by strongly attracting the water and making it “less volatile” which makes the



recovery of the solvent rather challenging and energy intensive. Only after heat integration, the use of ILs appeared to be more attractive, yielding 16% of energy savings compared to the heat integrated conventional process. The recovery conditions and the relatively low energy savings might limit the applicability of ILs for the separation of ethanol – water by extractive distillation.

### Overall

Finally, it can be concluded that, although ionic liquids can be suitable extractive distillation solvents, special attention should be paid to the solvent recovery technology and its heat integration with the extractive distillation column. In this study the most successful case was the separation of toluene/methylcyclohexane, where tetracyanoborate-based IL [HMIM][TCB] yielded 50% energy savings compared to the conventional solvent.

## Contents

<b>1. Introduction</b> .....	<b>1</b>
1.1 Advanced distillation technologies .....	1
1.2 Solvents for extractive distillation.....	4
1.2.1 Solvent selection criteria .....	4
1.2.2 Solvent selection methodology .....	5
1.2.3 Current solvent classification.....	7
1.3 Ionic liquids in extractive distillation.....	8
1.4 Scope of the research.....	11
1.5 Thesis outline .....	13
1.6 References.....	13
<b>2. COSMO-RS based IL selection for extractive distillation processes</b> .....	<b>17</b>
2.1 Introduction .....	17
2.2 Thermodynamic analysis in extractive distillation .....	18
2.3 COSMO-RS theory .....	20
2.3.1 Why COSMO-RS and <i>COSMOtherm</i> ? .....	21
2.4 Methodology.....	23
2.5 IL design and preselection.....	23
2.5.1 Separation of methylcyclohexane/toluene .....	23
2.5.2 Separation of 1-hexene/ <i>n</i> -hexane .....	28
2.5.3 Separation of ethanol/water .....	29
2.6 Experimental section.....	32
2.6.1 Chemicals.....	32
2.6.2 Experimental methods and procedure .....	33
2.6.3 Experimental results and discussion.....	35
2.7 Conclusions .....	39
2.8 References.....	40
Appendix 2.1: Abbreviations .....	45
<b>3. Thermodynamic properties and model for the mixture methylcyclohexane (1), toluene (2) and [HMIM][TCB] (3)/[BMIM][TCB] (3)</b> .....	<b>47</b>
3.1 Introduction .....	47

3.2	Theory .....	48
3.3	Experimental section.....	49
3.3.1	Materials.....	49
3.3.2	Experimental methods and procedure .....	50
3.4	Results and discussion.....	50
3.4.1	Binary and ternary liquid-liquid experiments .....	50
3.4.2	Vapor-liquid equilibrium experiments.....	53
3.4.3	Comparison of experimental and correlated data.....	54
3.5	Conclusions .....	57
3.6	References.....	58
	Appendix 3.1: Experimental data for the ternary LLE.....	61
<b>4.</b>	<b>Vapor-liquid equilibrium for the system ethanol (1) + water (2) + ionic liquids (3)...</b>	<b>63</b>
4.1	Introduction .....	63
4.2	Theory .....	64
4.3	Experimental section.....	66
4.3.1	Materials.....	66
4.3.2	Experimental method and procedure.....	66
4.4	Results and discussion.....	66
4.4.1	Vapor-liquid equilibrium experiments.....	66
4.4.2	Comparison of experimental, regressed and predicted data .....	68
4.5	Conclusions .....	71
4.6	References.....	71
<b>5.</b>	<b>Extractive distillation process design for the separation of toluene + methylcyclohexane using ionic liquids .....</b>	<b>75</b>
5.1	Introduction .....	75
5.2	Thermodynamic and simulation data .....	76
5.3	Conventional extractive distillation process using NMP .....	76
5.4	Extractive distillation column using ionic liquids .....	78
5.5	Ionic liquid recovery techniques .....	79
5.5.1	Recovery using flash evaporation .....	79
5.5.2	Recovery using stripping with hot nitrogen.....	81

5.5.3	Recovery using flash and stripping with hot nitrogen .....	82
5.5.4	Recovery using stripping with hot methylcyclohexane .....	84
5.5.5	Recovery using supercritical CO <sub>2</sub> extraction .....	85
5.5.6	Summary .....	87
5.6	Energy analysis .....	88
5.7	Conclusions .....	90
5.8	References.....	91
	Appendix 5.1: Thermodynamic and physical properties .....	93
	Appendix 5.2: Extractive distillation column (EDC) profiles for the separation of MCH and toluene.....	97
	Appendix 5.3: Heat exchanger networks (HEN's).....	99
<b>6.</b>	<b>Extractive distillation process design for the separation of ethanol + water using ionic liquids .....</b>	<b>105</b>
6.1	Introduction .....	105
6.2	Thermodynamic and simulation data .....	106
6.3	Conventional extractive distillation process using EG .....	107
6.4	Extractive distillation column using ionic liquids .....	109
6.5	Ionic liquid recovery techniques .....	111
6.5.1	Recovery using flash evaporation .....	111
6.5.2	Recovery using stripping with hot nitrogen.....	113
6.5.3	Recovery using flash and stripping with hot nitrogen .....	114
6.5.4	Recovery using stripping with hot ethanol vapor .....	115
6.5.5	Recovery using supercritical CO <sub>2</sub> extraction .....	117
6.5.6	Summary.....	117
6.6	Energy analysis .....	119
6.7	Conclusions .....	120
6.8	References.....	121
	Appendix 6.1: Thermodynamic and physical properties .....	123
	Appendix 6.2 Extractive distillation column (EDC) profiles for the separation of ethanol and water .....	127
	Appendix 6.3: Process flow diagrams .....	129
	Appendix 6.4: Heat exchanger networks (HEN's).....	131

<b>7. Conclusions and recommendations for future work .....</b>	<b>137</b>
7.1 Ionic liquid selection .....	137
7.2 Extractive distillation process .....	137
7.3 Recommendations for future work.....	138
7.4 References.....	139
<b>List of publications .....</b>	<b>141</b>
<b>Acknowledgments.....</b>	<b>145</b>
<b>Curriculum Vitae .....</b>	<b>147</b>

# 1. Introduction

## 1.1 Advanced distillation technologies

In the history of chemical separations, conventional distillation has been applied to more commercial processes than all other techniques combined [1]. This well-known operation takes advantage of the difference in boiling points of chemical compounds, and it is suitable for separating a variety of mixtures. However, not all liquid mixtures are possible to separate with ordinary fractional distillation. For instance, low relative volatility mixtures (including azeotropic mixtures) are difficult or economically unfeasible to separate by ordinary distillation.

One of the most useful ways to obtain chemicals which cannot be separated by conventional distillation is to employ selective solvents. They take advantage of the non-ideality of a mixture of components having different chemical structures. Three separation processes can be used as examples of the use of solvents: Liquid-liquid extraction, azeotropic distillation and extractive distillation.

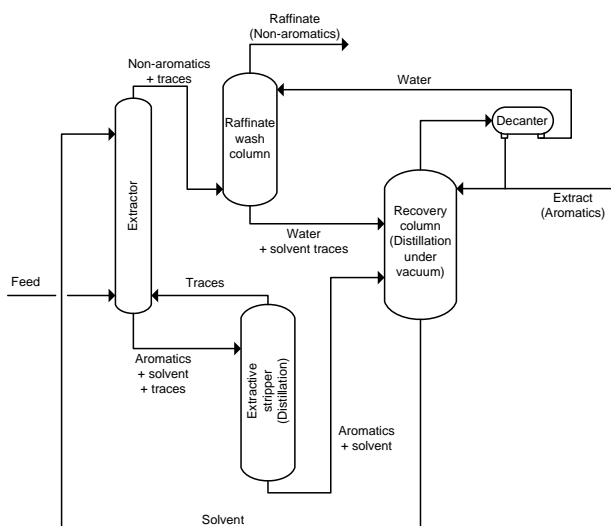


Figure 1.1: Liquid-liquid extraction process (adapted from [2])

*Liquid-liquid extraction:* Used to separate the components of a liquid mixture (feed) by contacting it with a second liquid phase (solvent). The process takes advantage of differences in the chemical properties of the feed components, such as differences in polarity and hydrophilic/hydrophobic character. A liquid-liquid extraction process produces a solvent-rich stream called the extract and an extracted-feed stream called the raffinate. A commercial process almost always includes two or more extra units in addition to the extraction column itself [3]. These unit operations are needed to purify the extract and raffinate streams and isolate the desired products. For instance, the liquid-liquid extraction process using sulfolane as the solvent for the separation of aromatics from non-aromatics mixtures requires four major process units (Figure 1.1).

**Azeotropic distillation:** This process involves the formation of an azeotrope, or the use of an existing azeotrope, to effect the desired separation. The azeotrope can be formed by the addition of a third component (entrainer) to the system. There are two kinds of azeotropic distillation (AD) processes: homogeneous (single liquid phase) and heterogeneous (two liquid phases) AD. Figure 1.2 illustrates a common example, the ethanol dehydration using benzene as a heterogeneous azeotropic entrainer [4].

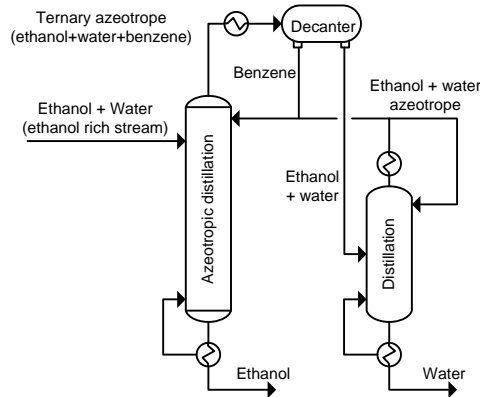


Figure 1.2: Azeotropic distillation process

**Extractive distillation:** This technology is widely used in the chemical and petrochemical industries for separating azeotropic, close-boiling and low relative volatility mixtures [1]. In extractive distillation, like azeotropic distillation, an additional solvent is used in order to interact with the components of different chemical structure within the mixture. The activity coefficients are modified in such a way that the relative volatility (equation 1.1) is increased.

$$\alpha_{ij} = \frac{y_i/x_i}{y_j/x_j} = \frac{\gamma_i P_{i,0}}{\gamma_j P_{j,0}} \tag{1.1}$$

Table 1.1 summarizes the basic advantages and disadvantages of liquid-liquid extraction, azeotropic distillation and extractive distillation.

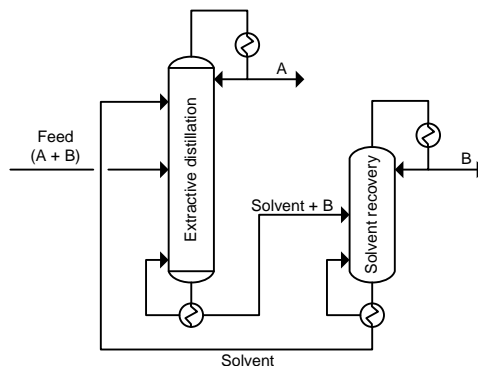
The main advantage of the extractive distillation process is that it can make use of two key variables: the solubility or affinity of the solvent and the boiling point differences of the key components to be separated. In contrast, the liquid-liquid extraction is based on only one variable, the solubility.

Figure 1.3 illustrates a typical extractive distillation (ED) process. As shown in the figure, the feed enters in the middle part of the extractive distillation column (EDC), while the low volatile solvent is introduced into the column near to the condenser. The component with the higher volatility in the presence of the solvent (not necessarily the component with the lowest boiling point) is obtained overhead as a relatively pure distillate. The other component leaves the column through the bottom mixed with the solvent. The solvent is then separated in a second unit from the remaining components, typically by distillation

(or evaporation), and recycled to the EDC. From Table 1.1 it can be concluded that AD uses larger quantities of solvents than ED. This might result in an enlargement of the column diameter and/or increase the pressure drop inside the column increasing the energy requirements [5].

**Table 1.1: Comparison among solvent-based technologies (adapted from [3, 5, 6])**

Process	Advantages	Disadvantages
<b>Liquid-liquid extraction</b>	Can separate classes of chemicals having wide range of boiling points. Can separate heat-sensitive materials. Can recover non-volatile compounds.	Equipment can be sensitive to fouling. Usually requires additional purification steps for trace solvent removal. Systems must form two liquid phases with limited miscibility between the phases. Equipment design is more complex and usually more costly than the other options.
<b>Azeotropic distillation</b>	Can efficiently remove dilute concentrations of more volatile components. Can be more capital and energy efficient for some systems.	Systems must form an azeotrope. Requires a separate technique to break the azeotrope and recover the products. Relatively large amount of entrainer. Entrainer and volatile components must be vaporized and be obtained as distillate product.
<b>Extractive distillation</b>	Complete, standalone operation. More degrees of freedom in design than the other options, allowing greater flexibility in implementation. Can process a higher capacity than liquid-liquid extraction operations in similar size equipment. Heat integration technology can be applied between both columns. Easy operability and controllability. Products are obtained free of solvent. Amount of solvent is usually lower than azeotropic entrainer in AD. Not all the solvent needs to be vaporized (solvent obtained as bottom product). Lower energy requirements than in AD.	Requires substantial volatility difference among components to be separated. Becomes less efficient with extremely wide boiling range feedstocks. May not be suitable for thermally sensitive materials.



**Figure 1.3: Conventional extractive distillation process**



## 1.2 Solvents for extractive distillation

### 1.2.1 Solvent selection criteria

The effectiveness of an extractive distillation process relies on the choice of extractive agent. This is the primary design consideration for processes based on a mass separating agent [7]. In the procedure of selecting the solvent both explicit and implicit properties must be considered. Explicit properties can be calculated or computed according to the thermodynamic behavior while implicit properties that cannot be computed are characteristics of the solvent itself e.g. toxicity, cost, stability, etc. However, the problem of estimating the effectiveness of solvents for specific separations becomes, in the initial part of the selection process, a matter of estimating activity coefficients (relative volatility) of the solutes in the presence of the solvents i.e. an explicit property. Since the ratio of saturation pressures is constant for isothermal systems, the only way that the relative volatility can be affected is by changing the ratio of the activity coefficients. This ratio, in the presence of the solvent, is called selectivity,  $S_{ij}$ .

$$S_{ij} = \left( \gamma_i / \gamma_j \right)_s \quad 1.2$$

The solvent with the highest selectivity is always considered to be the most promising for the separation of the mixture. This has been a widely accepted criterion for solvent selection [8, 9], indicating that the use of the solvent with the highest selectivity will yield the lowest total annual cost (TAC) of the extractive distillation process [5]. Nevertheless, the total energy demand of the process and the cost of the solvent can influence its selection [10]. In extractive distillation processes, two-way interactions between the solvent and each of the components should be taken into account; this will give an insight of the ease of the recovery of the solvent. For example, consider a solvent providing the highest selectivity by decreasing the activity coefficient of the  $j$  component in equation 1.2. In this case, the separation of the solvent and the  $j$  component (in the solvent recovery unit) becomes more difficult and more energy is required to obtain the pure solvent again.

The activity coefficients and therefore the selectivity (equation 1.2) depend on the concentration in the liquid phase and the temperature. A rigorous comparison of the candidate solvents requires their selectivities to be determined at a consistent solvent concentration and key components ratio. Generally, the activity coefficient (and thereby the selectivity) of each key component is determined at infinite dilution in each of the potential solvents. In most of the cases, the selectivity increases, often almost linearly, with solvent concentration [1]. Thus, the solvent with the largest selectivity at infinite dilution usually has the largest selectivity at the lower solvent concentrations. Therefore, the selectivity between two solutes at infinite dilution in the solvent (equation 1.3) provides a good estimation of the effectiveness of the solvents [11].

$$S_{ij}^{\infty} = \left( \frac{\gamma_i^{\infty}}{\gamma_j^{\infty}} \right)_s \quad 1.3$$

In addition to the solvent selectivities, there are some other desired characteristics the solvent must have to be suitable [3]:

- The solvent must not form azeotropes with the components in the mixture to be separated. This can be guaranteed by choosing solvents with a boiling point (bp) 30-40°C higher than the heaviest component to be separated [1]. This difference also influences and facilitates the recovery of the solvent.
- The solvent must be thermally and chemically stable, at temperatures encountered in the extractive distillation process, to prevent degradation or reaction.
- It should be non-corrosive to minimize the cost of construction materials.
- It must be non-toxic and environmentally friendly.
- It is desirable that the solvent has a reasonable solubility in the feed mixture at the temperatures and concentrations in the extractive distillation process. However, this is not a requirement to develop a successful separation system.
- The solvent must be easily separable from the components associated with it (the bottoms of the extractive distillation column).

In most of the cases, criteria like thermal stability, corrosion, reactivity and solubility can be dealt with by optimizing the process and operating conditions. Hence, the most important variables to choose the solvents are the selectivity and solubility. If a solvent causes a second liquid phase to form during the distillation, much of the selectivity enhancement can be lost [1]. Since high selectivities are achieved by increasing the non-ideality of the mixture, and mixtures with large non-idealities often have limited miscibilities, often a compromise between high selectivity and low miscibility needs to be made [1].

### 1.2.2 Solvent selection methodology

While it is possible to find solvents that increase or decrease the ratio of activity coefficients, it is usually preferable to select a solvent that accentuates the natural differences in vapor pressures of the components to be separated. A heuristic, therefore, is to favor solvents with selectivities greater than 1.0 [1]. To force the natural behavior of the mixture and obtain the most volatile compound  $i$  in the top of the column, the solvent should increase the activity coefficient of  $i$  (positive deviation of the Raoult's law), decrease the activity coefficient of  $j$  (negative deviation of the Raoult's law) or the combined effect (increase  $\gamma_i$  and decrease  $\gamma_j$ ). Because systems showing positive deviations are more common, the usual approach is to select a solvent that increases the activity coefficient of  $i$ .

Table 1.2: Recommended solvents in accordance to the polarity of the mixture (adapted from [1])

Mixture to be separated	Recommended solvent
Highly polar	Polar or non-polar
Non-polar	Polar
More volatile: polar. Less volatile: non-polar	Polar or non-polar*
More volatile: non-polar. Less volatile: polar	Polar
Moderately polar	Polar or non-polar

\*The polar solvents may reverse the relative volatility

Strong deviations from ideality are often associated with hydrogen bonding between molecules and many successful extractive distillation solvents are compounds capable to form strong hydrogen bonds. Therefore, for cases where either a polar or a non-polar solvent is recommended, polar compounds are preferred because they typically cause the solution to be more non-ideal. Some tables, similar to Table 1.2, based on the hydrogen-bonding properties to predict the kind of the deviation from Raoult's law can be found in the literature [1, 10, 12]. With the help of these qualitative tables, several solvents can be identified but each solvent needs to be ranked according to the specific application.

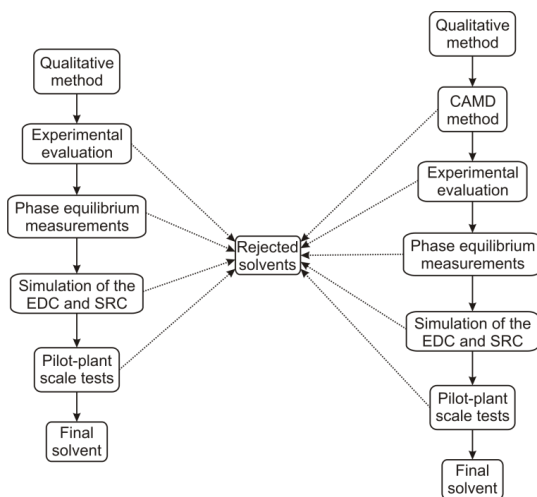


Figure 1.4: Solvent selection approach totally based in experimental evaluation (left) and using CAMD method (right)

Although many heuristic methods and rules of thumb have been developed in order to assist in the choice and ranking of solvents, these are mostly qualitative. Experimental solvent screening methods yield good results, but they are time consuming and expensive [6, 13]. A more effective, but less accurate, method to select solvents is Computer-Aided Molecular Design (CAMD). In these methods the required properties of a solvent are specified and its structure is then calculated through the use of e.g. group contribution methods [10, 14]. CAMD is essentially the inverse of property prediction by group contribution methods. It has been shown that UNIFAC (and related) can be useful as a guide for solvent selection [7, 12, 15, 16]. The problem statement of this method is: given a mixture and certain separation goals, synthesize, from the set of UNIFAC groups, feasible molecular structures with the desired solvent properties. However, this relatively simple method is limited to “typical separations” where the necessary interaction parameters of the solvents and substances are available [11, 12, 16].

The conductor like screening model for real solvents (COSMO-RS) is a promising, although relatively new, CAMD method to predict the activity coefficients and other thermophysical properties based on unimolecular quantum chemical calculations. It has the advantage of being applicable to molecules where the group contribution methods fail or some parameters are missing [17].

Figure 1.4 shows the solvent selection approach without and with the CAMD method. It should be mentioned that the methodology using CAMD method is used in this work. In the first step (qualitative method) the identification of general classes of compounds or functional groups that may make effective solvents for a given separation is done. After this step, the CAMD method can be introduced to filter the group of pre-selected solvents. With these methods, some solvents can be rejected saving some experimental work. The solvents are evaluated by simple experimental methods measuring the selectivity or relative volatility for a fixed composition of the components to be separated (e.g. 50% of each component) at several solvent to feed ratios. The solvents that show the highest selectivities are selected and can be evaluated in more accurate experimental equipment to determine the phase equilibrium between the mixture and each of the solvents. After the equilibrium data is obtained, simulations can be performed to design and predict the behavior of the extractive distillation process. The energy requirements of the extractive distillation process is an important variable that must be taken into account [10] and this can be assessed with process simulator software. With a pilot plant scale evaluation, the final solvent that can be applied in the industry is selected. Both methodologies shown in Figure 1.4 must give as a result the same final solvent. However, the CAMD method can reduce time and money investments in the solvent selection process.

### 1.2.3 Current solvent classification

One important characteristic of extractive distillation is that the solvent increases the liquid load inside the column. The vapor flow in the column is relatively low in comparison with the liquid flow. Thus, the design of the liquid channels is very important. “Perfect” solvents should decrease the solvent to feed ratio and the liquid load of the column and, therefore, make the operation easily implemented. Currently, there are four kinds of solvents that are reported to be used in or suitable for extractive distillation: liquid solvents, solid salts, combination of solid salt and liquid solvent and non-volatile components like ionic liquids and hyperbranched polymers [5, 18, 19].

*Liquid solvents:* This is the most common class of solvents used in extractive distillation processes. The main advantage of these solvents is the easy operation and handling in an EDC. Due to their characteristics, they can be recovered in a conventional distillation column and recycled again to the extractive distillation column. The solubility or capacity, equation 1.4, is a measure of the concentration (molar composition) in one of the liquid phases when the compound is highly concentrated in the other liquid phase [20]. It is desirable to have solvents with high selectivity (high degree of separation) and high solubility (avoid formation of a second liquid phase).

$$C_i^\infty = \frac{1}{\gamma_i^\infty} \quad 1.4$$

In general, solvents with high selectivity will have a reduced capacity [3]. It has been proposed to blend high selective (low capacity) with high soluble solvents to improve the separation ability and reduce the formation of a second liquid phase in the extractive distillation column [5]. The main disadvantage of the liquid solvents is the possible pollution of the top products of both the extractive distillation and the solvent recovery

column, despite of their low vapor pressure, and the requirement of large solvent to feed mass ratios (reaching values of 7-8 in industry) [5].

*Solid salt:* In certain systems it is possible to use a solid salt dissolved into the liquid phase. The so-called “salt effect in vapor-liquid equilibrium” refers to the ability of a solid salt to alter the equilibrium behavior by changing the activity coefficients in the liquid phase. The process of an extractive distillation with salt is somewhat different from the process showed in Figure 1.3 (especially the recovery column). The salt is not recovered by means of distillation, but generally it is separated by evaporation. One advantage of this process is the easy recovery of the salt [5]. The separation of ethanol and water is the most important application of this technology. In systems where the salts can be employed, generally, the solvent to feed ratios are smaller than that of the liquid solvents which results in lower energy requirements. However, in industrial operations there are problems with dissolution, reuse, corrosion and transportation of the salt. These disadvantages make the extractive distillation with solid salt not widely applied in the industry [5].

*Combination of liquid solvent and solid salt:* Some systems permit to use a combination of liquid solvent and solid salt dissolved into the liquid phase as the separating agent. The extractive distillation process using this combination is the same as the process shown in Figure 1.3. The combination of these two solvents integrates the advantages of liquid solvents (easy operation) and solid salt (high separation ability with low solvent to feed ratios) and can be suitable for separating polar or non-polar systems [5]. However, the corrosive effect of the solid salts is a disadvantage that is still present. On the other hand, due to the solubility limitation of the solid salts, the amount added to the liquid solvents is often small and the improvement of the separation is limited. Besides, liquid solvents are, in some degree, volatiles which still can pollute the distillates.

*Hyperbranched polymers:* This class of solvents are highly branched, polydisperse, three-dimensional macromolecules. Their applications are based on the non-volatility associated with these polymers and the large number of functional groups that are attached to the molecule, allowing for tailoring of their physical and thermodynamical properties. The hyperbranched polymers have been mainly studied in the separation of the polar mixtures, e.g. ethanol-water and tetrahydrofuran-water, by means of extractive distillation and solvent extraction, respectively. However, there are only a few hyperbranched polymers commercially available at present which meet the requirements of an entrainer or solvent (large scale availability, low viscosity, low melting temperatures, stability, selectivity and capacity) [18]. As a remark, hyperbranched polymers applied to extractive distillation process are out of the scope of this work and just few words will be devoted to these components mostly comparing them with ILs, taking data from the literature.

### 1.3 Ionic liquids in extractive distillation

The term Ionic Liquid (IL) is used for a class of chemical composed entirely of ions with a melting temperature below 100°C. This arbitrary limit is defined as a response to the dramatically increasing number of possible applications of the ILs below this temperature in industrial processes [21]. They are formed by an organic cation and an inorganic or

organic anion [22]. Since there are many known and potential ions, the number of ionic liquids is rather large [23]. Suitable cations and anions can be chosen to obtain ILs with the desired properties for specific applications and, like the liquid solvents, they can be mixed to improve their behavior. Therefore, it is possible to design an IL for a particular application by combining a cation with an anion to obtain the desired melting point, viscosity, density, hydrophobicity, miscibility, etc. This is the reason why the ILs are also referred like “designer solvents”. In spite of the complexity of the ILs, Joglekar et al [22] and Wasserscheid and Welton [24] have reported some general properties and the effects of some cation-anion combination.

Although ILs have been known for 100 years, it is only during the past decade that the interest and applications have increased dramatically in many fields of the chemical industry. They are being used as solvents replacing volatile organic compounds (VOC), catalyst in chemical reactions, extraction media for separation processes, lubricants, thermofluids, plasticizers, and electrically conductive liquids in electrochemistry, to name but a few [24]. For application in extractive distillation ionic liquids are promising solvents due to their unique characteristics [5, 24, 25]:

- Negligible vapor pressure which is reflected in the purity of the vapor products and in the feasibility to be recycled after recovery.
- Wide liquid range of about 300°C with a melting point around room temperature. They are chemically, thermally stable with or without water under the operation temperature of extractive distillation<sup>1</sup>. Moreover, it is believed that they can be easily recycled and mixed with the reflux stream of the EDC introducing none of the less volatile compounds at the top of the column.
- A wide range of materials, including organic, inorganic and even polymers, are soluble in ionic liquids which ensures that the ionic liquids have the enough solubility for the components to be separated, and can be selected to increase the relative volatility of the liquid mixtures avoiding the formation of several liquid phases.
- They are much less corrosive than conventional high melting point salts.

Near zero VOC emissions makes the ILs perfect chemicals to be used in industry. However, even if the ionic liquids do not evaporate and contribute to air pollution, most of them are water soluble and can enter to the environment by this means. The toxicity, corrosion behavior and physical properties for most of the ionic liquids should be known for a successful industrial application of these chemicals. Therefore, this lack of knowledge can be considered the biggest disadvantage of the ILs [26]. Nevertheless, there are some other disadvantages like the non-availability of characterization techniques, deficient understanding of the mechanism of synthesis and the high prices of these solvents. However, if the demand of the ILs increases, the production in a larger scale would also increase, and the prices would decrease.

---

<sup>1</sup> The upper limit temperature of the liquid phase is defined in many cases by decomposition of the IL's rather than vaporization.

**Table 1.3: Simulation results for the ethanol water separation by extractive distillation (adapted from [25])**

	Ethylene glycol (EG)	[EMIM][BF4]
<b>S/F (molar)</b>	0.9	0.60
<b>S/F (mass)</b>	1.47	3.13
<b>Reboiler heat duty (kW)</b>	3276	2958
<b>Overall heat duty (kW)</b>	3959	2963

In Table 1.3 some simulation results using the conventional solvent (ethylene glycol – EG) and one ionic liquid (1-ethyl-3-methyl-imidazolium tetrafluoroborate – [EMIM][BF4]) for the separation of ethanol-water by extractive distillation are shown. The main fixed column parameters are as follows: Feed flow rate = 200 kmol/h (7600 kg/h), pressure = 1 bar, theoretical stages = 28, ethanol molar composition in the feed = 0.7, feed entered the column in its boiling point, ethanol molar purity in the distillate = 0.998. Detailed information can be found in [25]. Due to the molecular weight of the IL, the solvent to feed mass ratio (S/F) is two times larger than the conventional process using EG. However, because it higher selectivity and the non volatility of the solvent (no evaporation of the solvent), the energy requirements of the column using IL can be 10% lower. Taking into account the solvent recovery unit, the energy savings can be even higher than 20% using a non-optimized IL for the specific separation of ethanol-water [25]. This indicates that ionic liquids represent promising classes of components to be used in extractive distillation processes.

The large amount of possible ILs makes the experimental evaluation for a specific separation problem unfeasible. Additionally, the mechanisms that lead to an efficient IL solvent are not yet completely understood [17]. Therefore, the design of ILs as additives can only be based on the study of different kinds of structural variations by means of a non-experimental, less time-consuming and less cost-intensive method, at least in the initial stage of the solvent selection process [27]. The common CAMD approaches based on group contribution methods like UNIFAC are limited because the interaction parameters of many ILs systems are not yet available [28, 29].

Klamt and co-workers had proposed a new perspective in fluid-phase thermodynamics and developed a quantum chemical approach (COSMO-RS) for the prediction of the thermodynamic properties of pure and mixed fluids (polar and non-polar) using only structural information of the molecules [30]. The COSMO-RS model was developed for conventional solvents. However, it can also predict thermodynamic properties for ILs with the same accuracy that is observed for organic solvents, without any change in the theory or the use of specific parameters [30].

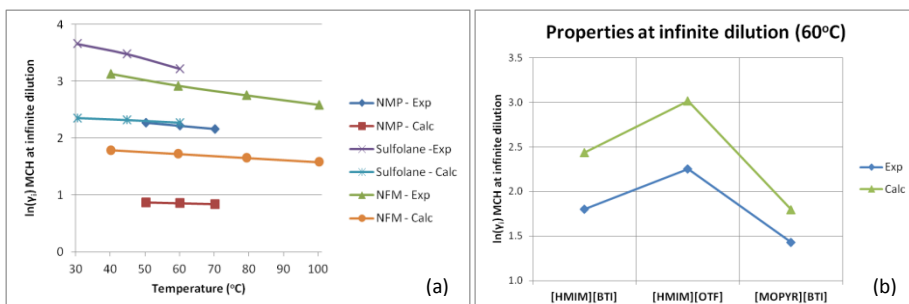


Figure 1.5: Methylcyclohexane activity coefficients predicted with *COSMOtherm* and comparison with experimental values. (a) Conventional solvents and (b) ionic liquids

The *COSMOtherm* software package (Version C2.1 Release 01.11a) has been used to predict the activity coefficients at infinite dilution and phase equilibrium data for polar and non-polar compounds in ILs. The results (some of them depicted in Figure 1.5) show that it can be used as a qualitative tool for the pre-selection of solvents for extractive processes, giving better results for the prediction of vapor-liquid equilibrium than liquid-liquid equilibrium [27, 30-34]. As can be seen in Figure 1.5(a), *COSMOtherm* under-predicts the activity coefficients at infinite dilution of methylcyclohexane in conventional solvents. However, Figure 1.5(b) illustrates that it over-predicts those thermodynamic properties in the presence of ionic liquids. Nevertheless, it can qualitatively predict the trend in the interactions among the components and the type of solvents as well as the temperature. This means that the most promising solvents and ionic liquids can be selected with a non-experimental method – *COSMOtherm* software package. This software and its results are further discussed in Chapter 2.

When an IL is used in extractive distillation processes it acts as a conventional solvent. The IL is fed in the top of the column and is obtained at the column's bottom stream in combination with the less volatile components. The IL increases the relative volatility of the mixture and a very pure stream can be obtained in the distillate. If the relative volatility with ILs is higher than with the conventional solvents, energy saving in this column can be achieved. However, because of its non-volatility, it is said that energy savings in the recovery process can be obtained. It is commonly mentioned in the literature that ILs can be easily recovered and recycled back to the extractive distillation column by evaporation, crystallization, stripping among others [25, 35, 36]. However, in the literature, a complete analysis, design and study of the performance of extractive distillation processes using ionic liquids, including their recovery, was not found.

#### 1.4 Scope of the research

Three case studies have been selected which differ from each other in polarity and chemical structure of the components.

- Water/ethanol
- Aromatics/non-aromatics
- Olefins/paraffins



Ethanol is an important base chemical which is produced from petrochemical streams or bioprocesses. It has been used as solvent, in cosmetic and food industry, among others. However, ethanol as a (partial) replacement of gasoline has influenced its worldwide demand. Just in USA,  $42 \times 10^6 \text{ m}^3$  ( $33 \times 10^6$  tons) of ethanol were added to gasoline in 2009 accounting for about 8% of gasoline consumption by volume [37, 38]. Water is involved in the ethanol production chain. This mixture forms an azeotrope with an ethanol mass composition of 0.956 and its challenging energy-efficient separation has been widely reported [39]. Aromatics are among the most important chemical raw materials; they are used in the manufacture of plastics, synthetic rubber and synthetic fiber [40]. The total production in 2009 in Western Europe of benzene, toluene and p-xylene was about  $7.2 \times 10^6$ ,  $1.6 \times 10^6$  and  $1.7 \times 10^6$  tons, respectively [41]. Because of the low relative volatility, external agents are used to increase the economic feasibility of the distillation units, e.g. N-methyl-2-pyrrolidone, sulfolane, among others [2]. The principal uses for  $\alpha$ -olefins are as polyethylene co-monomer, detergent alcohols, poly(olefins), plasticizers, among others [42, 43]. According to Sasol, the projected demand for 2012 of C6-C8 olefins is around  $0.85 \times 10^6$  tons [44]. Due to the close boiling components obtained in the olefin production and to the low relative volatility of the system (e.g. at 0.1 MPa the relative volatility of the systems 1-hexene/*n*-hexane and cyclohexane/cyclohexene are 1.18 and 1.07, respectively [45]), the separation of olefins and paraffins is energy intensive and all the commercially available processes for the production of olefins use several fractional distillation columns.

In this work, methylcyclohexane, toluene, 1-hexene and *n*-hexane were chosen as representative components of non-aromatic, aromatic, olefin and paraffin, respectively. The separation cases together with the separation technologies commonly applied are listed in Table 1.4.

**Table 1.4: Cases studied in this work**

Mixture	Polarity	Separation technologies applied
<b>Water – Ethanol</b>	Polar & Polar	Azeotropic distillation, extractive distillation, extractive fermentation, adsorption, membrane separations [39].
<b>Methylcyclohexane – Toluene</b>	Non-polar & Non-polar	Liquid-liquid extraction, azeotropic distillation, extractive distillation, adsorption, membranes and sometimes crystallization by freezing [40, 46].
<b>1-Hexene – <i>n</i>-Hexane</b>	Non-polar & Non-polar	Low temperature distillation, extractive distillation, adsorption, absorption and membranes [47].

Ionic liquids are a new class of components with high potential to replace existing solvents in extractive distillation and achieve energy/capital savings >20% [25]. However, at this moment negligible knowledge exist on the optimal properties for ionic liquids to be employed and their implementation in actual process systems.

The objective of this work is to establish this knowledge by investigating the relation between the molecular structure of ionic liquids and their performance in extractive distillation processes for various applications: aromatics/non-aromatics (toluene/methylcyclohexane), olefins/paraffins (1-hexene/*n*-hexane) and alcohol/water (ethanol/water). Part of the research will be devoted to establish suitable ionic liquid

structures and their optimal properties from a conceptual point of view. A combination of high-throughput experimental screening techniques, molecular modeling based simulation tools such as COSMO-RS and flow sheeting models in Aspen Plus will be applied to establish a solvent selection methodology for extractive distillation processes. Both liquid-liquid and vapor-liquid equilibrium experiments are performed to determine the actual performance of the ionic liquids in the presence of the mixtures. The selectivity and relative volatility of the volatile components are analyzed and the final selection of the solvents is based in experiments. Experimental data is taken to allow the regression of the parameters of a thermodynamic model (NRTL and UNIQUAC are mainly used as default thermodynamic models in this work). After the thermodynamic parameters are obtained, simulations in Aspen Plus (or another flow sheet simulator) are performed and analysis of the energy requirements with heat integration of the extractive distillation process is done. The recovery technology of the ionic liquids has not been analyzed in detail in the literature. In this work, several recovery technologies are investigated and the final extractive distillation process with ionic liquids is proposed and evaluated taking into account the energy requirements involved in the separation process.

## 1.5 Thesis outline

As was mentioned in previous paragraph, the main goal of this research is to analyze the selection and performance of ionic liquids in extractive distillation processes. In order to do this, Chapter 2 addresses the question “which properties are affecting the extractive distillation processes?” Theoretical ionic liquid design and selection for each mixture is done and experimental data is taken to confirm the predicted properties of the ionic liquids. These properties are compared with the conventional solvents and their feasible application to extractive distillation processes is analyzed. In Chapter 3, the thermodynamic properties for the mixture methylcyclohexane + toluene + ionic liquids are presented, the thermodynamic model is selected and its parameters are regressed. In Chapter 4, the thermodynamic properties, selection of the thermodynamic model and its parameters are presented for the mixture ethanol + water + ionic liquids. In Chapter 5, the process design of an extractive distillation process using an ionic liquid for the separation of methylcyclohexane and toluene mixture has been executed. The extractive distillation column and the recovery technology design are shown and the heat integration analysis for the extractive distillation process is done. In Chapter 6, the process design, including the recovery units, for the separation of the mixture ethanol + water is shown. This thesis is concluded in Chapter 7. In this chapter, recommendations for future research are included.

## 1.6 References

1. Doherty, M.F. and J.P. Knapp, *Distillation, Azeotropic and Extractive*, in *Kirk-Othmer Encyclopedia of Chemical Technology* 2004, John Wiley & Sons, Inc.
2. Meyers, R.A., *Handbook of petroleum refining processes*. 3rd ed. McGraw-Hill handbooks2004, New York: McGraw-Hill. 1 v. (various pagings).
3. Lee, F.M. and J.C. Gentry, *Don't Overlook Extractive Distillation*. *Chemical Engineering Progress*, 1997. **93**(10): p. 56-64.
4. Lee, F.M., R.W. Wytcherley and D.W. Ian, *DISTILLATION | Azeotropic Distillation in Encyclopedia of Separation Science* 2000, Academic Press: Oxford. p. 990-995.

5. Lei, Z., C. Li and B. Chen, *Extractive Distillation: A Review*. Separation and Purification Reviews, 2003. **32**(2): p. 121 - 213.
6. Gentry, J.C., S. Kumar and R. Wright-Wytcherley, *Use extractive distillation to simplify petrochemical processes* Hydrocarbon Processing, 2004(June).
7. Gani, R. and E.A. Brignole, *Molecular design of solvents for liquid extraction based on UNIFAC*. Fluid Phase Equilibria, 1983. **13**: p. 331-340.
8. Jiménez, L. and J. Costa López, *Solvent Selection for a Reactive and Extractive Distillation Process by Headspace Gas Chromatography*. Separation Science and Technology, 2003. **38**(1): p. 21 - 37.
9. Kyle, B.G. and D.E. Leng, *Solvent Selection for Extractive Distillation*. Ind. Eng. Chem., 1965. **57**(2): p. 43-48.
10. Kossack, S., K. Kraemer, R. Gani and W. Marquardt. *A Systematic Synthesis Framework for Extractive Distillation Processes*. in *European Congress of Chemical Engineering (ECCE-6)*. 2007. Copenhagen.
11. Bastos, J.C., M.E. Soares and A.G. Medina, *Selection of solvents for extractive distillation. A data bank for activity coefficients at infinite dilution*. Ind. Eng. Chem. Proc. Des. Dev., 1985. **24**(2): p. 420-426.
12. Chen, B., Z. Lei, Q. Li and C. Li, *Application of CAMD in separating hydrocarbons by extractive distillation*. AIChE Journal, 2005. **51**(12): p. 3114-3121.
13. Bieker, T. and K.H. Simmrock, *Knowledge integrating system for the selection of solvents for extractive and azeotropic distillation*. Computers & Chemical Engineering, 1994. **18**: p. S25-S29.
14. van Dyk, B. and I. Nieuwoudt, *Design of Solvents for Extractive Distillation*. Ind. Eng. Chem. Res., 2000. **39**(5): p. 1423-1429.
15. Brignole, E.A., S. Bottini and R. Gani, *A strategy for the design and selection of solvents for separation processes*. Fluid Phase Equilibria, 1986. **29**: p. 125-132.
16. Pretel, E.J., P.A. López, S.B. Bottini and E.A. Brignole, *Computer-aided molecular design of solvents for separation processes*. AIChE Journal, 1994. **40**(8): p. 1349-1360.
17. Jork, C., C. Kristen, D. Pieraccini, A. Stark, C. Chiappe, Y.A. Beste and W. Arlt, *Tailor-made ionic liquids*. The Journal of Chemical Thermodynamics, 2005. **37**(6): p. 537-558.
18. Seiler, M., *Hyperbranched polymers: Phase behavior and new applications in the field of chemical engineering*. Fluid Phase Equilibria, 2006. **241**(1-2): p. 155-174.
19. Seiler, M., D. Köhler and W. Arlt, *Hyperbranched polymers: new selective solvents for extractive distillation and solvent extraction*. Separation and Purification Technology, 2003. **30**(2): p. 179-197.
20. Sandler, S.I., *Chemical, biochemical, and engineering thermodynamics*. 4th ed2006, Hoboken, N.J.: John Wiley. xiv, 945 p.
21. Jork, C., M. Seiler, Y.A. Beste and W. Arlt, *Influence of Ionic Liquids on the Phase Behavior of Aqueous Azeotropic Systems*. J. Chem. Eng. Data, 2004. **49**(4): p. 852-857.
22. Joglekar, Hemant G., I. Rahman and B.D. Kulkarni, *The Path Ahead for Ionic Liquids*. Chemical Engineering & Technology, 2007. **30**(7): p. 819-828.
23. Nebig, S., V. Liebert and J. Gmehling, *Measurement and prediction of activity coefficients at infinite dilution ( $\gamma_{\infty}$ ), vapor-liquid equilibria (VLE)*

- and excess enthalpies (HE) of binary systems with 1,1-dialkyl-pyrrolidinium bis(trifluoromethylsulfonyl)imide using mod. UNIFAC (Dortmund).* Fluid Phase Equilibria, 2009. **277**(1): p. 61-67.
24. Wasserscheid, P. and T. Welton, *Ionic liquids in synthesis* 2003, Weinheim: Wiley-VCH. xvi, 364 p.
  25. Seiler, M., C. Jork, A. Kavarnou, W. Arlt and R. Hirsch, *Separation of azeotropic mixtures using hyperbranched polymers or ionic liquids.* AIChE Journal, 2004. **50**(10): p. 2439-2454.
  26. Meindersma, G.W., *Extraction of aromatics from naphtha with ionic liquids.* PhD Thesis, 2005, University of Twente: Enschede.
  27. Palomar, J., V.R. Ferro, J.S. Torrecilla and F. Rodriguez, *Density and Molar Volume Predictions Using COSMO-RS for Ionic Liquids. An Approach to Solvent Design.* Ind. Eng. Chem. Res., 2007. **46**(18): p. 6041-6048.
  28. Lei, Z., J. Zhang, Q. Li and B. Chen, *UNIFAC Model for Ionic Liquids.* Industrial & Engineering Chemistry Research, 2009. **48**(5): p. 2697-2704.
  29. Alevizou, E.I., G.D. Pappa and E.C. Voutsas, *Prediction of phase equilibrium in mixtures containing ionic liquids using UNIFAC.* Fluid Phase Equilibria, 2009. **284**(2): p. 99-105.
  30. Diedenhofen, M., F. Eckert and A. Klamt, *Prediction of Infinite Dilution Activity Coefficients of Organic Compounds in Ionic Liquids Using COSMO-RS.* J. Chem. Eng. Data, 2003. **48**(3): p. 475-479.
  31. Banerjee, T. and A. Khanna, *Infinite Dilution Activity Coefficients for Trihexyltetradecyl Phosphonium Ionic Liquids: Measurements and COSMO-RS Prediction.* J. Chem. Eng. Data, 2006. **51**(6): p. 2170-2177.
  32. Freire, M.G., S.P.M. Ventura, L.M.N.B.F. Santos, I.M. Marrucho and J.A.P. Coutinho, *Evaluation of COSMO-RS for the prediction of LLE and VLE of water and ionic liquids binary systems.* Fluid Phase Equilibria, 2008. **268**(1-2): p. 74-84.
  33. Freire, M.G., L.M.N.B.F. Santos, I.M. Marrucho and J.A.P. Coutinho, *Evaluation of COSMO-RS for the prediction of LLE and VLE of alcohols + ionic liquids.* Fluid Phase Equilibria, 2007. **255**(2): p. 167-178.
  34. Banerjee, T., R.K. Sahoo, S.S. Rath, R. Kumar and A. Khanna, *Multicomponent Liquid-Liquid Equilibria Prediction for Aromatic Extraction Systems Using COSMO-RS.* Ind. Eng. Chem. Res., 2007. **46**(4): p. 1292-1304.
  35. Arlt, W., M. Seiler, C. Jork and T. Schneider. *Ionic liquids as selective additives for separation of close boiling or azeotropic mixtures.* 2004. Patent US20040133058 A1.
  36. Orchilles, A.V., P.J. Miguel, E. Vercher and A. Martinez-Andreu, *Ionic Liquids as Entrainers in Extractive Distillation: Isobaric Vapor-Liquid Equilibria for Acetone + Methanol + 1-Ethyl-3-methylimidazolium Trifluoromethanesulfonate.* J. Chem. Eng. Data, 2007. **52**(1): p. 141-147.
  37. Kumar, S., N. Singh and R. Prasad, *Anhydrous ethanol: A renewable source of energy.* Renewable & Sustainable Energy Reviews, 2010. **14**(7): p. 1830-1844.
  38. McPhail, L.L., *Assessing the impact of US ethanol on fossil fuel markets: A structural VAR approach.* Energy Economics. **In Press, Corrected Proof.**

39. Huang, H.-J., S. Ramaswamy, U.W. Tschirner and B.V. Ramarao, *A review of separation technologies in current and future biorefineries*. Separation and Purification Technology, 2008. **62**(1): p. 1-21.
40. Weissermel, K. and H.J. Arpe, *Industrial Organic Chemistry*. 4 ed 2003: WILEY-VCH. 491.
41. *Association of petrochemicals producers in europe (appe)*. [cited 2011 28/06/2011]; Available from: <http://www.petrochemistry.net>.
42. Griesbaum, K., A. Behr, D. Biedenkapp, H.-W. Voges, D. Garbe, C. Paetz, G. Collin, D. Mayer and H. Höke, *Hydrocarbons*, in *Ullmann's Encyclopedia of Industrial Chemistry* 2000, Wiley-VCH Verlag GmbH & Co. KGaA.
43. Lappin, G.R., L.H. Nemeč, J.D. Sauer and J.D. Wagner, *Olefins, Higher*, in *Kirk-Othmer Encyclopedia of Chemical Technology* 2000, John Wiley & Sons, Inc.
44. *Sasol to double octene production*. Additives for Polymers, 2003. **2003**(6): p. 10-10.
45. Marrufo, B., A. Aucejo, M. Sanchotello and S. Loras, *Isobaric vapor-liquid equilibrium for binary mixtures of 1-hexene + n-hexane and cyclohexane + cyclohexene at 30, 60 and 101.3 kPa*. Fluid Phase Equilibria, 2009. **279**(1): p. 11-16.
46. Koenitzer, B.A. *Polyurethane-imide membranes and their use for the separation of aromatics from non-aromatics*. 1990. Patent 4929358.
47. Eldrige, R.B., *Olefin/paraffin separation technology: a review*. Industrial & Engineering Chemistry Research, 1993. **32**(10): p. 2208-2212.

## 2. COSMO-RS based IL selection for extractive distillation processes

### Abstract

In this chapter, a solvent selection methodology for extractive distillation processes is applied to identify promising ionic liquid (IL) solvents for the following separation cases: methylcyclohexane/toluene, 1-hexene/*n*-hexane and ethanol/water. Thermodynamic and phase stability analysis are done in order to understand the strong interactions between the solutes and the ionic liquids (solvents) and vice versa. The solvent preselection is done with *COSMOtherm* software (version C2.1 Release 01.11a) and selectivities and relative volatilities are obtained experimentally and compared with the predicted values. Variations in the IL structure (in the cations and anions) and their effect in the solubility and selectivity are theoretically studied and experimentally confirmed. Suitable ILs are selected by experimentation at finite dilution (real solutions). A suitable IL for the separation of 1-hexene from *n*-hexane yielding a better performance than the conventional solvent *N*-methyl-2-pyrrolidone (NMP) was not found. Tetracyanoborate-based ILs seem to be promising solvents for the extractive distillation of toluene from methylcyclohexane as a replacement of the conventional solvent NMP. For the separation of ethanol from water, the ILs 1-ethyl-3-methyl-imidazolium acetate and 1-ethyl-3-methyl-imidazolium dicyanamide (due to its thermal stability) seem to be suitable candidates and possible replacements of ethylene glycol (EG), which is used as a conventional solvent for the separation of this mixture.

### 2.1 Introduction

Group contribution methods (GCM) are the most reliable and widely accepted way to predict and calculate activity coefficients and other thermodynamic properties in liquid (multicomponent) mixtures [1-4]. This information is of high value for chemical engineers to synthesize and design chemical processes. Among several methods, (modified) UNIFAC is the most used and one of the most accurate of such GCMs [3-5]. This method involves, in the initial and developing stage, the fitting of some set of experimental data to obtain interaction parameters necessary for further predictions. Thus, the thermodynamic calculation is interpolated (or extrapolated) from those experimental values. Nevertheless, the performance of these models depends upon the availability and quality of the interaction parameters. Moreover, although GCMs are the most used, these methods cannot be applied for molecules not present in the database.

Nowadays there are some new methods that are basically independent of experimental data. The necessary information is obtained from the molecular structure. A new model called COSMO-RS, the conductor-like screening model for real solvents, is based on unimolecular quantum chemical calculations of the individual species in the system (pure components) [6-9]. This model is especially suitable for property calculations of some substances if reliable experimental data is missing or not available [10-13]. COSMO-RS combines an electrostatic theory of locally interacting molecular surface descriptors,

which are available from quantum chemical calculations, with a statistical thermodynamics methodology [13].

In this chapter, a systematic solvent selection methodology for extractive distillation (ED) processes is established. Some methodologies for conventional solvent selection have been reported in the literature [1, 14, 15]. They are based on the strength of the interactions between the solutes and the solvents at infinite dilution, which is represented by the selectivity,  $S_{ij}^{\infty}$  (equation 2.1).

$$S_{ij}^{\infty} = \left( \frac{\gamma_i^{\infty}}{\gamma_j^{\infty}} \right)_S \quad 2.1$$

where  $\gamma_i^{\infty}$  refers to the activity coefficient of component  $i$  at infinite dilution in a solvent  $S$ . Activity coefficients and selectivities at infinite dilution are abundant in the literature [16-29]. However, these data do not accurately represent industrial operations. As it will be shown later in this chapter, when strong interactions between the solvents and the solutes occur, the conventional methodologies cannot be applied. The proposed approach will be focused to the implementation of ILs in extractive distillation (ED) processes; nevertheless, it can also be applied to conventional solvents and other extractive processes.

In this chapter, a systematic solvent selection methodology for ED processes is established. Thermodynamic analysis was done in order to understand the interactions involved in ED processes. Three cases were studied: separation of methylcyclohexane/toluene, 1-hexene/ $n$ -hexane and ethanol/water. A theoretical screening was done with *COSMOtherm* software (version C2.1 Release 01.11a) in order to make a preselection of cations and anions suitable for every case study. Selected cations were then combined with 27 anions to identify the most suitable combinations of ions. It should be mentioned that not only ILs with high selectivities were selected, but also with reasonable solubility to avoid possible formation of a second liquid phase, i.e. the phase stability analysis is taken into account. Some ILs were experimentally tested: selectivities, solubilities and relative volatilities at finite dilution are obtained and compared with the predicted values. Following this procedure, the most suitable ILs were finally selected for every case study according to the experimental relative volatilities/selectivities at finite dilution (real solutions), which are more representative data of industrial processes.

## 2.2 Thermodynamic analysis in extractive distillation

Phase splitting due to thermodynamic instability of liquid mixtures plays an important role in simulation and processes design. In ED, for example, the formation of two liquid phases due to the addition of the solvent is undesirable. Immiscibility in the distillation column leads to lower efficiency, control challenges, and creates foaming, which can drastically lower the capacity and lead to premature flooding, liquid carryover and solvent losses [30, 31].

The criterion for the existence of more than one liquid phase in a binary mixture is

$$\left(\frac{\partial^2 \Delta G_{mix}}{\partial x_1^2}\right)_{T,P} < 0 \quad 2.2$$

The molar Gibbs energy of mixing  $\Delta G_{mix}$  is expressed as

$$\frac{\Delta G_{mix}}{RT} = \frac{G^{ex}}{RT} + \frac{\Delta G_{mix}^{is}}{RT} \quad 2.3$$

where the molar excess Gibbs energy ( $G^{ex}$ ) is commonly predicted with activity models e.g. NRTL, UNIQUAC, UNIFAC among others. The molar Gibbs energy of mixing for an ideal mixture  $\Delta G_{mix}^{is}$  is expressed as

$$\frac{\Delta G_{mix}^{is}}{RT} = \sum_i x_i \ln(x_i) \quad 2.4$$

In this work, the NRTL (Non-Random Two Liquids) method introduced by Renon and Prausnitz [32] is used. It is one of the most frequently employed tools in correlating phase equilibrium data. The NRTL expression for the molar excess Gibbs energy is

$$\frac{G^{ex}}{RT} = \sum_i x_i \frac{\sum_j \tau_{ji} G_{ji} x_j}{\sum_k G_{ki} x_k} \quad 2.5$$

where:

$$\begin{aligned} G_{ij} &= \exp(-\alpha_{ij} \tau_{ij}) \\ \tau_{ij} &= a_{ij} + b_{ij}/T; \quad \tau_{ii} = 0; \quad G_{ii} = 1 \end{aligned} \quad 2.6$$

$a_{ij}$ ,  $b_{ij}$ , are unsymmetrical, i.e.  $ij \neq ji$

Experimental data are necessary for the regression of the above parameters. However, the following simplifications may be done in order to analyze the phase splitting of a mixture in an approximate manner:

- $a_{ij} = 0$
- $\alpha_{ij}$  is user-defined (commonly 0.2 – 0.3)

In this way, the model for a binary system depends on two adjustable parameters ( $b_{12}$  and  $b_{21}$ ). Thus, just two experimental points are theoretically necessary to determine those parameters. The accuracy of the model increases with the number of experimental data used. However, in this work, the activity coefficients at infinite dilution are going to be used as experimental data, i.e.  $\gamma_{12}^\infty$  of the component 1 in the solvent (2) and  $\gamma_{21}^\infty$  of the solvent (2) in the component (1).

The activity coefficients at infinite dilution for a binary mixture in accordance with the NRTL model are expressed by the following equations:

$$\begin{aligned} \ln(\gamma_{12}^\infty) &= \tau_{21} + G_{12} \tau_{12} \\ \ln(\gamma_{21}^\infty) &= \tau_{12} + G_{21} \tau_{21} \end{aligned} \quad 2.7$$



Thus, there are two equations to solve with two unknown variables ( $\tau_{ij}$ ). With these parameters, the entire equilibrium of the binary mixture can be obtained. Therefore, given the activity coefficients at infinite dilution in a binary mixture, the parameters of the NRTL model can be obtained, the phase behavior of the mixture can be predicted and the stability analysis can be performed.

It is interesting to know the combination of parameters (or activity coefficients at infinite dilution) that causes the formation of two liquid phases. When the above criterion is applied, Figure 2.1 is obtained.

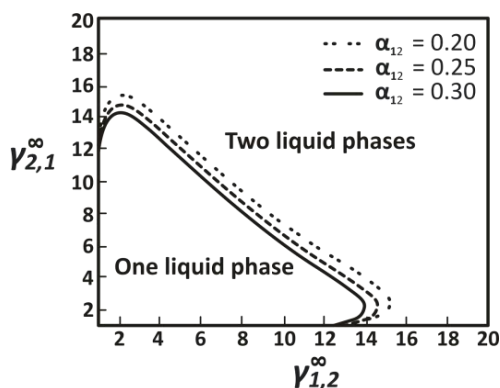


Figure 2.1: Phase stability analysis for a binary mixture

As can be seen in Figure 2.1, there is a triangular region where only one liquid phase exists. The interactions (or activity coefficients at infinite dilution) between the components to be separated and the solvent (and vice versa) should be located inside that area. Therefore, the solvent selection should be based on the analysis of the activity coefficients of the components in the solvent and the solvent in the components. The interactions between the components to be separated and the solvent are as important as the interaction between the solvent and components.

### 2.3 COSMO-RS theory

The Conductor-like Screening Model for Real Solvents (COSMO-RS) was originally published in 1995 [11]. This method was generalized and parameterized in 1998 [33]. In numerous publications [9, 10, 13, 34-39] it has been shown that COSMO-RS is a valuable tool for the handling of chemical engineering problems regarding activity coefficients and other thermodynamic data. COSMO-RS and the theory behind this method are out of the scope of this research; however a short introduction of its features will be given in this section. A more detailed explanation of the theory has been given by Klamt and Eckert, among others [11, 13, 33, 34, 38].

Description of a solute molecule in solution is complicated and time consuming due to the large number of solvent molecules required for a realistic representation and their interactions with the surrounding molecules. On the other hand, the group contribution methods (e.g. UNIFAC) are fast at the cost of the dependency of available parameters or enough experimental data to regress them. COSMO-RS is classified as a dielectric

continuum solvation model (CSM) which allows for a faster treatment of molecules in solutions than quantum chemistry methods by approximating the most important feature of solvents (electrostatic interaction with the solute) by classical dielectric theory.

Quantum chemical methods originally have been developed for isolated molecules (in vacuum or in the gas phase). Due to the importance of solvents in industry and to the practical impossibility of a rigorous representation of a molecular environment by quantum chemical approaches, attempts have been made to combine the quantum chemical descriptions with an approximate description of the surrounding solvent. Dielectric models, such as CSM, have been used to describe the electrostatic behavior of solvents and the Conductor-like Screening Model (COSMO) is an efficient variant of these CSMs. The COSMO model is based on the construction of an imaginary cavity for a given molecular geometry. This cavity is then discretized in  $m$  small segments, so that in each segment  $i$  a constant screening charge density  $\sigma_i$  can be assumed, resulting in a screening charge  $q_i = a_i \times \sigma_i$  with  $a_i$  being the area of the segment. With this basic information, the virtual conducting molecular contact surface (geometry of the cavity) is computed by the quantum chemical COSMO method. In addition, the screening charge density on each position of the molecular contact surface and the dielectric interaction energy (measure of the polarity of molecules) of the solute with the continuum is known.

In reality there is not such a conducting medium (segments of the cavity) between the molecules as it is assumed in COSMO model. This cavity has to be “removed” and here is where COSMO-RS plays its role. If these surface charge densities are averaged over the contact segment, an effective probability function,  $p(\sigma)$ , can be derived. This property is called the  $\sigma$ -profile, and describes the amount of surface in the ensemble having a screening charge density between  $\sigma$  and  $\sigma + d\sigma$ . This model replaces the ensemble of interacting molecules with the corresponding ensemble of interacting surface pieces, in other words, now the interacting molecules are entirely described by their  $\sigma$ -profiles which vary considerably between different molecules, and even conformers. With this information, statistical thermodynamics can be used to obtain the chemical potential and the activity coefficients of the components in the mixture [10].

### 2.3.1 Why COSMO-RS and *COSMOtherm*?

COSMO-RS is a promising tool for the calculations and prediction of thermodynamic properties of pure components (vapor pressures) and mixtures (activity coefficients, excess properties, phase diagrams, solubility of liquids and solids). This model takes into account the most important molecular interaction energy modes, electrostatics, hydrogen bonding and, in a more approximate way, van der Waals interactions [40].

*COSMOtherm* is a software package for the quantitative calculation that uses COSMO-RS theory. This software (version C2.1 release 01.11a) is used in this work to obtain the thermodynamic properties of pure components and mixtures. It has a large database; however, the amount of ILs present in it is limited. New molecules can be easily created and stored in the database. This has to be done only once for each new compound. These COSMO-files contain the  $\sigma$ -profiles and charge distribution of the molecule, which is valuable information for the software. Thus, *COSMOtherm* can be run easily utilizing the stored molecular information.

The incorporation of new  $\sigma$ -profiles is done with help of molecular and quantum chemical simulation software (*HyperChem*, *Turbomole*, *MOPAC*, *Gaussian*, and *DMOL3*, among others). In this work, *HyperChem* (release 8.0.3) was used to draw the molecules and make a first molecular optimization. *Turbomole* (running under *Linux*) was used to create the COSMO files. The parameterization used in the *Turbomole* software package was BP-RIDFT/COSMO-density functional theory (DFT), with the TZVP (triple- $\xi$  valence quality augmented by one set of polarization functions) basis set which is utilized for accurate DFT quantitative calculations and is recommended for high quality prediction of thermophysical data [41, 42].

Compared to most of the GCMs, COSMO-RS depends on an extremely small number of adjustable parameters (sixteen in total [38]). However, they are not specific of functional groups or molecule types. The parameters depend on the quantum chemical method used and its basis set. COSMO-RS is parameterized for the elements H, C, N, O, Cl, F, Br, I, Si, P and S [10]. Molecules with other elements can be dealt with this package although the predictions may be less accurate [38].

Two approaches have been proposed to select solvents for extraction and extractive distillation: the calculation of activity coefficients at infinite dilution (quantitative method) and the qualitative method based on  $\sigma$ -profiles<sup>2</sup>. In this work, the quantitative method (based on activity coefficients) is used to select the group/sort of cations and anions which are suitable for extractive distillation of polar and non-polar mixtures taking into account their ability to increase selectivity and solubility.

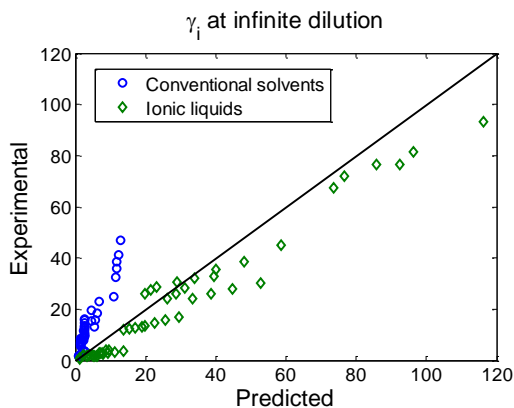


Figure 2.2: Accuracy of *COSMOtherm* prediction for several components and solvents

Activity coefficients at infinite dilution obtained experimentally [19, 26, 27, 43-46] were compared with the ones calculated with *COSMOtherm*. This thermodynamic data is valuable information for the selection and design of solvents for extraction and extractive distillation process.

<sup>2</sup> The  $\sigma$ -profiles are probability distribution plots of the charge density of the molecular surfaces of the compounds

The predicted and experimental values of activity coefficients at infinite dilution at several temperatures are shown in Figure 2.2. This figure shows the interactions between the components (*n*-heptane, *n*-hexane, 1-hexene, toluene, cyclohexane, ethanol and water) and the solvents, i.e. conventional (sulfolane, *N*-methyl-2-pyrrolidone, *N,N*-dimethylformamide, *N*-formylmorpholine) and ionic liquids (1-ethyl-3-methylimidazolium bis(trifluoromethylsulfonyl)imide, 1-butyl-3-methylimidazolium tetrafluoroborate and 1-hexyl-3-methylimidazolium thiocyanate). Figure 2.2 is intended to show the capability of *COSMOtherm* to predict activity coefficients at infinite dilution. As can be seen in Figure 2.2, *COSMOtherm* underestimates the activity coefficients in the conventional solvents, giving higher deviations at larger activity coefficients values. On the other hand, the predictions for the ILs seem to be more accurate; nevertheless, *COSMOtherm* tends to overestimate the activity coefficients at infinite dilution. As can be concluded from the figure, *COSMOtherm* software is able to predict qualitatively the strength of the interactions between the solutes and the solvents (conventional and ILs) which is very useful for the design and selection of the solvents. Besides this, *COSMOtherm* is even able to predict how these interactions are affected by the temperature [40].

## 2.4 Methodology

In this work, three separation cases had been selected to analyze the suitability of ILs used as solvents in ED processes: methylcyclohexane/toluene, olefin/paraffin and ethanol/water. A theoretical screening is done using *COSMOtherm* (version C2.1 release 01.11a) to make a preselection of cations and anions suitable for every case study. Activity coefficients and selectivities at infinite dilution are predicted, and the influence of the alkyl chain length and the degree of branching of every cation is analyzed for every case. Selected cations are then combined with 27 anions to identify the most suitable combinations of ions. It should be mentioned that not only ILs with high selectivities were selected, but also with reasonable solubility to avoid possible formation of a second liquid phase, i.e. the phase stability analysis is taken into account. Some ILs are experimentally tested: selectivities, solubilities and relative volatilities are obtained. Following this procedure, the most suitable IL is finally selected for every case study.

## 2.5 IL design and preselection

The ionic liquids can be decomposed in cations and anions. In this work, cations are roughly classified in several categories: a) non cyclic cations like ammonium-, phosphonium- and sulfonium-based cations; b) cyclic cations like piperidinium and pyrrolidonium, and c) aromatic-type cations like imidazolium-, pyridinium- and quinolinium-based cations. Abbreviations of cations and anions can be found in Table 2.1 in the appendix of this chapter. Compared to cations, anions are more varied and its classification is not as straightforward.

### 2.5.1 Separation of methylcyclohexane/toluene

#### 2.5.1.1 Cation screening

The influence of the alkyl chain length and branching of the cations on the activity coefficients at infinite dilution and selectivities (predicted with *COSMOtherm*) are predicted for several cations combined with the anion abbreviated as BTI in the appendix.

This particular anion has been reported as suitable for the separation of organic mixtures [17, 18, 23, 47, 48].

#### 2.5.1.1.1 Non-cyclic cations

In Figure 2.3, the non-cyclic cations studied in this work are shown, i.e. ammonium, phosphonium, sulfonium and guanidinium cations. The alkyl chains were modified in such a way that the influence of its length and the branching would have been predicted.

In Figure 2.4(a), several symmetric non-cyclic cations are shown with a propyl (C3) alkyl chain. As can be seen, the cation influences the activity coefficients and selectivity (equation 2.1). All the cations studied in this section give high activity coefficients between the IL and methylcyclohexane. The IL [6C3-Gua][BTI] gives the lower activity coefficient; however, its selectivity is also low.

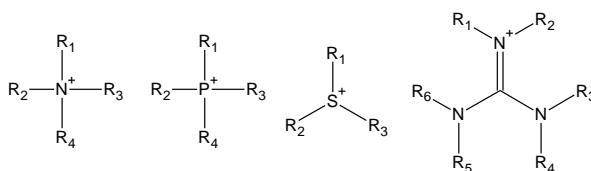


Figure 2.3: Non-cyclic cations. From left to right: ammonium, phosphonium, sulfonium and guanidinium

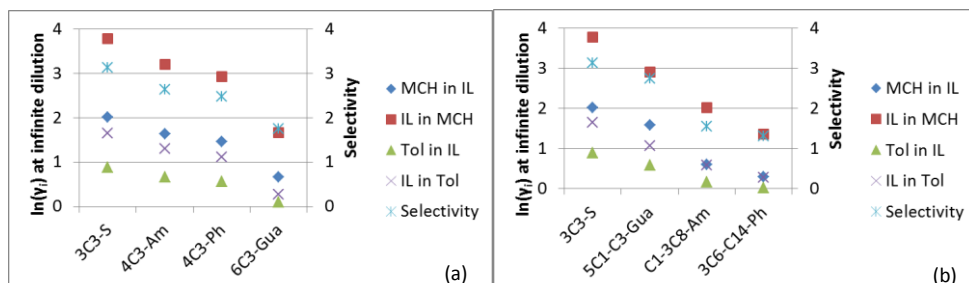


Figure 2.4: Activity coefficients and selectivities for non-cyclic cations. Influence of the (a) cation and (b) degree of branching

Once the cation [6C3-Gua] is changed for [5C1-C3-Gua], the selectivity increases 60% (Figure 2.4(b)); nevertheless, its solubility decreases. The selectivity and activity coefficients decrease when the alkyl chains are long and the degree of branching is high. The guanidinium cation does not look interesting considering the low selectivity compared to the other cations, e.g. ammonium- or phosphonium-based (Figure 2.4(a)). The sulfonium-based cations show the largest values for the activity coefficients at infinity dilution and selectivities. These cations are not attractive due to their high probability to form immiscible liquid phases. According to Figure 2.4(a), ammonium- and phosphonium-based cations have interactions similar to those of the components to be separated. These cations, and specifically the commercially available [C1-3C8-Am] and [3C6-C14-Ph], are selected to determine experimentally their solubility and selectivity.

#### 2.5.1.1.2 Cyclic cations

In Figure 2.5, the cyclic cations studied in this work are presented: pyrrolidonium and piperidinium. The length of each branch was modified and their influence is analyzed.

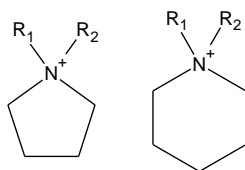


Figure 2.5: Cyclic cations. From left to right: Pyrrolidonium and piperidinium.

In Figure 2.6, the influence of the alkyl chain in pyrrolidonium-based (PYR) and piperidinium-based (PIP) cations is shown. For the same chain lengths, the pyrrolidonium and piperidinium cations show differences in the activity coefficients and selectivities. In all the cases, the PIP cations show lower values for both properties. The selectivity and activity coefficients decrease when the alkyl chain is long and the degree of branching is high. Because of their low activity coefficients, relatively high selectivities, and commercial availability, the cations 1-hexyl-1-methyl-pyrrolidonium [C6-C1-PYR] and 1-hexyl-1-methyl-piperidinium [C6-C1-PIP] are selected for further experimental analysis.

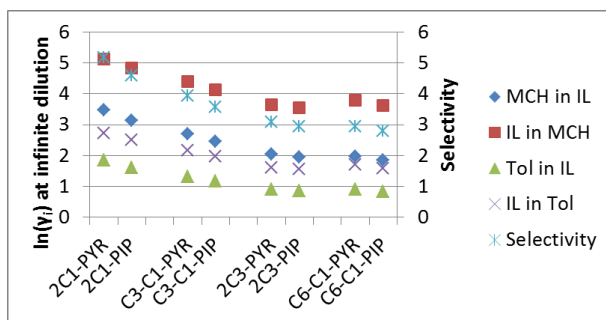


Figure 2.6: Activity coefficients and selectivity for cyclic cations

### 2.5.1.1.3 Aromatic-like cations

In this section, the imidazolium-, pyridinium- and quinolinium-based cations are studied. Their structures are shown in Figure 2.7. As can be seen in the Figure 2.8(a), when the length of the alkyl chain is increased, the activity coefficients and selectivities decrease (this behavior was also observed for quinolinium-based ILs, not shown in Figure 2.8). Besides, the degree of branching also influences these properties in the same way (Figure 2.8(b)). From Figure 2.8(c), it can be concluded that the degree of branching has more influence on the thermodynamic interactions between the components than the position of the alkyl chain. This same behavior was observed for other types of cations (results are not shown in this work). Cations having long alkyl chains, e.g. [C6-MIM], [C8-MIM], [C6-MPY], [C6-PY] and [C6-Qui] are selected for further experimental analysis.

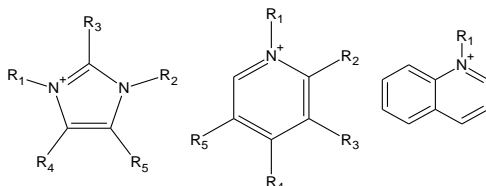


Figure 2.7: Aromatic-like cations. From left to right: imidazolium, pyridinium and quinolinium

### 2.5.1.2 Anion screening

Every cation selected in the previous subsection was combined with 27 different anions. The activity coefficients and selectivities were predicted. Some of the results are shown in Figure 2.9 and 2.10. It should be mentioned that the goal of the anion screening is to find the best combination of ions giving high selectivities (to make the separation easier) and relatively low values for the activity coefficients (to avoid the formation of two liquid phases). In the Figure 2.9 and 2.10, the anions are organized with respect to the values of  $\gamma_{IL-MCH}^{\infty}$ .

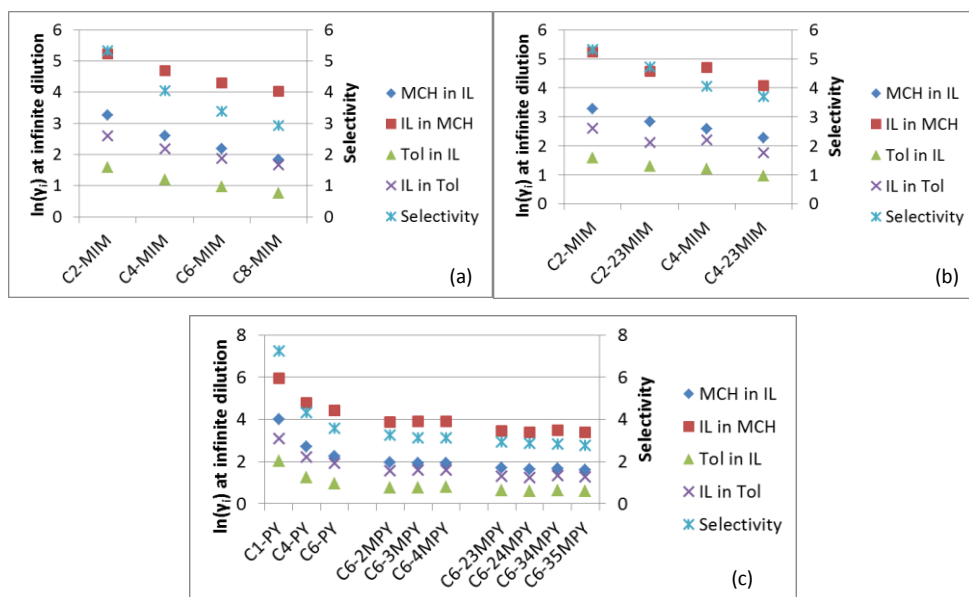


Figure 2.8: Activity coefficients and selectivities for aromatic-like cations. (a) Alkyl chain length, (b) degree of branching and (c) degree of branching and positioning of the alkyl groups in pyridinium cations

Methyl-tri(octyl)-ammonium ([C1-3C8-Am]) was selected as a representative of the non-cyclic cations and the results are shown in Figure 2.9(a). As can be seen, just by modification of the anion, the selectivity can be changed from 1.2 for the tris(pentafluoroethyl)trifluorophosphate (FAP) anion to 2.1 for the tetracyanoborate (TCB) anion. The solubility also can be changed drastically. The phosphate anion ( $H_2PO_4$ ) gives  $\gamma_{IL-MCH}^{\infty} = 20000$  which means that the IL methyl-tri(octyl)-ammonium phosphate is immiscible with methylcyclohexane. On the other hand, the IL [C1-3C8-Am][FAP] gives a value of 3.1 for the same property making this IL miscible with both methylcyclohexane and toluene. However, the anion FAP also gives the lowest selectivity. As can be seen in Figure 2.9(a), a high solubility and/or selectivity is reached with the anions TCB, tricyanomethanide (TCM), and bis((trifluoromethyl)sulfonyl)imide (BTI). Because of commercial availability, the IL methyl-tri(octyl)-ammonium bis((trifluoromethyl)sulfonyl)imide ([C1-3C8-Am][BTI]) was chosen for further studies.

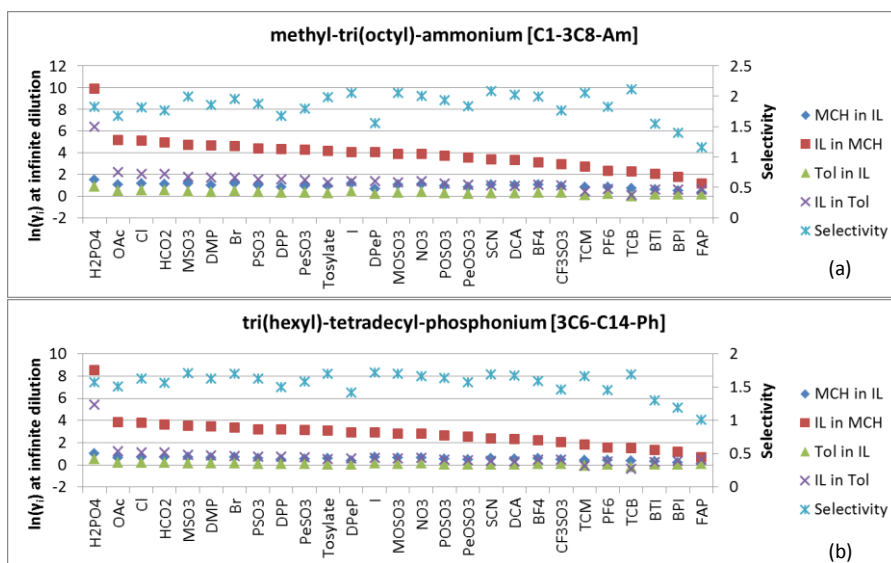


Figure 2.9: Activity coefficients and selectivities: anion screening for the cation (a) methyl-tri(octyl)-ammonium and (b) tri(hexyl)-tetradecyl-phosphonium

For the phosphonium-based cation, the same conclusions can be drawn, as can be seen in Figure 2.9(b). The IL tri(hexyl)-tetradecyl-phosphonium bis((trifluoromethyl)sulfonyl)imide ([3C6-C14-Ph][BTI]) was also chosen for further studies.

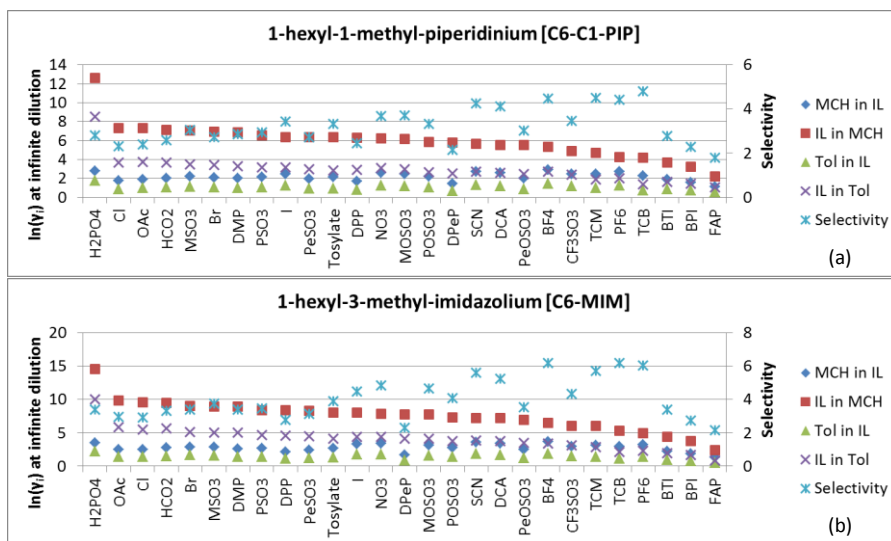


Figure 2.10: Activity coefficients and selectivities: anion screening for the cation 1-hexyl-1-methyl-piperidinium (a) and 1-hexyl-3-methyl-imidazolium (b)

The cation 1-hexyl-1-methyl-piperidinium ([C6-C1-PIP]) was chosen as representative for the cyclic cations; however, the same conclusions as those for [C6-C1-PIP] apply to 1-hexyl-1-methyl-pyrrolidonium ([C6-C1-PYR]). In Figure 2.10(a), it can be seen that the solubility is affected by the anion similarly to that in the non-cyclic cations, which means



that the organic components interact separately with the ions in the IL. However, it should be noted that the ratio of the interactions (selectivity) can be affected in a different way. Because of commercial availability, 1-hexyl-1-methyl-piperidinium bis((trifluoromethyl)sulfonyl)imide ([C6-C1-PIP][BTI]) and 1-hexyl-1-methyl-pyrrolidonium bis((trifluoromethyl)sulfonyl)imide ([C6-C1-PYR][BTI]) were chosen for further studies. In the aromatic-like category, the same conclusions can be drawn, as illustrated in Figure 2.10(b). 1-Hexyl-3-methyl-imidazolium ([C6-MIM]) was chosen as representative; although the same behavior was observed for 1-hexyl-1-methyl-pyridinium [C6-MPY] and 1-hexyl-quinolinium [C6-Qui].

As a result of the cation and anion screening, the following ILs are selected for further experimental study. The conventional solvent NMP (N-methyl-2-pyrrolidone) is also included in the experiments as a benchmark.

- [C6-MIM][BTI]
- [C4-MIM][BTI]
- [C6-Qui][BTI]
- [C6-PY][BTI]
- [C6-MIM][TCB]
- [C4-MIM][TCB]
- [C6-C1-PIP][BTI]
- [C6-C1-PYR][BTI]
- [3C6-C14-Ph][BTI]
- [C1-3C8-Am][BTI]
- [C8-MIM][TCB]
- NMP

### 2.5.2 Separation of 1-hexene/*n*-hexane

*COSMOtherm* activity coefficients at infinite dilution were used to select suitable ILs for the case study 1-hexene/*n*-hexane. Non-cyclic, cyclic and aromatic-like cations were tested in this software. Some of the results are shown in Figure 2.11.

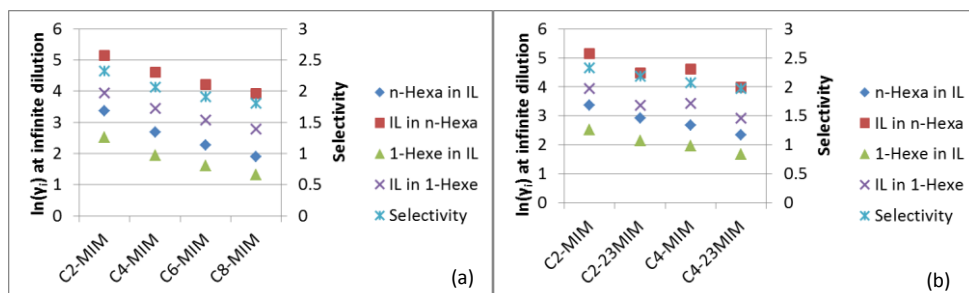


Figure 2.11: Cation screening for the system 1-hexene/*n*-hexane. (a) Alkyl chain and (b) degree of branching effects

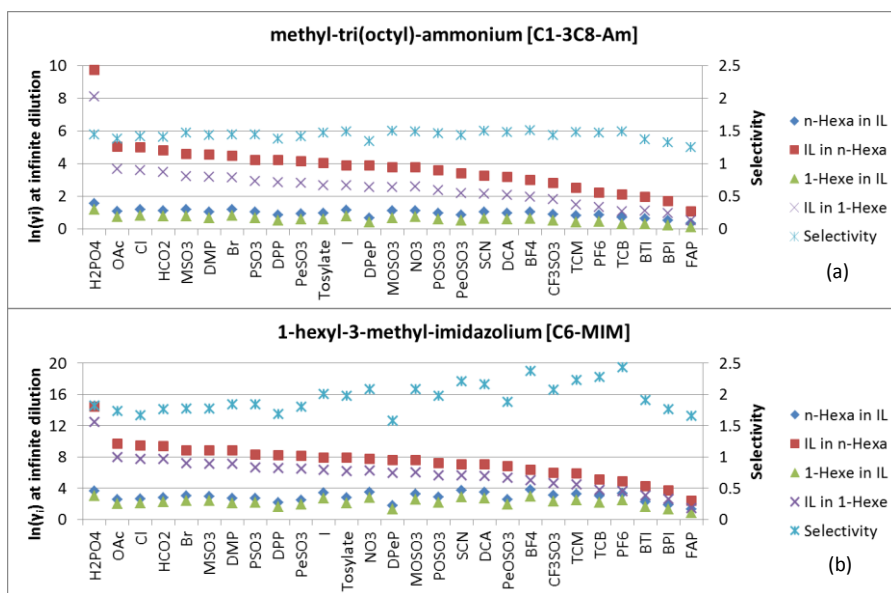


Figure 2.12: Anion screening for the system 1-hexene/*n*-hexane. (a) ammonium-based and (b) imidazolium-based cation

In Figure 2.11, the imidazolium-based cations are shown; however, the conclusions also apply to the other families of cations. As predicted in the aromatic/non-aromatic case, the longer the alkyl chain, the lower the selectivity and activity coefficients (higher solubility), as can be seen in Figure 2.11(a). The degree of branching also has the same influence on the selectivity and solubility of the components as that in the aromatic/non-aromatic case (Figure 2.11(b)). The higher the degree of branching, the lower the selectivity; meanwhile the solubility increases because of the decrease of the activity coefficients. For these reasons, the same cations as those in the aromatic/non-aromatic case were chosen to study the influence of the anion in the activity coefficients predicted by *COSMOtherm*. The results are shown in Figure 2.12.

It should be noted that *COSMOtherm* predicts lower selectivities for the separation of olefins/paraffins than for the separation of aromatic/non-aromatic for the same (or similar) ILs. Besides, the predicted activity coefficients for aromatic/non-aromatic are lower than for the olefins/paraffins. According to *COSMOtherm* and phase stability analysis, more solubility issues can be expected for the separation of 1-hexene/*n*-hexane. Comparing the anion screening for both organic case studies, it can be concluded that the influence of the anion on the activity coefficients and selectivity follows the same trend. Therefore, the ILs selected for the separation case aromatics/non-aromatics are also considered suitable for the separation of olefin/paraffin, and they will be experimentally studied in following sections.

### 2.5.3 Separation of ethanol/water

Selectivities and activity coefficients at infinity dilution were predicted for the system ethanol, water and IL. In this case, ethylene glycol (EG) is considered as the conventional

solvent and benchmark for the extractive distillation process [49]. A similar procedure was applied to make the selection of suitable ILs for this mixture.

### 2.5.3.1 Cation screening

The anion selected to analyze suitable cations was  $\text{Cl}^-$  (chloride) because of its suitability for the separation of polar mixtures [50]. As shown in Figure 2.13, the activity coefficients for IL/water in a  $\text{Cl}^-$ -based IL are very low, implying more attractive forces between these two species. These attraction forces can play an important role in the separation of the pure components, especially unfavorable for the recovery of the solvent [50, 51].

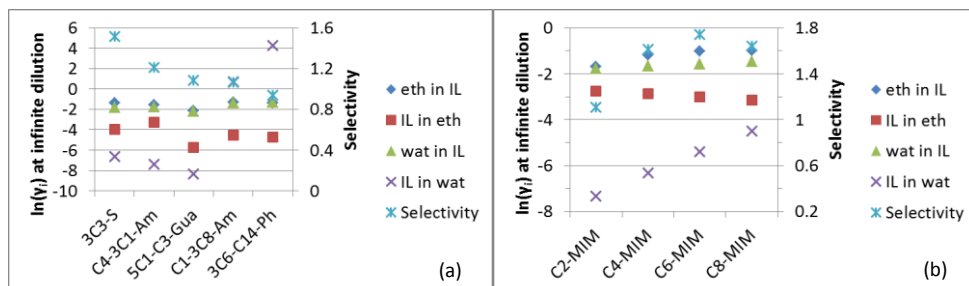


Figure 2.13: Cation screening for the system ethanol/water: (a) non-cyclic cations and (b) imidazolium-based cation

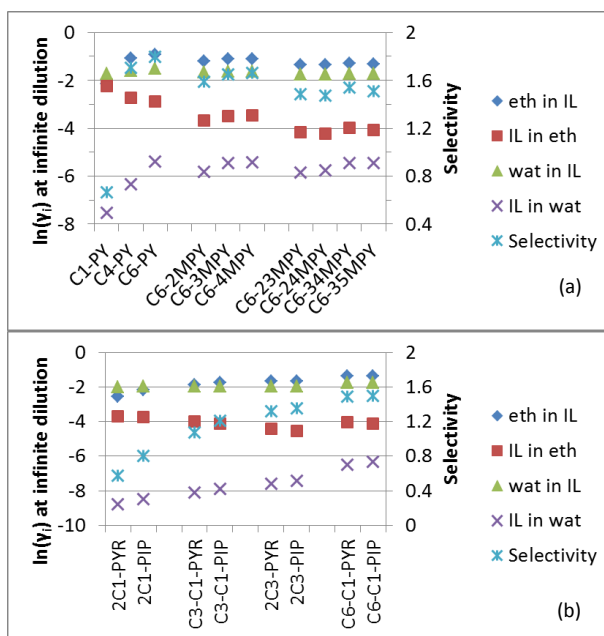


Figure 2.14: Cation screening for the system ethanol/water: (a) pyridinium-based and (b) cyclic cations

In Figure 2.13, the non-cyclic cation seems to have little influence on the activity coefficients of ethanol and water in the ILs; however, the selectivity is being affected by the cation. The alkyl chain length and degree of branching effects are shown in Figure 2.14 for (a) pyridinium-based and (b) cyclic cations. It can be concluded that the longer the alkyl

chains attached to the cation, the higher the selectivity and the activity coefficients, except for  $\gamma_{IL-eth}^{\infty}$ . The degree of branching decreases the selectivity and activity coefficients, as can be seen in Figure 2.14. Besides, these thermodynamic properties are slightly affected by the location of the branches.

For non-cyclic, cyclic and aromatic-like cations, the results are similar and the conclusions can be generalized to different classes of cations. They seem to have little influence on the activity coefficients of ethanol and water in ILs. According to this, it can be concluded that the cations should not have extra alkyl chains (low degree of branching) and the alkyl chain should be relatively long. Comparing the previous results, it can be concluded that the imidazolium-based cations showed the highest selectivities at infinite dilution for this mixture. For this reason, two imidazolium based cations (1-ethyl-3-methyl-imidazolium and 1-hexyl-3-methyl-imidazolium), the non-cyclic cations butyl-tri(methyl)-ammonium and tri(propyl)-sulfonium, the cyclic cation 1-hexyl-1-methyl-piperidinium, and the aromatic-like cation 1-hexyl-pyridinium were chosen to determine the anion influence on the selectivities and activity coefficients.

### 2.5.3.2 Anion screening

Each cation mentioned in the previous section was combined with 28 different anions, and the selectivity and activity coefficients were predicted. The results are shown in Figure 2.15 for the cations 1-ethyl-3-methyl-imidazolium (a) and butyl-tri(methyl)-ammonium (b). The anions are arranged according to the activity coefficient of the pair IL/water. The results and conclusions were the same for the other cations selected in the previous section.

As can be seen in Figure 2.15, the more hydrophobic anions (left side of the figures) showed the lowest selectivities and the acetate (OAc) anion showed the highest selectivity. Considering the large activity coefficient of the pair IL/water for the hydrophobic anions, the formation of two liquid phases between the ILs and water is expected. The influence of the cations on the selectivity seems to be significantly lower than the influence of the anion. From Figure 2.15, it can be noticed that the highest selectivities are reached with the anions: acetate (OAc), phosphate (H<sub>2</sub>PO<sub>4</sub>), dimethylphosphate (DMP) and lactate (Lac). However, the phosphate anion (as well as the chloride anion) is known to be corrosive [52]. Because of the commercial availability of the methanesulfonate (MSO<sub>3</sub>) and dicyanamide (DCA) anions and the theoretical performance of acetate and lactate anions, the following ILs are selected for further experimental study (determination of the relative volatility) for the separation of ethanol/water mixture:

- 1-ethyl-3-methyl-imidazolium methanesulfonate [C2-MIM][MSO<sub>3</sub>]
- 1-ethyl-3-methyl-imidazolium acetate [C2-MIM][OAc]
- 1-ethyl-3-methyl-imidazolium lactate [C2-MIM][Lac]
- 1-ethyl-3-methyl-imidazolium dicyanamide [C2-MIM][DCA]
- Butyl-tri(methyl)-ammonium acetate [BTMA][OAc]

From the COSMOtherm screening it can be concluded that introduction of a double bond in the n-alkane or aromatization of components (i.e. toluene) decreases the activity

coefficients. This may be due to the  $\pi$ -interactions occurring between the components and the cations or anions. For the toluene/MCH and 1-hexene/*n*-hexane cases, cations with localized charges (ammonium, phosphonium and sulfonium) present better solubility than cations with non-localized charges. This may be due to the so called cation- $\pi$  interactions also known as Dougherty effect [53]. The anions with delocalized charge (BTI, BPI, FAP) exhibited stronger interactions (higher solubilities) than Cl or OAc for toluene/MCH and 1-hexene/*n*-hexane separation. The interactions of anions are highly complex [54, 55], although it is clear that increasing size and charge delocalization of the anion, the hydrogen bonding ability decreases and the interactions become weaker.

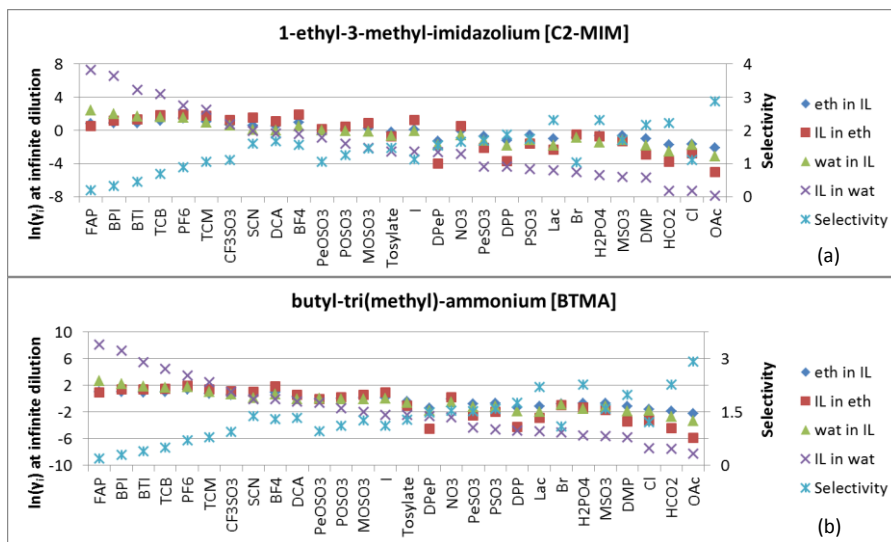


Figure 2.15: Anion screening for the system ethanol/water. (a) 1-ethyl-3-methyl-imidazolium and (b) butyl-tri(methyl)-ammonium cation

For the mixture ethanol/water the main interactions are hydrogen bonds which are formed between the polar molecules and the ions. In particular, the ions with localized charge become more important. That is the case of [C2-MIM][OAc], which has a cation with a delocalized charge and an anion with a localized charge or [C4-3C1-Am][OAc] in which both ions have a localized charge, both with ability to form hydrogen bonds.

## 2.6 Experimental section

### 2.6.1 Chemicals

In the following, the mass fraction purity is given. The ILs [3C6-C14-Ph][BTI] (>0.99), [C1-3C8-Am][BTI] (>0.99), [C6-C1-PIP][BTI] (>0.99), [C6-Qui][BTI] (>0.98), [C6-MIM][BTI] (>0.99), [C6-PY][BTI] (>0.98), [C6-C1-PYR][BTI] (>0.99), [C4-MIM][BTI] (>0.99), [C2-MIM][Lac] (>0.98), [C2-MIM][MSO3] (>0.99), [C2-MIM][OAc] (>0.99), [C2-MIM][DCA] (>0.98) and [C4-3C1-Am][OAc] (>0.95) were purchased from Iolitec. The ILs [C4-MIM][TCB] (for synthesis), [C6-MIM][TCB] (for synthesis) and [C8-MIM][TCB] (for synthesis) were purchased from Merck. Toluene (>0.999), N-methyl-2-pyrrolidone (NMP; 0.995), 1-hexene (>0.97), *n*-hexane (>0.95), *n*-heptane (>0.97), methanol (>0.998), 1-butanol (>0.99) and acetone (>0.99) were purchased from Sigma-Aldrich. Methylcyclohexane (>0.98) and

ethylbenzene (>0.99) were purchased from Fluka. Ethylene glycol (EG; >0.9999) was purchased from VWR and ethanol (>0.995) from Merck. It should be mentioned that ethylbenzene, *n*-heptane and 1-butanol were used as internal standards in the gas chromatography (GC) analysis of aromatics/non-aromatics, olefins/paraffins and water/ethanol mixtures, respectively. Besides, acetone and methanol were used as diluents for organic and alcohol mixtures, respectively. After every experiment, the ILs were purified under vacuum (<1.0 kPa) at  $T = 333$  K for a minimum of 5 h in a rotary evaporator (Büchi Rotavapour R-200 equipped with a Büchi heating bath B-490).

## 2.6.2 Experimental methods and procedure

### 2.6.2.1 Solubility and selectivity experiments

Liquid–liquid extraction experiments were carried out in jacketed vessels with a volume of approximately  $70\text{ cm}^3$ . The experimental procedure mentioned in the work of Meindersma et al [56-58] was followed. The top of the vessel was closed using a PVC cover, through which a stirrer shaft was passed. Two stainless steel propellers equipped with an electronic stirrer control were used. The vessels were jacketed to circulate water from a water bath in order to maintain a constant temperature inside the vessels. The extraction temperature was set at  $333.15\text{ K}$ . For each experiment, maximum  $50\text{ cm}^3$  of mixture (IL + organics) were placed in the vessels, and they were closed. When the desired temperature was reached, the mixture was stirred for 1 h (Meindersma et al. [56-58] established that the equilibration time for extractions with ILs takes approximately 10 min). Samples ( $0.1\text{ cm}^3$ ) from both phases were taken after 30 min of settling down. Ethylbenzene ( $0.1\text{ cm}^3$ ) was added as the internal standard for the GC analysis, and  $1\text{ cm}^3$  of acetone was added to completely solubilize the sample and avoid phase splitting. Analysis of the samples was done by a Varian CP-3800 gas chromatograph (GC) with a Varian CP-SIL5CB ( $50\text{ m} \times 0.32\text{ mm} \times 0.45\text{ mm}$ ) capillary column. Because the ionic liquid has no vapor pressure, it cannot be analyzed by GC. The IL was collected in a cup-liner and a precolumn in order to do not disrupt the analysis. The IL was determined by mass balance of the measured mole fractions of the hydrocarbons. The experiments were carried out in duplicate in order to exclude experimental errors, and the GC analyses were carried out in triplicate in order to be able to exclude possible errors in the analytical technique. For all the measurements, the uncertainty for the temperature measurements is estimated at  $\pm 0.05\text{ K}$  and for the tie-line measurements is estimated within  $\pm 0.001$  in mole fraction.

### 2.6.2.2 Relative volatility experiments

To determine experimental relative volatilities, two techniques were used according to the components present in the samples. For methylcyclohexane/toluene and 1-hexene/*n*-hexane, a headspace technique was used. Because of the presence of water in the ethanol case and the analytical equipment used in this research, the static headspace technique cannot be applied to this mixture. Ebulliometric equipment (Fischer Labodest VLE 602) was used to determine the relative volatility of the mixture ethanol/water in the presence of several solvents.

### 2.6.2.2.1 Headspace technique

Headspace GC (HSGC) was used for measuring the relative volatilities of the organic components in the solvents. Among other thermodynamic properties, this technique has been used to determine relative volatilities and vapor-liquid equilibrium [59]. HSGC is used for the analysis of volatile and semi-volatile organics in a solid or liquid matrix. It analyzes the gas space of a sealed chromatography vial located above the sample. A schematic representation of the equipment is shown in Figure 2.16.

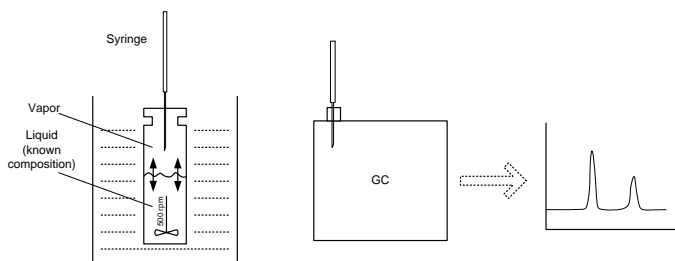


Figure 2.16: Headspace schematic representation

First, liquid samples ( $10 \text{ cm}^3$ ) with a known composition were placed into  $20 \text{ cm}^3$  threaded headspace vials having a gas volume above it. Then, they were closed with magnetic screw caps. They were placed onto temperature-controlled racks with a total capacity for 72 vials and maintained at a constant temperature of 303.15 K. After 12 h of incubation, the experimental determination and analysis of the samples were allowed to start. Before injection, every vial was agitated at 500 rpm for 1 hr. The agitator is temperature-controlled with an uncertainty of  $\pm 0.05 \text{ K}$ , provided by the manufacturer. In this agitator, the temperature was set as 303.15 K. Then an aliquot of the vial's gas phase (the headspace) was introduced into the carrier gas stream of a gas chromatograph where it is analyzed in the usual way. In this work, the analysis was done by a Varian CP-3800 gas chromatograph (GC) with a Varian CP-SIL5CB ( $30 \text{ m} \times 0.25 \text{ mm} \times 0.25 \mu\text{m}$ ) capillary column. Because the IL and the solvents used in this work have negligible vapor pressure, they cannot be detected by GC. The experiments were carried out in duplicate in order to exclude experimental errors. The gas samples were taken by an ATAS CombiPAL autosampler equipped with a  $2.5 \text{ cm}^3$  gastight syringe. For all of the measurements, the injected volume was set as  $0.3 \text{ cm}^3$  and the uncertainty for the vapor composition is estimated at  $\pm 0.005$ .

Because the peak area obtained in the HSGC ( $A_i$ ) is proportional to the partial pressure of the component in the vapor phase ( $p_i$ ), then

$$A_i = c_i p_i \quad 2.8$$

where  $c_i$  is constant. Raoult's law can be combined with the equation 2.8,

$$A_i = c_i x_i \gamma_i P_i^{sat} \quad 2.9$$

For a pure component ( $x_i = 1$  and  $\gamma_i = 1$ ), the above equation can be written as

$$A_i^0 = c_i P_i^{sat} \quad 2.10$$

After equations 2.9 and 2.10 are combined and reorganized, the relative volatility can be calculated with equation 2.11.

$$\alpha_{12} = \frac{y_1/x_1}{y_2/x_2} = \frac{A_1 P_1^{sat} / A_1^0 x_1}{A_2 P_2^{sat} / A_2^0 x_2} \quad 2.11$$

#### 2.6.2.2.2 Ebulliometric technique

For the ethanol/water case, vapor-liquid equilibrium data were obtained by ebulliometric measurements using a Fischer technology Labodest unit (VLE 602D). The equilibrium apparatus is a dynamic recirculating still that ensures intimate contact of the liquid and vapor phase.

The apparatus is depicted in Figure 2.17. It is equipped with a PT100 temperature sensor, with an uncertainty of  $\pm 0.01\text{K}$ , and a digital pressure controller, with an uncertainty of  $\pm 0.001\text{kPa}$ , according to the manufacturer. Equilibrium conditions were assumed when constant temperature and pressure were obtained for 30 min or longer. Then, samples ( $0.1\text{ cm}^3$ ) of the liquid and condensed vapor were taken for analysis. 1-Butanol ( $0.1\text{ cm}^3$ ) was added as the internal standard for the GC analysis, and  $1\text{ cm}^3$  of methanol was added to completely solubilize the sample. The concentration of the liquid and vapor samples were obtained with a Varian 430-GC gas chromatograph using a capillary column (Supelco Nukol,  $15\text{ m} \times 0.53\text{ mm} \times 0.5\text{ }\mu\text{m}$ ). The IL was collected in a cup-liner and a precolumn in order to do not disrupt the analysis. The water content was determined with an automatic Karl Fischer titrator (Metrohm 795 KFT) combined with a Sartorius CPA 3245 mass balance ( $\pm 0.1\text{ mg}$ ). The uncertainty for the vapor and liquid compositions is estimated at  $\pm 0.001$ .

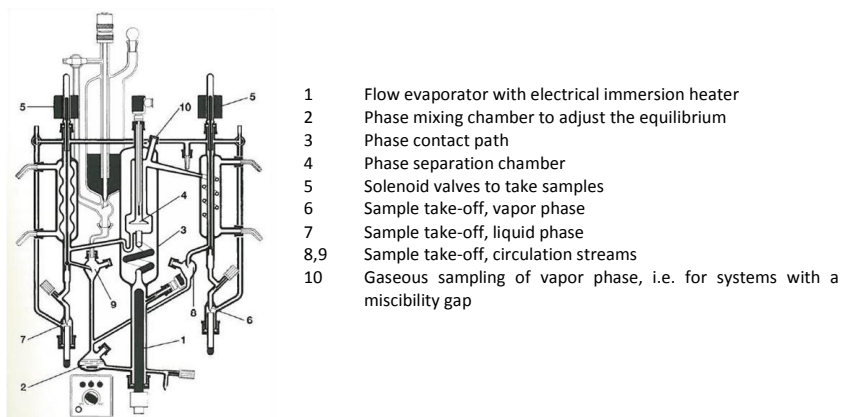


Figure 2.17: Labodest VLE apparatus

### 2.6.3 Experimental results and discussion

#### 2.6.3.1 Separation of methylcyclohexane/toluene

The experimental (liquid + liquid) equilibrium data measured at  $333.15\text{ K}$  at atmospheric pressure for the binary systems (methylcyclohexane + IL) and (toluene + IL) are presented in Figure 2.18. For numerical and analytical reasons it was assumed that the solubility of ionic liquids in the organic phase was very low, as in the work carried out by Meindersma



[56, 60]. For binary extractions, Shiflett and Niehaus [61] reported values of 0% of ionic liquid in the organic phase for several substituted benzene components. In this work, the molar compositions of the ionic liquids in the organic phase were set to  $10^{-4}$ .

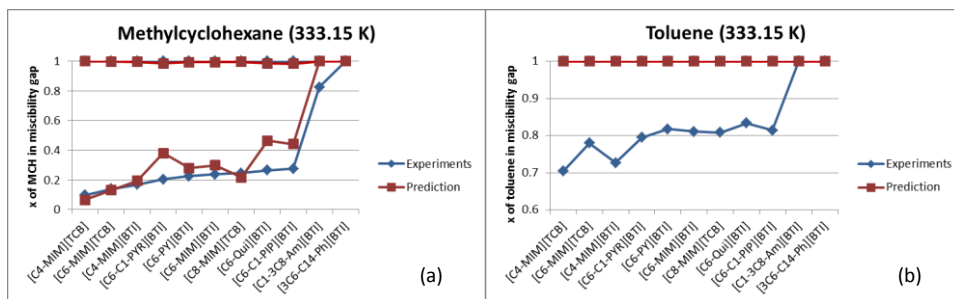


Figure 2.18: Binary solubilities of methylcyclohexane and toluene with ILs at 333.15 K

Figure 2.18 shows the comparison between the experimental and the *COSMOtherm* prediction for the solubility of methylcyclohexane and ILs. It should be mentioned that *COSMOtherm* predicted total solubility of toluene in ILs. As can be seen in the ion screening section, the activity coefficients where toluene is involved are much lower than where methylcyclohexane is present. For the anions studied in this section, the predicted activity coefficients at infinite dilution for the combination toluene+IL fall inside the one-liquid phase area of Figure 2.1. For the IL [C1-3C8-Am][BTI], *COSMOtherm* was unable to predict the phase splitting when it is mixed with methylcyclohexane. Besides this, *COSMOtherm* predicts, accurately, that [3C6-C14-Ph][BTI] is totally soluble with both methylcyclohexane and toluene. In extractive distillation processes it is desirable to have completely miscible solvents. From the solubility results shown Figure 2.18, the most suited ILs to be used in extractive distillation processes are [C1-3C8-Am][BTI] and [3C6-C14-Ph][BTI] due to their high miscibility; however, the relative volatility (or selectivity) is the determining property for the solvent selection.

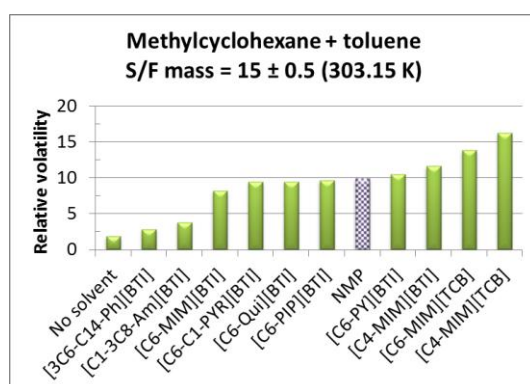


Figure 2.19: Relative volatility for methylcyclohexane/toluene with several ILs

The experimental relative volatilities obtained with the HSGC technique measured at 303.15 K for the ternary system methylcyclohexane (1) + toluene (2) + solvent (3) are shown in Figure 2.19. The mass compositions expressed on a solvent free basis for all the measurements are 0.3 and 0.7 for methylcyclohexane and toluene, respectively. For all of

the measurements, a solvent to feed (S/F) mass ratio of around 15 was maintained. The high values for S/F were chosen to avoid a second liquid-phase formation during the experiments according to the solubility values reported in Figure 2.18.

In Figure 2.19 it can be seen that the relative volatility for the real solution of methylcyclohexane + toluene + solvent increased when any of the solvents are added. Taking as a benchmark the conventional solvent NMP, it can be concluded that [3C6-C14-Ph][BTI] and [C1-3C8-Am][BTI] do not increase significantly the relative volatility of the mixture, even though they are the most soluble ILs. The solvents [C6-MIM][BTI], [C6-C1-PYR][BTI], [C6-Qui][BTI] and [C6-C1-PIP][BTI] do not show any improvement in the benchmark's selectivity, therefore, those ILs are not suitable solvents for the separation of aromatics/non-aromatics. As predicted by *COSMOtherm*, the selectivity (or relative volatility) increases when the alkyl chain attached to the anion is reduced, i.e. in terms of selectivity, [C4-MIM][BTI] > [C6-MIM][BTI] and [C4-MIM][TCB] > [C6-MIM][TCB]. According to *COSMOtherm*, the TCB anion was a suitable anion. As can be observed in Figure 2.19, the ILs composed with the TCB anion showed the highest relative volatility for the separation of aromatics/non-aromatics. The ILs [C4-MIM][TCB] and [C6-MIM][TCB] appear to be the most promising replacements for the conventional solvent (NMP) to separate this mixture by extractive distillation.

### 2.6.3.2 Separation of 1-hexene/n-hexane

The experimental relative volatilities obtained with the HSGC technique measured at 303.15 K for the ternary system *n*-hexane (1) + 1-hexene (2) + solvent (3) are shown in Figure 2.20, for conventional solvents (a) and ILs (b). The mass compositions expressed on a solvent-free basis for all the measurements are 0.2 and 0.8 for *n*-hexane and 1-hexene, respectively. For all the measurements, a solvent to feed (S/F) mass ratio of around 16 for conventional solvents and 20 for ILs was maintained. The high values for S/F were chosen to avoid second liquid phase formation during the experiments.

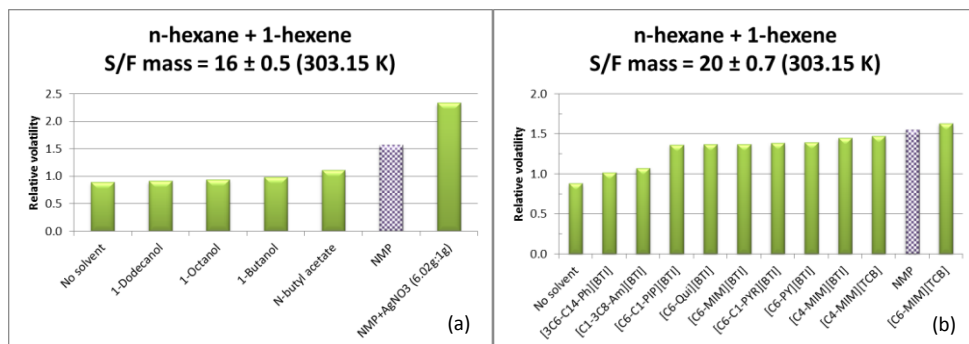


Figure 2.20: Relative volatility for the system 1-hexene (80 wt%)/n-hexane(20 wt%) using conventional solvents (a) and ILs (b) at 303.15 K

Berg (1995) [62] reported in his patent several suited solvents (e.g. alcohols, acetates and formates) for the separation of olefins/paraffins. In Figure 2.20(a), the relative volatilities for such conventional solvents are shown, including acetate and alcohols. It can be concluded that alcohols do not affect the relative volatility of the components significantly making them unsuitable solvents. In this work, NMP is taken as a benchmark. When some

silver nitrate is added to NMP (1 g of  $\text{AgNO}_3$  per 6.02 g of NMP) the relative volatility increases nearly 50%. The effect of silver in olefins and the metal-olefin complex formation has been widely reported in literature [63, 64] and it is out of the scope of this research.

In Figure 2.20(b), the relative volatility for the mixture 1-hexene/*n*-hexane using ILs as solvents is shown. None of the ILs studied in this work is able to significantly increase the relative volatility at finite dilution (real solution) in comparison with the conventional solvent NMP. Only the IL [C6-MIM][TCB] reached a slightly higher relative volatility. However, the increase is not big enough to consider this solvent as a suitable replacement. Besides this, the ILs have solubility constraints that force the use of large solvent to feed ratios to avoid the formation of two liquid phases.

Due to this unsuitability of ILs to replace conventional solvents in extractive distillation for the separation of 1-hexene/*n*-hexane, this mixture won't be studied anymore in this work.

### 2.6.3.3 Separation of ethanol/water

The relative volatilities for the selected ILs and the conventional solvent (ethylene glycol – EG) were determined experimentally with the ebulliometric technique. The vapor – liquid equilibrium was measured at ambient pressure (0.1 MPa). The mass compositions of the feed mixture, expressed in a solvent free basis, for all of the measurements are 0.9 and 0.1 for ethanol and water, respectively, using a solvent to feed mass ratio of around 1 was used.

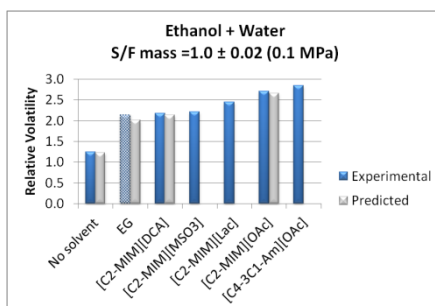


Figure 2.21: Relative volatility for the system ethanol (10 wt%)/water (90 wt%) with several solvents at 0.1 MPa

The experimental relative volatilities for the water/ethanol system are shown in Figure 2.21. As a benchmark, the values of the mixtures without solvent and using EG as the solvent are also reported. Besides, the relative volatility predicted using *Aspen Plus* is also shown for those two cases. As can be seen, the predicted and experimental relative volatilities for the cases without solvent and using EG are in agreement, confirming the reliability and accuracy of the method and equipment used in this research. Comparing the imidazolium-based ILs, it can be noticed that the acetate anion is able to reach a relative volatility of 2.7, which is an increase of 23% in comparison with the conventional solvent and 120% in comparison with the mixture without solvent. The ionic liquid [C2-MIM][OAc] is selected as a promising solvent for the extractive distillation of ethanol/water.

The solvent [C4-3C1-Am][OAc] showed the largest increase in the relative volatility of the mixture; however, it is a solid component. Due to the disadvantages of using solid components in extractive distillation (described in Chapter 1), it was decided to discard this IL as a suitable solvent. The dicyanamide- (DCA) and methanesulfonate- (MSO<sub>3</sub>) based ILs exhibited increases in their relative volatilities similar to that of EG. However, it should be mentioned that the DCA-based ILs have shown to be more thermally stable than MSO<sub>3</sub>-based ILs [65, 66].

From the results above, it can be concluded that [C2-MIM][OAc] is the most promising IL for the separation of the mixture ethanol/water by extractive distillation. This result is in agreement with the experimental findings of Ge et al., which confirms the applicability and usefulness of the systematic IL selection methodology presented in this work. The ILs [C2-MIM][OAc] and [C2-MIM][DCA] will be studied in more detailed in Chapter 4.

## 2.7 Conclusions

Thermodynamic analysis and solvent selection methodology for extractive distillation process for the separation of methylcyclohexane/toluene, 1-hexene/*n*-hexane and ethanol/water were established. For ILs not only the selectivity and activity coefficients of the components in the solvent should be taken into account to select the solvent, but also the activity coefficients of the solvent in the components. For all the ILs, the large interactions between these compounds and the solutes are leading (in most of the cases where organics are involved) to the formation of two liquid phases. A critical triangular area which relates the activity coefficients at infinite dilution with the formation of two liquid phases was identified. It is desirable to increase the selectivity by increasing the activity coefficients; however, miscibility problems should be avoided. There is a clear trade-off between the selectivity and solubility, as it can be seen in this work.

The screening and experiments showed that no suitable IL exists which can replace the conventional solvent NMP for the separation of 1-hexene/*n*-hexane. The non-polarity of this mixture does not lead to sufficiently strong interactions with the solvents to increase its selectivity. Besides, the ILs studied in this work formed two liquid phases with these organic components and the experimental relative volatility demonstrated that the conventional solvent NMP performs better than any IL studied in this work.

For the aromatic/non-aromatic and olefin/paraffin separation cases, *COSMOtherm* predicts a decrease in the activity coefficients when the alkyl chain and the degree of branching are increased. This was confirmed with experimental data. Two ILs having tetracyanoborate (TCB) as anion were selected. This anion has lower molecular weight and higher selectivity than most of the fluorinated anions. The ILs 1-hexyl-3-methyl-imidazolium tetracyanoborate [C6-MIM][TCB] and 1-butyl-3-methyl-imidazolium tetracyanoborate [C4-MIM][TCB] are considered as promising solvents for the separation of aromatics/non-aromatics by extractive distillation and they will be studied in more detailed in Chapter 3.

For the more polar case, ethanol/water, the predictions have to be taken more carefully. According to *COSMOtherm*, the effect of the anion in the selectivity (or relative volatility) is more pronounced than the effect of the cation. The IL 1-ethyl-3-methyl-imidazolium

acetate [C2-MIM][OAc] showed a reasonable increase in the selectivity, in comparison with the conventional solvent (EG). A more detailed study of this IL and [C2-MIM][DCA] will be performed in Chapter 4. According to the *COSMOtherm* results shown in this work, it can be concluded that the ILs increase the selectivity and relative volatility by attracting the water, which might negatively influence the IL recovery. A more detailed analysis of this effect is done in Chapter 4 and 6.

## 2.8 References

1. Harper, P.M. and R. Gani, *A multi-step and multi-level approach for computer aided molecular design*. Computers & Chemical Engineering, 2000. **24**(2-7): p. 677-683.
2. Karunanithi, A.T., L.E.K. Achenie and R. Gani, *A New Decomposition-Based Computer-Aided Molecular/Mixture Design Methodology for the Design of Optimal Solvents and Solvent Mixtures*. Ind. Eng. Chem. Res., 2005. **44**(13): p. 4785-4797.
3. Kossack, S., K. Kraemer, R. Gani and W. Marquardt. *A Systematic Synthesis Framework for Extractive Distillation Processes*. in *European Congress of Chemical Engineering (ECCE-6)*. 2007. Copenhagen.
4. Pretel, E.J., P.A. López, S.B. Bottini and E.A. Brignole, *Computer-aided molecular design of solvents for separation processes*. AIChE Journal, 1994. **40**(8): p. 1349-1360.
5. Kossack, S., K. Kraemer, R. Gani and W. Marquardt, *A systematic synthesis framework for extractive distillation processes*. Chemical Engineering Research and Design, 2008. **86**(7): p. 781-792.
6. Banerjee, T. and A. Khanna, *Infinite Dilution Activity Coefficients for Trihexyltetradecyl Phosphonium Ionic Liquids: Measurements and COSMO-RS Prediction*. J. Chem. Eng. Data, 2006. **51**(6): p. 2170-2177.
7. Banerjee, T., R.K. Sahoo, S.S. Rath, R. Kumar and A. Khanna, *Multicomponent Liquid-Liquid Equilibria Prediction for Aromatic Extraction Systems Using COSMO-RS*. Ind. Eng. Chem. Res., 2007. **46**(4): p. 1292-1304.
8. Banerjee, T., M.K. Singh and A. Khanna, *Prediction of Binary VLE for Imidazolium Based Ionic Liquid Systems Using COSMO-RS*. Ind. Eng. Chem. Res., 2006. **45**(9): p. 3207-3219.
9. Banerjee, T., K.K. Verma and A. Khanna, *Liquid-liquid equilibrium for ionic liquid systems using COSMO-RS: Effect of cation and anion dissociation*. AIChE Journal, 2008. **54**(7): p. 1874-1885.
10. Klamt, A., *COSMO-RS. From Quantum Chemistry to Fluid Phase Thermodynamics and Drug Design*. 1st ed 2005: Elsevier.
11. Klamt, A., *Conductor-like Screening Model for Real Solvents: A New Approach to the Quantitative Calculation of Solvation Phenomena*. The Journal of Physical Chemistry, 1995. **99**(7): p. 2224-2235.
12. Klamt, A. and F. Eckert, *Prediction of vapor liquid equilibria using COSMOtherm*. Fluid Phase Equilibria, 2004. **217**(1): p. 53-57.
13. Klamt, A. and F. Eckert, *COSMO-RS: a novel and efficient method for the a priori prediction of thermophysical data of liquids*. Fluid Phase Equilibria, 2000. **172**(1): p. 43-72.

14. Jiménez, L. and J. Costa López, *Solvent Selection for a Reactive and Extractive Distillation Process by Headspace Gas Chromatography*. Separation Science and Technology, 2003. **38**(1): p. 21 - 37.
15. Kyle, B.G. and D.E. Leng, *Solvent Selection for Extractive Distillation*. Ind. Eng. Chem., 1965. **57**(2): p. 43-48.
16. Marciniak, A., *Influence of cation and anion structure of the ionic liquid on extraction processes based on activity coefficients at infinite dilution. A review*. Fluid Phase Equilibria, 2010. **294**(1–2): p. 213-233.
17. Marciniak, A. and M. Wlazło, *Activity coefficients at infinite dilution and physicochemical properties for organic solutes and water in the ionic liquid 1-(2-methoxyethyl)-1-methylpiperidinium bis(trifluoromethylsulfonyl)-amide*. The Journal of Chemical Thermodynamics, 2012. **49**(0): p. 137-145.
18. Marciniak, A. and M. Wlazło, *Activity coefficients at infinite dilution and physicochemical properties for organic solutes and water in the ionic liquid 4-(2-methoxyethyl)-4-methylmorpholinium bis(trifluoromethylsulfonyl)-amide*. The Journal of Chemical Thermodynamics, 2012. **47**(0): p. 382-388.
19. Domańska, U., A. Marciniak, M. Królikowska and M. Arasimowicz, *Activity Coefficients at Infinite Dilution Measurements for Organic Solutes and Water in the Ionic Liquid 1-Hexyl-3-methylimidazolium Thiocyanate*. Journal of Chemical & Engineering Data, 2010. **55**(7): p. 2532-2536.
20. Domanska, U. and A. Marciniak, *Measurements of activity coefficients at infinite dilution of aromatic and aliphatic hydrocarbons, alcohols, and water in the new ionic liquid [EMIM][SCN] using GLC*. The Journal of Chemical Thermodynamics, 2008. **40**(5): p. 860-866.
21. Domanska, U. and A. Marciniak, *Activity Coefficients at Infinite Dilution Measurements for Organic Solutes and Water in the Ionic Liquid 1-Ethyl-3-methylimidazolium Trifluoroacetate*. J. Phys. Chem. B, 2007. **111**(41): p. 11984-11988.
22. Letcher, T.M., A. Marciniak, M. Marciniak and U. Domanska, *Determination of Activity Coefficients at Infinite Dilution of Solutes in the Ionic Liquid 1-Butyl-3-methylimidazolium Octyl Sulfate Using Gas-Liquid Chromatography at a Temperature of 298.15 K, 313.15 K, or 328.15 K*. J. Chem. Eng. Data, 2005. **50**(4): p. 1294-1298.
23. Letcher, T.M., A. Marciniak, M. Marciniak and U. Domanska, *Activity coefficients at infinite dilution measurements for organic solutes in the ionic liquid 1-hexyl-3-methyl-imidazolium bis(trifluoromethylsulfonyl)-imide using g.l.c. at T = (298.15, 313.15, and 333.15) K*. The Journal of Chemical Thermodynamics, 2005. **37**(12): p. 1327-1331.
24. Gruber, D., M. Topphoff and J. Gmehling, *Measurement of Activity Coefficients at Infinite Dilution Using Gas-Liquid Chromatography. 9. Results for Various Solutes with the Stationary Phases 2-Pyrrolidone and N-Methylformamide*. J. Chem. Eng. Data, 1998. **43**(6): p. 935-940.
25. Gruber, D., D. Langenheim, W. Moollan and J. Gmehling, *Measurement of Activity Coefficients at Infinite Dilution Using Gas-Liquid Chromatography. 7. Results for Various Solutes with N-Methyl-2-piperidone as Stationary Phase*. J. Chem. Eng. Data, 1998. **43**(2): p. 226-229.

26. Möllmann, C. and J. Gmehling, *Measurement of Activity Coefficients at Infinite Dilution Using Gas-Liquid Chromatography. 5. Results for N-Methylacetamide, N,N-Dimethylacetamide, N,N-Dibutylformamide, and Sulfolane as Stationary Phases*. J. Chem. Eng. Data, 1997. **42**(1): p. 35-40.
27. Letcher, T.M. and P.G. Whitehead, *The determination of activity coefficients of alkanes, alkenes, cycloalkanes, and alkynes at infinite dilution with the polar solvents dimethyl sulphoxide (DMSO), or N,N-dimethylformamide (DMF), or N-methyl-2-pyrrolidinone (NMP) using a g.l.c. technique at the temperatures 283.15 K and 298.15 K*. The Journal of Chemical Thermodynamics, 1997. **29**(11): p. 1261-1268.
28. Fischer, K. and J. Gmehling, *Vapor-liquid equilibria, activity coefficients at infinite dilution and heats of mixing for mixtures of N-methyl pyrrolidone-2 with C5 or C6 hydrocarbons and for hydrocarbon mixtures*. Fluid Phase Equilibria, 1996. **119**(1-2): p. 113-130.
29. Bastos, J.C., M.E. Soares and A.G. Medina, *Selection of solvents for extractive distillation. A data bank for activity coefficients at infinite dilution*. Ind. Eng. Chem. Proc. Des. Dev., 1985. **24**(2): p. 420-426.
30. Kister, H.Z., *Distillation design* 1992, New York: McGraw-Hill. xix, 710 p.
31. Kister, H.Z., *Distillation operations* 1990, New York: McGraw-Hill. xvii, 729 p.
32. Renon, H. and J.M. Prausnitz, *Local compositions in thermodynamic excess functions for liquid mixtures*. AIChE Journal, 1968. **14**(1): p. 135-144.
33. Klamt, A., V. Jonas, T. Bürger and J.C.W. Lohrenz, *Refinement and Parametrization of COSMO-RS*. The Journal of Physical Chemistry A, 1998. **102**(26): p. 5074-5085.
34. Schäfer, A., A. Klamt, D. Sattel, J.C.W. Lohrenz and F. Eckert, *COSMO Implementation in TURBOMOLE: Extension of an efficient quantum chemical code towards liquid systems*. Phys. Chem. Chem. Phys., 2000(2): p. 2187-2193.
35. Anantharaj, R. and T. Banerjee, *COSMO-RS-Based Screening of Ionic Liquids as Green Solvents in Denitrification Studies*. Industrial & Engineering Chemistry Research, 2010. **49**(18): p. 8705-8725.
36. Freire, M.G., L.M.N.B.F. Santos, I.M. Marrucho and J.A.P. Coutinho, *Evaluation of COSMO-RS for the prediction of LLE and VLE of alcohols + ionic liquids*. Fluid Phase Equilibria, 2007. **255**(2): p. 167-178.
37. Freire, M.G., S.P.M. Ventura, L.M.N.B.F. Santos, I.M. Marrucho and J.A.P. Coutinho, *Evaluation of COSMO-RS for the prediction of LLE and VLE of water and ionic liquids binary systems*. Fluid Phase Equilibria, 2008. **268**(1-2): p. 74-84.
38. Frank Eckert, A.K., *Fast solvent screening via quantum chemistry: COSMO-RS approach*. AIChE Journal, 2002. **48**(2): p. 369-385.
39. Mu, T., J. Rarey and J. Gmehling, *Performance of COSMO-RS with Sigma Profiles from Different Model Chemistries*. Industrial & Engineering Chemistry Research, 2007. **46**(20): p. 6612-6629.
40. Diedenhofen, M., F. Eckert and A. Klamt, *Prediction of Infinite Dilution Activity Coefficients of Organic Compounds in Ionic Liquids Using COSMO-RS*. J. Chem. Eng. Data, 2003. **48**(3): p. 475-479.
41. *Turbomole. User's manual*, 2008.
42. Eckert, F., *COSMOtherm Users Manual. Version C2.1 Release 01.082008*.

43. Weidlich, U., H.J. Roehm and J. Gmehling, *Measurement of  $\gamma^\infty$  using GLC. 2. Results for the stationary phases N-formylmorpholine and N-methylpyrrolidone*. J. Chem. Eng. Data, 1987. **32**(4): p. 450-453.
44. Schult, C.J., B.J. Neely, R.L. Robinson, K.A.M. Gasem and B.A. Todd, *Infinite-dilution activity coefficients for several solutes in hexadecane and in n-methyl-2-pyrrolidone (NMP): experimental measurements and UNIFAC predictions*. Fluid Phase Equilibria, 2001. **179**(1-2): p. 117-129.
45. Krummen, M., P. Wasserscheid and J. Gmehling, *Measurement of Activity Coefficients at Infinite Dilution in Ionic Liquids Using the Dilutor Technique*. J. Chem. Eng. Data, 2002. **47**(6): p. 1411-1417.
46. Foco, G.M., S.B. Bottini, N. Quezada, J.C. de la Fuente and C.J. Peters, *Activity Coefficients at Infinite Dilution in 1-Alkyl-3-methylimidazolium Tetrafluoroborate Ionic Liquids*. J. Chem. Eng. Data, 2006. **51**(3): p. 1088-1091.
47. Liebert, V., S. Nebig and J. Gmehling, *Experimental and predicted phase equilibria and excess properties for systems with ionic liquids*. Fluid Phase Equilibria, 2008. **268**(1-2): p. 14-20.
48. Jork, C., C. Kristen, D. Pieraccini, A. Stark, C. Chiappe, Y.A. Beste and W. Arlt, *Tailor-made ionic liquids*. The Journal of Chemical Thermodynamics, 2005. **37**(6): p. 537-558.
49. Gil, I.D., A.M. Uyazan, J.L. Aguilar, G. Rodriguez and L.A. Caicedo, *Separation of ethanol and water by extractive distillation with salt and solvent as entrainer: Process simulation*. Brazilian Journal of Chemical Engineering, 2008. **25**(1): p. 207-215.
50. Ge, Y., L. Zhang, X. Yuan, W. Geng and J. Ji, *Selection of ionic liquids as entrainers for separation of (water + ethanol)*. The Journal of Chemical Thermodynamics, 2008. **40**(8): p. 1248-1252.
51. Zhang, L., J. Han, D. Deng and J. Ji, *Selection of ionic liquids as entrainers for separation of water and 2-propanol*. Fluid Phase Equilibria, 2007. **255**(2): p. 179-185.
52. Uerdingen, M., C. Treber, M. Balsler, G. Schmitt and C. Werner, *Corrosion behaviour of ionic liquids*. Green Chemistry, 2005. **7**(5): p. 321-325.
53. Ma, J.C. and D.A. Dougherty, *The Cation- $\pi$  Interaction*. Chemical Reviews, 1997. **97**(5): p. 1303-1324.
54. Hansmeier, A., *Ionic liquids as alternative solvents for aromatics extractions*, 2010, Eindhoven University of Technology.
55. Meindersma, G.W., L.M.G. Sanchez, A.R. Hansmeier and A.B. de Haan, *Application of task-specific ionic liquids for intensified separations*. Monatshefte Fur Chemie, 2007. **138**(11): p. 1125-1136.
56. Meindersma, G.W., A. Podt, M.G. Meseguer and A.B. de Haan, *Ionic liquids as alternatives to organic solvents in liquid-liquid extraction of aromatics*. Ionic Liquids IIIB: Fundamentals, Progress, Challenges and Opportunities: Transformations and Processes, 2005. **902**: p. 57-71.
57. Meindersma, G.W., A. Podt and A.B. de Haan, *Selection of ionic liquids for the extraction of aromatic hydrocarbons from aromatic/aliphatic mixtures*. Fuel Processing Technology, 2005. **87**(1): p. 59-70.



58. Meindersma, G.W., A. Podt and A.B. de Haan, *Ternary Liquid–Liquid Equilibria for Mixtures of an Aromatic + an Aliphatic Hydrocarbon + 4-Methyl-N-butylpyridinium Tetrafluoroborate*. *Journal of Chemical & Engineering Data*, 2006. **51**(5): p. 1814-1819.
59. Kolb, B. and L.S. Ettre, *Static headspace-gas chromatography : theory and practice*. 2nd ed 2006, Hoboken, N.J.: Wiley. xxv, 349 p.
60. Meindersma, G.W., *Extraction of aromatics from naphtha with ionic liquids*. *PhD Thesis*, 2005, University of Twente: Enschede.
61. Shiflett, M.B. and A.M.S. Niehaus, *Liquid–Liquid Equilibria in Binary Mixtures Containing Substituted Benzenes with Ionic Liquid 1-Ethyl-3-methylimidazolium Bis(trifluoromethylsulfonyl)imide*. *Journal of Chemical & Engineering Data*, 2009. **55**(1): p. 346-353.
62. Berg, L. *Separation of 1-hexene from hexane by extractive distillation*. 1994. Patent US5460700.
63. Song, F., Y. Yu and J. Chen, *Separation of C6-Olefin Isomers in Reactive Extractants*. *Tsinghua Science & Technology*, 2008. **13**(5): p. 730-735.
64. Kuipers, N.J.M., A.E. Wentinkl, A.B. de Haan, J. Scholtz and H. Mulder, *Functionalized solvents for olefin isomer purification by reactive extractive distillation*. *Chemical Engineering Research & Design*, 2007. **85**(A1): p. 88-99.
65. Wooster, T.J., K.M. Johanson, K.J. Fraser, D.R. MacFarlane and J.L. Scott, *Thermal degradation of cyano containing ionic liquids*. *Green Chemistry*, 2006. **8**(8): p. 691-696.
66. Fredlake, C.P., J.M. Crosthwaite, D.G. Hert, S.N.V.K. Aki and J.F. Brennecke, *Thermophysical Properties of Imidazolium-Based Ionic Liquids*. *Journal of Chemical & Engineering Data*, 2004. **49**(4): p. 954-964.

## Appendix 2.1: Abbreviations

Table 2.1: Abbreviations for the cations and anions used in this chapter

<b>Cations</b>		<b>Anions</b>	
6C3-Gua	Hexa(propyl)-guanidinium	H <sub>2</sub> PO <sub>4</sub>	Phosphate
C3-5C1-Gua	Propyl-penta(methyl)-guanidinium	Lac	Lactate
5C1-C3-Gua	Pentamethyl-propyl-guanidinium	OAc	Acetate
3C3-S	Tripropyl-sulfonium	Cl	Chloride
4C3-Am	Tetrapropyl-ammonium	HCO <sub>2</sub>	Formate
C1-3C8-Am	Methyl-trioctyl-ammonium	MSO <sub>3</sub>	Methanesulfonate
C4-3C1-Am	Butyl-trimethyl-ammonium	DMP	Dimethylphosphate
4C3-Ph	Tetrapropyl-phosphonium	Br	Bromide
3C6-C14-Ph	Trihexyl-tetradecyl-phosphonium	PSO <sub>3</sub>	Propanesulfonate
2C1-PYR	Dimethyl-pyrrolidonium	DPP	Dipropylphosphate
2C3-PYR	Dipropyl-pyrrolidonium	PeSO <sub>3</sub>	Pentanesulfonate
C3-C1-PYR	Propyl-methyl-pyrrolidonium	Tosylate	Toluene-4-sulfonate
C6-C1-PYR	Hexyl-methyl-pyrrolidonium	DPeP	Dipentylphosphate
2C1-PIP	Dimethyl-piperidinium	I	Iodide
2C3-PIP	Dipropyl-piperidinium	MOSO <sub>3</sub>	Methylsulfate
C3-C1-PIP	Propyl-methyl-piperidinium	NO <sub>3</sub>	Nitrate
C6-C1-PIP	Hexyl-methyl-piperidinium	POSO <sub>3</sub>	Propylsulfate
C2-MIM	1-ethyl-3-methyl-imidazolium	PeOSO <sub>3</sub>	Pentylsulfate
C4-MIM	1-butyl-3-methyl-imidazolium	SCN	Thiocyanate
C6-MIM	1-hexyl-3-methyl-imidazolium	DCA	Dicyanamide
C8-MIM	1-octyl-3-methyl-imidazolium	BF <sub>4</sub>	Tetrafluoroborate
C2-23MIM	1-ethyl-2,3-dimethyl-imidazolium	CF <sub>3</sub> SO <sub>3</sub>	Trifluoromethane sulfonate
C4-23MIM	1-butyl-2,3-dimethyl-imidazolium	TCM	Tricyanomethanide
C1-PY	1-methyl-pyridinium	PF <sub>6</sub>	Hexafluorophosphate
C4-PY	1-butyl-pyridinium	TCB	Tetracyanoborate
C6-PY	1-hexyl-pyridinium	BTI	Bis((trifluoromethyl)sulfonyl)imide
C6-2MPY	1-hexyl-2-methyl-pyridinium	BPI	Bis((pentafluoroethyl)sulfonyl)imide
C6-3MPY	1-hexyl-3-methyl-pyridinium	FAP	Tris(pentafluoroethyl)trifluorophosphate
C6-4MPY	1-hexyl-4-methyl-pyridinium		
C6-23MPY	1-hexyl-2,3-dimethyl-pyridinium		
C6-24MPY	1-hexyl-2,4-dimethyl-pyridinium		
C6-34MPY	1-hexyl-3,4-dimethyl-pyridinium		
C6-35MPY	1-hexyl-3,5-dimethyl-pyridinium		
C3-Qui	Propyl-quinolinium		
C5-Qui	Pentyl-quinolinium		
C6-Qui	Hexyl-quinolinium		



### 3. Thermodynamic properties and model for the mixture methylcyclohexane (1), toluene (2) and [HMIM][TCB] (3)/[BMIM][TCB] (3)

#### *Abstract*

In this chapter, the study of the thermodynamic behavior of 1-hexyl-3-methylimidazolium tetracyanoborate [HMIM][TCB] and 1-butyl-3-methylimidazolium tetracyanoborate [BMIM][TCB] in combination with methylcyclohexane (MCH) and toluene, as representatives for non-aromatic and aromatic components, is presented. Binary and ternary liquid-liquid equilibrium data were collected at three different temperatures and at atmospheric pressure (0.1 MPa). The experimental data were well-correlated with the NRTL and UNIQUAC thermodynamic models; however, the UNIQUAC model gave better predictions than the NRTL, with a root mean square error below 0.02. The parameters obtained from the regressions of liquid-liquid equilibrium data were used to predict the vapor-liquid equilibrium (VLE). These were compared with experimental data taken by headspace technique at three different temperatures and solvent to feed ratios. The UNIQUAC model and its parameters are able to predict the VLE of the ternary systems with a maximum error of 0.2. The non-aromatic/aromatic selectivities and relative volatilities of the ionic liquids make them suitable solvents to be used in extractive distillation processes.

#### 3.1 Introduction

The separation of aromatics from non-aromatic components is one of the most important separation processes in the chemical industry. The recovery of aromatics can be done by several solvent-based technologies, e.g. azeotropic distillation, liquid-liquid extraction and extractive distillation. However, depending on the aromatic composition, extractive distillation has several advantages over the other technologies: it is operated like a conventional distillation process, uses two key variables such as polarity and boiling point differences, it does not require additional steps to purify products [1]. This process utilizes polar solvents e.g. Sulfolane, N-methyl-2-pyrrolidone (NMP) and N-formylmorpholine (NFM) [2]. NMP is one of the most used conventional separating agents. It has several advantages over other solvents: nontoxic, relatively easy recovery and totally soluble in both aromatic and non-aromatic compounds [3]. Methylcyclohexane and toluene have been chosen as representatives for the non-aromatic and aromatic components, respectively.

In the last years, ionic liquids (ILs) have attracted the attention of the scientific community and have been investigated as separating agents in several industrial processes. They are organic salts which are liquid at low temperature (<100 °C) and consist of large organic cations and organic or inorganic anions. Therefore, it is possible to design an IL for a particular application by combining the ions to obtain the desired melting point, viscosity, density, hydrophobicity, miscibility, etc. This is the reason why the ILs are also referred as “designer solvents”. This interest is directly related to the unique properties of the ILs,

such as negligible vapor pressure, thermal and chemical stability, capabilities to be used as replacements of conventional solvents, wide liquidus range and less corrosive than conventional salts with high boiling points. ILs are being studied for several years; however, the information about their properties is still scarce. Experimental phase equilibrium data are required to develop thermodynamic models which can describe the systems containing these components.

Wilson, NRTL (Non Random Two Liquid), UNIQUAC and UNIFAC equations have been used for the correlation of systems involving ILs in several studies [4-6]. Even some equations of state have been adapted to predict the thermodynamic behavior of the ILs and their mixtures with organic components [7-9]. However, NRTL and UNIQUAC give the best description of activity coefficients, being the most commonly used models [9]. Although these models have been theoretically developed for non-electrolyte systems, it usually leads to good correlations for systems containing ILs [2].

In this chapter, the feasibility of implementing ILs in extractive distillation (ED) processes is studied. The ILs 1-hexyl-3-methylimidazolium tetracyanoborate [HMIM][TCB] and 1-butyl-3-methylimidazolium tetracyanoborate [BMIM][TCB] are studied and ternary phase equilibrium data with the mixture methylcyclohexane (MCH) and toluene are reported. NRTL and UNIQUAC models are analyzed and a comparison of both thermodynamic models is carried out.

## 3.2 Theory

There are several thermodynamic models to describe phase equilibrium, some of them are empirical, e.g. Margules and van Laar models, and others are based on local composition theory, e.g. Wilson, NRTL models. The UNIQUAC model is also derived from local composition theory but has a more theoretical background. There are also models which use the group contribution concept (e.g. UNIFAC and ASOG). However, the NRTL and UNIQUAC models have been applied to (partial) immiscible systems. The equations of the NRTL model for the computation of activity coefficients in multicomponent systems are:

$$\ln(\gamma_i) = \frac{\sum_j x_j \tau_{ji} G_{ji}}{\sum_k x_k G_{ki}} + \sum_j \frac{x_j G_{ij}}{\sum_k x_k G_{kj}} \left( \tau_{ij} - \frac{\sum_m x_m \tau_{mj} G_{mj}}{\sum_k x_k G_{kj}} \right) \quad 3.1$$

where:

$$\begin{aligned} G_{ij} &= \exp(-\alpha_{ij} \tau_{ij}) \\ \tau_{ij} &= a_{ij} + b_{ij}/T \\ \tau_{ii} &= 0; \quad G_{ii} = 1 \end{aligned} \quad 3.2$$

As can be seen in equations 3.1 and 3.2, the model consists of three parameters; however,  $a_{ij}$  and  $b_{ij}$  are unsymmetrical, i.e.  $ij \neq ji$ .  $\alpha_{ij}$  is user-defined (commonly fixed) and it can

be chosen according to the polarity, immiscibility and characteristics of the components and system [10]. In this work, a value of 0.2 was set in all the regressions for the systems which were forming two liquid phases. Then, for each binary system there are four parameters in total to be regressed.

The equations of the UNIQUAC model for the computation of activity coefficients in multicomponent systems are [11]:

$$\begin{aligned} \ln(\gamma_i) = & \ln \frac{\Phi_i}{x_i} + \frac{z}{2} q_i \ln \frac{\theta_i}{\Phi_i} + l_i - \frac{\Phi_i}{x_i} \sum_j x_j l_j \\ & - q_i \ln \left( \sum_j \theta_j \tau_{ji} \right) + q_i \\ & - q_i \sum_j \frac{\theta_j \tau_{ij}}{\sum_k \theta_k \tau_{kj}} \end{aligned} \quad 3.3$$

where

$$\begin{aligned} \Phi_i &= \frac{r_i x_i}{\sum_k r_k x_k} \quad ; \quad \theta_i = \frac{q_i x_i}{\sum_k q_k x_k} \\ l_i &= \frac{z}{2} (r_i - q_i) + 1 - r_i; \quad z = 10 \\ \tau_{ij} &= \exp \left( a_{ij} + \frac{b_{ij}}{T} \right) \end{aligned} \quad 3.4$$

As can be seen in equations 3.3 and 3.4, the UNIQUAC model consists of two pure-component molecular structure constants ( $r_i$  and  $q_i$ , which represent the van der Waals volume and surface area parameter, respectively) and two binary parameters ( $a_{ij}$  and  $b_{ij}$ ); however, they are unsymmetrical. Then, for each binary system there are four parameters in total to be regressed and two constants to be specified.

### 3.3 Experimental section

#### 3.3.1 Materials

The ILs 1-hexyl-3-methylimidazolium tetracyanoborate [HMIM][TCB] (for synthesis) and 1-butyl-3-methylimidazolium tetracyanoborate [BMIM][TCB] (for synthesis) were purchased from Merck. In the following, mass fraction purity is given. Toluene (>0.999) and acetone (>0.99) were purchased from Sigma-Aldrich. Methylcyclohexane MCH (>0.98) and ethylbenzene (>0.99), which was used as the internal standard in the gas chromatography analysis, were purchased from Fluka. After every experiment, the ILs were purified under vacuum (<1.0 kPa) at  $T = 333$  K for minimum 5 h in a rotary evaporator (Büchi Rotavapor R-200 equipped with a Büchi heating bath B-490).

### 3.3.2 Experimental methods and procedure

#### 3.3.2.1 Liquid-liquid equilibrium

Liquid-liquid extraction experiments were carried out in jacketed vessels with a volume of approximately 70 cm<sup>3</sup>. The experimental procedure mentioned in the work of G.W. Meindersma et al. [2, 12, 13] was followed. The top of the vessel was closed using a PVC cover, through which a stirrer shaft was passed. Two stainless steel propellers equipped with an electronic stirrer control were used. The vessels were jacketed to circulate water from a water bath in order to maintain a constant temperature inside the vessels. The extraction temperature was changed from 293.15 to 333.15 K. For each experiment, maximum 50 cm<sup>3</sup> of mixture (IL + organics) was placed into the vessels and they were closed. When the desired temperature was reached, the mixture was stirred for 1 h (Meindersma et al. [2, 12, 13] established that the equilibration time for extractions with ILs takes approximately 10 min). Samples (0.1 cm<sup>3</sup>) from both phases were taken after a 30 min of settling down. The experiments were carried out in duplicate in order to exclude experimental errors.

Ethylbenzene (0.1 cm<sup>3</sup>) was added to the samples as the internal standard for the gas chromatography (GC) analysis, and 1 cm<sup>3</sup> of acetone was added to completely solubilize the sample and avoid possible phase splitting. The concentration of every sample was obtained with a Varian CP-3800 gas chromatograph using a capillary column (CP-SIL5CB, 50 m x 0.32 mm x 0.45 mm). The IL was collected in a cup-liner and a precolumn in order to do not disrupt the analysis. The IL was determined by mass balance of the measured mole fractions of the hydrocarbons. GC analyses were carried out in triplicate in order to be able to exclude possible errors in the analytical equipment. For all the measurements, the uncertainty for the temperature measurements is estimated at  $\pm 0.05$  K and for the tie-line measurements is estimated within  $\pm 0.001$  in mole fraction.

#### 3.3.2.2 Vapor-liquid equilibrium

For measuring the relative volatilities and vapor-liquid equilibrium of the organic components when the ILs were added, the Headspace gas chromatography (HSGC) was used. A more detailed description of the procedure and experimental method is presented in section 2.6.2.2.1. For all the measurements, the uncertainty for the vapor composition is estimated at  $\pm 0.005$  and for the temperature measurements is estimated at  $\pm 0.05$  K.

## 3.4 Results and discussion

### 3.4.1 Binary and ternary liquid-liquid experiments

The experimental liquid-liquid equilibrium data measured at T/K = (293.15, 313.15 and 333.15) at atmospheric pressure for the binary systems methylcyclohexane + IL and toluene + IL are listed in Table 3.1.

Table 3.1: Binary liquid-liquid equilibrium molar compositions of organic components and ionic liquids

T (K)	Methylcyclohexane extraction		Toluene extraction	
	[HMIM][TCB]	[BMIM][TCB]	[HMIM][TCB]	[BMIM][TCB]
	$x_{MCH}^{II}$	$x_{MCH}^{II}$	$x_{Tol}^{II}$	$x_{Tol}^{II}$
293.15	0.1239	0.0884	0.7663	0.7341
313.15	0.1288	0.0814	0.7756	0.7235
333.15	0.1392	0.0973	0.7799	0.7042

The ternary systems methylcyclohexane + toluene + ILs are listed in Table 3.7 in the appendix section. In these tables, the superscripts *I* and *II* refer to organic-rich and IL-rich phase, respectively. For numerical and analytical reasons it was assumed that the solubility of ILs in the organic phase was very low, as in the work carried out by G. W. Meindersma [2, 12, 13]. For binary extractions, Shiflett and Niehaus [14] reported values of 0% of IL in the organic phase for several substituted benzenes components. In this work, the molar compositions of the ionic liquids in the organic phase were set to  $10^{-4}$ .

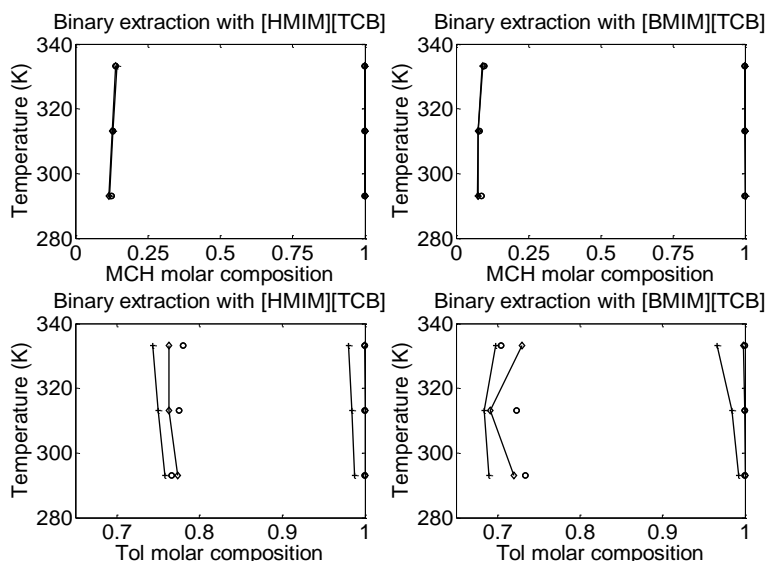


Figure 3.1: Binary liquid-liquid equilibrium for the systems methylcyclohexane and toluene with ILs. (o) Experimental results, (+) calculated values with NRTL model, (◊) calculated values with UNIQUAC model.

Figure 3.1 shows the liquid-liquid equilibrium results (T-x-x diagrams) for the binary mixtures methylcyclohexane and toluene with the ILs. Regressed data in the following figures are explained in section 3.4.3. As can be seen in Figure 3.1, the solubility of toluene in the ILs is higher than the methylcyclohexane (MCH). The polarity of the organic compounds plays an important role in determining the solubility in the solvent. It is known that toluene is a more polar compound than MCH due to its double bonds, and the ILs, being also polar components, have higher affinity to the toluene (this is known as the rule of “like dissolves like”). Comparing the experimental results of both ILs in the binary extractions, it can be seen that both organic components are more soluble in



[HMIM][TCB] than [BMIM][TCB]. The temperature does not have a remarkable influence in the solubility of the organic components. This behavior is commonly reported for immiscible systems containing ILs [14].

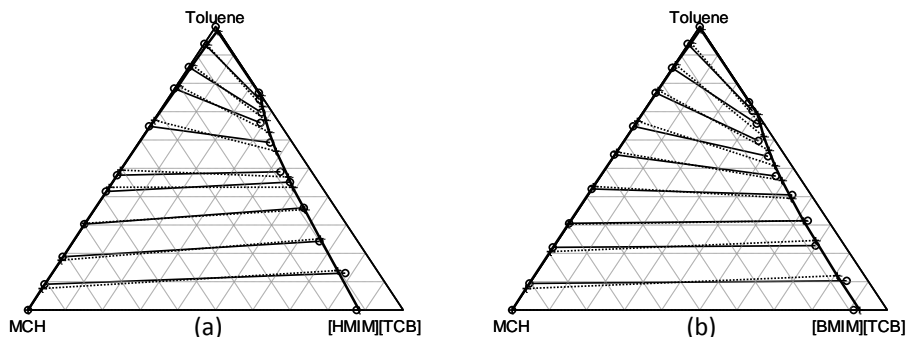


Figure 3.2: Ternary liquid-liquid equilibrium for the systems containing (a) [HMIM][TCB] and (b) [BMIM][TCB] at 293.15K. (o) Experimental results, (+) calculated values with NRTL model.

Figure 3.2 and 3.3 show the liquid-liquid equilibrium results (T-x-x diagrams) for the ternary mixtures MCH, toluene and the ILs. Similar figures were obtained for  $T/K = (313.15 \text{ and } 333.15)$ , but they are not shown in this work. The experimental data is reported in Table 3.7 of the appendix of this chapter. As can be seen in these figures, both ILs have partial miscibility with the organic components, however, the miscible area for [HMIM][TCB] is higher than for [BMIM][TCB], i.e. the former IL has better solubility with the compounds. A deeper analysis of the experimental and correlated data is performed in section 3.4.3.1.

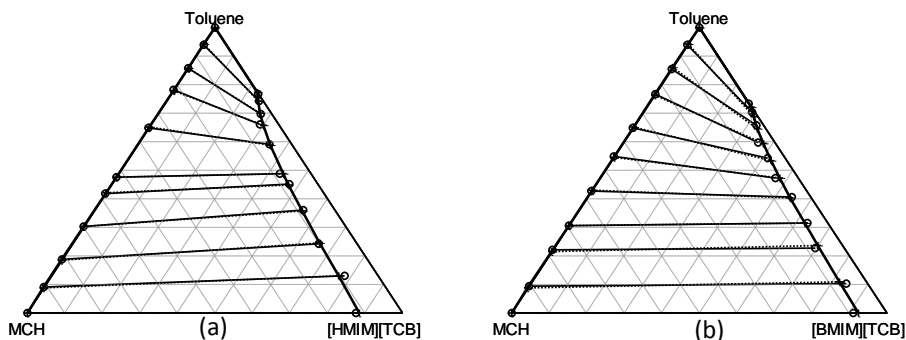


Figure 3.3: Ternary liquid-liquid equilibrium for the systems containing (a) [HMIM][TCB] and (b) [BMIM][TCB] at 293.15K. (o) Experimental results, (+) calculated values with UNIQUAC model.

Figure 3.4 shows the selectivity of both ILs and their change with the MCH molar composition in the organic-rich liquid phase (expressed as solvent-free basis). The selectivities of the ILs were determined from equation 3.5.

$$S = \frac{x_{MCH}^I / x_{MCH}^{II}}{x_{Tol}^I / x_{Tol}^{II}}$$

3.5

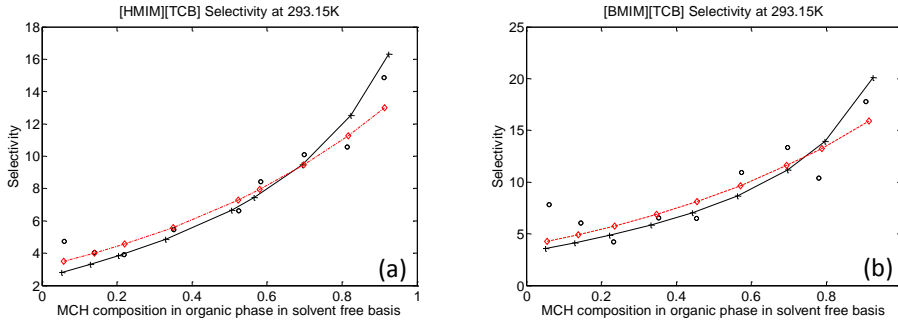


Figure 3.4: Selectivities of the ILs for methylcyclohexane. (a) [HMIM][TCB] and (b) [BMIM][TCB]. (o) Experimental results, (+) calculated values with NRTL model, (o) calculated values with UNIQUAC model.

It can be seen in Figure 3.4 that the selectivity increases with increasing the MCH composition. This figure also shows that the selectivity of [BMIM][TCB] is around 20% higher than the selectivity of [HMIM][TCB]; however, it should be noted that its solubility is lower. This is a common property of the solvents used in extraction processes, the higher the selectivity the lower the solubility [15].

### 3.4.2 Vapor-liquid equilibrium experiments

The experimental vapor-liquid equilibrium data were measured at  $T/K = (303.15, 313.15$  and  $323.15)$  for the ternary systems MCH + toluene + [HMIM][TCB] or [BMIM][TCB] and the relative volatilities are reported in Figure 3.5(a) and (b), respectively. Three different solvent to feed mass ratios were used for both ILs. Because of the non-volatility of these compounds, they are not detected by the headspace technique. Predicted data, represented by lines in Figure 3.5, are explained in section 3.4.3.

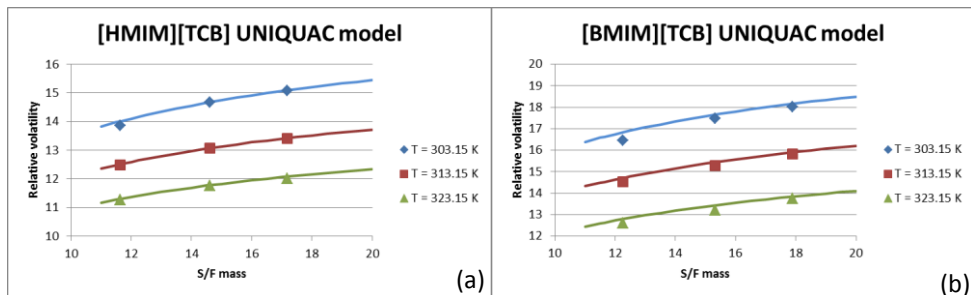


Figure 3.5: Vapor-liquid equilibrium for the mixture (a) MCH (1) + Toluene (2) + [HMIM][TCB] (3) and (b) MCH (1) + Toluene (2) + [BMIM][TCB] (3) at  $T/K = 303.15, 313.15$  and  $323.15$ . The lines represent UNIQUAC predictions

In Figure 3.5 it can be seen that the relative volatility increases with the solvent to feed mass ratio; however, it decreases with the temperature. As it was explained above, the ILs

(polar components) have stronger interactions with the most polar compound in the mixture (toluene), making the MCH more volatile. Contrary to the liquid-liquid equilibrium results, the temperature dependence of the vapor-liquid equilibrium is higher than the liquid-liquid equilibrium. More toluene appears in vapor phase, resulting in a decrease in the relative volatility of the mixture; however, its value is high enough to make these solvents suitable for the extractive distillation process. It should be mentioned that the solvent to feed mass ratios used were higher than 10 to avoid formation of two liquid phases during the experiments.

From Figure 3.5 it can be concluded that the relative volatilities of the IL [BMIM][TCB] are higher than [HMIM][TCB]. This is explained by the length of the alkyl chain attached to the imidazolium cation, as mentioned in Chapter 2. From the experimental results, it can be concluded that both ILs are suitable solvents for the extractive distillation of MCH and toluene.

### 3.4.3 Comparison of experimental and correlated data

#### 3.4.3.1 Liquid-liquid equilibrium

For the correlation of the experimental data, the NRTL and UNIQUAC models were used. To obtain reliable results for the whole composition range and the temperature range, the binary and ternary sets were included in the regression. In order to consider temperature dependency in both models, linear temperature-dependent binary interaction parameters ( $\tau_{ij}$ ) were taken into account.

The parameters for the NRTL and UNIQUAC models were obtained using *Aspen Plus V7.2*. In the regressions, the ILs were treated as a non-dissociating component. Since the ILs have no vapor pressure and their concentrations in the organic phase is close to zero, the parameter regression is not asked to fulfill the equation for the equality of the fugacity for the ILs, just as in the parameter regression reported by Meindersma [13]. The binary parameters for MCH and toluene were taken from *Aspen Plus*. As mentioned before, a value of 0.2 was chosen for the NRTL parameter  $\alpha_{ij}$ . The required van der Waals parameters  $r_i$  and  $q_i$  of the UNIQUAC model for the ILs were estimated with the correlation proposed by Domanska [16, 17].

$$r_i = 0.029281V_i \quad 3.6$$

$$q_i = \frac{(z-2)r_i}{z} + \frac{2}{z}$$

Where  $V_i$  is the molar volume in  $cm^3mol^{-1}$  of the IL at  $T/K = 298.15$  and  $z$  is the coordination number assumed to be equal to 10. The properties are listed in Table 3.2.

Table 3.2: Properties of the ILs

	[HMIM][TCB]	[BMIM][TCB]
MW	282.2	254.1
$V_j$ ( $cm^3/mol$ )	278.7	244.7

In Table 3.2, molar volumes of both ILs were predicted with software package *COSMOtherm* (version C2.1 release 01.11a). The van der Waals volume and surface area parameters are listed in **Error! Not a valid bookmark self-reference..** The values for the organic components were estimated using the Bondi method [11].

Table 3.3: van der Waals volume and surface parameters for UNIQUAC model

	MCH	Toluene	[HMIM][TCB]	[BMIM][TCB]
$r_i$	4.7200	3.9228	8.1611	7.1645
$q_i$	3.7760	2.9680	6.7289	5.9316

It should be noted that the values of  $r_i$  and  $q_i$  predicted for the ILs in this work are in accordance with the values reported for other ILs [17-19]. The NRTL and UNIQUAC parameters obtained after the regression of the experimental data are listed in Table 3.4.

Table 3.4: NRTL and UNIQUAC interaction parameters

	MCH (i) Toluene (j)		MCH (i) HMIMTCB (j)		MCH (i) BMIMTCB (j)		Toluene (i) HMIMTCB (j)		Toluene (i) BMIMTCB (j)	
	NRTL	UNIQUAC	NRTL	UNIQUAC	NRTL	UNIQUAC	NRTL	UNIQUAC	NRTL	UNIQUAC
	$a_{ii}$	0	0	11.296	-3.58	-29.428	6.97	1.3551	2.567	-6.323
$a_{ji}$	0	0	-0.5689	0.829	-4.952	-0.865	-0.1575	0.240	1.564	-0.728
$b_{ij}$	-43.24	-25.30	-1245.91	378.55	11675.6	-2804.83	1674.28	-1733.29	3928.6	-3515.55
$b_{ji}$	134.06	-2.31	373.86	-166.26	1936.43	310.42	-670.01	220.37	-1089.33	488.98
$\alpha_{ij}$	0.3	0	0.2	0	0.2	0	0.2	0	0.2	0

As can be seen in the results depicted in the figures, the experimental liquid-liquid equilibrium data are well correlated with both thermodynamic models. In Figure 3.1, the binary equilibrium between MCH and the ILs is well correlated by the parameters; however, in the toluene case, there are high deviations, even the calculated temperature dependence with NRTL model is opposite to the one obtained in the experiments. This can be due to the fact that during the regression of the parameters, the ternary data were considered as more important than the binary data (the weight of the ternary data was set twice as big as the binary data).

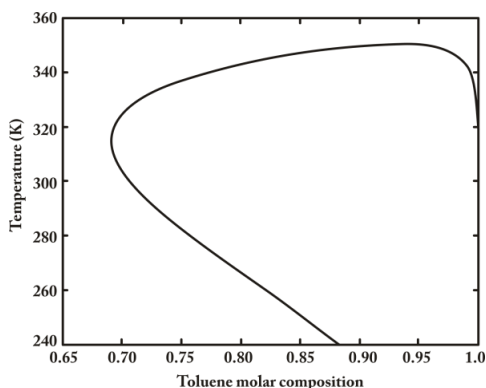


Figure 3.6: Liquid-liquid phase diagram for toluene and [BMIM][TCB] predicted with UNIQUAC

The curvature in the calculated values for the binary equilibrium between toluene and [BMIM][TCB] shown in Figure 3.1 is caused by the parameters obtained for the thermodynamic models. In Figure 3.6, the liquid-liquid phase diagram for the binary system toluene + [BMIM][TCB] calculated with UNIQUAC model is shown. The model shows a binodal curve that defines an “island” [10, 20] with a clear *upper critical solution temperature* (350.2 K). The experimental data does not show such a trend, which drives us to the conclusion that the NRTL/UNIQUAC binary parameters obtained with ternary data for the system toluene + IL should be used with caution in order to avoid miscalculations for the binary system.

The NRTL model is able to represent the ternary equilibrium envelope with reasonable accuracy as can be seen in Figure 3.2; however, UNIQUAC model (Figure 3.3) is more accurate. The experimental and correlated tie lines in the ternary diagrams are very close to each other, especially for UNIQUAC model where they overlap (Figure 3.3). Similar figures were obtained at T/K = (313.15 and 333.15) which shows the ability of the models to represent the temperature dependence of the equilibrium. In Figure 3.4, the experimental and correlated selectivities are shown. It can be seen that the parameters are able to represent the increase of the selectivity with increasing the MCH composition in the organic-rich liquid phase.

The goodness of fit was determined with the root mean square error (*RMS*) which is defined as:

$$RMS = \sqrt{\frac{1}{NE} \sum_k \sum_i \sum_p (x_{i,k}^{p,exp} - x_{i,k}^{p,pred})^2} \quad 3.7$$

where *k* and *NE* refers to the number of the experiment and total number of experiments, respectively, *x* to molar composition of the component *i* and *p* to the liquid phase. The values of *RMS* for the ILs and different models are presented in Table 3.5. As can be inferred from these values, the goodness of fit of the correlation is very satisfactory for both models; however, UNIQUAC is able to correlate in a more accurate way the liquid-liquid equilibrium for both ILs. It also can be seen in Table 3.5 that both models presented better correlation for the ionic liquid [HMIM][TCB].

Table 3.5: Goodness of fit for the models (liquid-liquid equilibrium)

	<i>RMS</i>	
	NRTL	UNIQUAC
[HMIM][TCB]	0.0383	0.0116
[BMIM][TCB]	0.0460	0.0221

### 3.4.3.2 Vapor-liquid equilibrium

In Figure 3.5, the relative volatilities for both ILs are shown (points) together with the predicted values using the UNIQUAC model (lines) utilizing the parameters regressed from liquid-liquid equilibrium data (Table 3.4).

It can be seen in Figure 3.5 that the UNIQUAC model and its regressed parameters are able to predict vapor-liquid equilibrium behavior for both ILs.

Table 3.6: Goodness of prediction of the models for VLE data

	RMS for VLE predictions	
	NRTL	UNIQUAC
[HMIM][TCB]	6.43	0.0557
[BMIM][TCB]	6.23	0.2047

$$RMS = \sqrt{\frac{1}{NE} \sum_k^{NE} (\alpha_k^{exp} - \alpha_k^{pred})^2} \quad 3.8$$

The deviations of the predicted relative volatilities and the experimental values were calculated with equation 3.8 and are shown in Table 3.6. It can be seen that UNIQUAC model is able to predict vapor-liquid equilibrium with a maximum deviation of 0.2. Meanwhile, the NRTL model and its parameters exhibited a higher deviation, reaching values as high as 6.4. In Figure 3.7 it can be seen the deviations between the experimental VLE data and the predictions with the NRTL model and parameters.

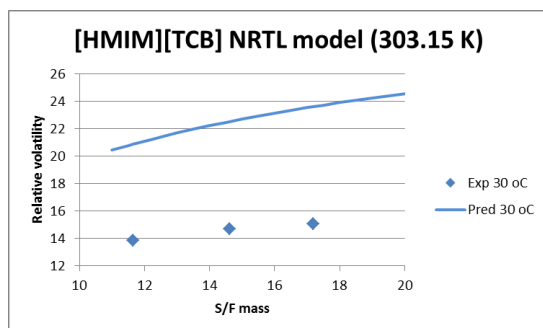


Figure 3.7: Vapor-liquid equilibrium for the mixture MCH (1) + Toluene (2) + [HMIM][TCB] at 303.15 K and prediction with NRTL model

### 3.5 Conclusions

Binary and ternary liquid-liquid experimental data for the systems MCH + toluene + [HMIM][TCB] and [BMIM][TCB] were collected at three different temperatures, T/K = (293.15, 313.15 and 333.15). Although, the binary regressions were not very satisfactory, the NRTL and UNIQUAC parameters obtained in this work can be used to calculate the liquid-liquid phase splitting for ternary systems. All the liquid-liquid experimental data were well correlated by the thermodynamic models with a maximum *RMS* value of 0.0460. However, the NRTL model (using the parameters obtained from LLE data) is not able to predict the vapor-liquid equilibrium. UNIQUAC model gives a better predictions having a maximum *RMS* of 0.2 for the system containing [BMIM][TCB]. The calculated selectivities and relative volatilities using UNIQUAC model and its parameters are in good agreement with the experimental values. This thermodynamic model and the parameters reported in this work are used in the process design which is shown and analyzed in

Chapter 5. The ILs studied have a high selectivity and can be interesting for extractive distillation and their thermodynamic behavior can be represented with the UNIQUAC model and the parameters obtained in this work.

### 3.6 References

1. Lee, F.M. and J.C. Gentry, *Don't Overlook Extractive Distillation*. Chemical Engineering Progress, 1997. **93**(10): p. 56-64.
2. Meindersma, G.W., A. Podt and A.B. de Haan, *Selection of ionic liquids for the extraction of aromatic hydrocarbons from aromatic/aliphatic mixtures*. Fuel Processing Technology, 2005. **87**(1): p. 59-70.
3. Chen, B., Z. Lei and J. Li, *Separation on Aromatics and Non-aromatics by extractive distillation with NMP*. Journal of Chemical Engineering of Japan, 2003. **36**(1): p. 20-24.
4. Simoni, L.D., L.E. Ficke, C.A. Lambert, M.A. Stadtherr and J.F. Brennecke, *Measurement and Prediction of Vapor-Liquid Equilibrium of Aqueous 1-Ethyl-3-methylimidazolium-Based Ionic Liquid Systems*. Industrial & Engineering Chemistry Research, 2010. **49**(8): p. 3893-3901.
5. Deenadayalu, N., S.H. Thango, T.M. Letcher and D. Ramjugernath, *Measurement of activity coefficients at infinite dilution using polar and non-polar solutes in the ionic liquid 1-methyl-3-octyl-imidazolium diethyleneglycolmonomethylethersulfate at T = (288.15, 298.15, and 313.15) K*. The Journal of Chemical Thermodynamics, 2006. **38**(5): p. 542-546.
6. Domanska, U. and A. Marciniak, *Measurements of activity coefficients at infinite dilution of aromatic and aliphatic hydrocarbons, alcohols, and water in the new ionic liquid [EMIM][SCN] using GLC*. The Journal of Chemical Thermodynamics, 2008. **40**(5): p. 860-866.
7. Li, J., Q. He, C. He, C. Peng and H. Liu, *Representation of Phase Behavior of Ionic Liquids Using the Equation of State for Square-well Chain Fluids with Variable Range*. Chinese Journal of Chemical Engineering, 2009. **17**(6): p. 983-989.
8. Tsiptsias, C., I. Tsvintzelis and C. Panayiotou, *Equation-of-state modeling of mixtures with ionic liquids*. Physical Chemistry Chemical Physics, 2010. **12**(18): p. 4843-4851.
9. Döker, M. and J. Gmehling, *Measurement and prediction of vapor-liquid equilibria of ternary systems containing ionic liquids*. Fluid Phase Equilibria, 2005. **227**(2): p. 255-266.
10. Sandler, S.I., *Chemical, biochemical, and engineering thermodynamics*. 4th ed2006, Hoboken, N.J.: John Wiley. xiv, 945 p.
11. Poling, B.E., J.M. Prausnitz and J.P. O'Connell, *The properties of gases and liquids*. 5th ed2001, New York: McGraw-Hill. 1 v. (various pagings).
12. Meindersma, G.W., L.M.G. Sanchez, A.R. Hansmeier and A.B. de Haan, *Application of task-specific ionic liquids for intensified separations*. Monatshefte Fur Chemie, 2007. **138**(11): p. 1125-1136.
13. Meindersma, G.W., A. Podt and A.B. de Haan, *Ternary Liquid-Liquid Equilibria for Mixtures of an Aromatic + an Aliphatic Hydrocarbon + 4-Methyl-N-*

- butylpyridinium Tetrafluoroborate*. Journal of Chemical & Engineering Data, 2006. **51**(5): p. 1814-1819.
14. Shiflett, M.B. and A.M.S. Niehaus, *Liquid-Liquid Equilibria in Binary Mixtures Containing Substituted Benzenes with Ionic Liquid 1-Ethyl-3-methylimidazolium Bis(trifluoromethylsulfonyl)imide*. Journal of Chemical & Engineering Data, 2009. **55**(1): p. 346-353.
  15. Jork, C., C. Kristen, D. Pieraccini, A. Stark, C. Chiappe, Y.A. Beste and W. Arlt, *Tailor-made ionic liquids*. The Journal of Chemical Thermodynamics, 2005. **37**(6): p. 537-558.
  16. Domanska, U., *Solubility of n-alkanols (C16,C18,C20) in binary solvent mixtures*. Fluid Phase Equilibria, 1989. **46**(2-3): p. 223-248.
  17. Gutierrez, J.P., W. Meindersma and A.B. de Haan, *Binary and ternary (liquid-liquid) equilibrium for {methylcyclohexane (1)+toluene (2)+1-hexyl-3-methylimidazolium tetracyanoborate (3)/1-butyl-3-methylimidazolium tetracyanoborate (3)}*. The Journal of Chemical Thermodynamics, 2011. **43**(11): p. 1672-1677.
  18. Lei, Z., J. Zhang, Q. Li and B. Chen, *UNIFAC Model for Ionic Liquids*. Industrial & Engineering Chemistry Research, 2009. **48**(5): p. 2697-2704.
  19. Kato, R., M. Krummen and J. Gmehling, *Measurement and correlation of vapor-liquid equilibria and excess enthalpies of binary systems containing ionic liquids and hydrocarbons*. Fluid Phase Equilibria, 2004. **224**(1): p. 47-54.
  20. Smith, J.M., H.C. Van Ness and M.M. Abbott, *Introduction to chemical engineering thermodynamics*. 7th ed. McGraw-Hill chemical engineering series 2005, Boston: McGraw-Hill. xviii, 817 p.





## Appendix 3.1: Experimental data for the ternary LLE

Table 3.7: Experimental molar compositions and selectivities for the ternary liquid-liquid equilibrium for [HMIM][TCB] and [BMIM][TCB].

IL used: [HMIM][TCB]					IL used: [BMIM][TCB]				
$x_{MCH}^I$	$x_{Tol}^I$	$x_{MCH}^{II}$	$x_{Tol}^{II}$	$S$	$x_{MCH}^I$	$x_{Tol}^I$	$x_{MCH}^{II}$	$x_{Tol}^{II}$	$S$
<b>T/K = 293.15</b>					<b>T/K = 293.15</b>				
0.9118	0.0882	0.0894	0.1284	14.86	0.9058	0.0942	0.0553	0.1021	17.76
0.8142	0.1857	0.1007	0.2426	10.56	0.7790	0.2210	0.0772	0.2272	10.38
0.6988	0.3012	0.0828	0.3601	10.09	0.6958	0.3042	0.0539	0.3147	13.36
0.5835	0.4165	0.0752	0.4513	8.41	0.5738	0.4262	0.0500	0.4052	10.91
0.5252	0.4748	0.0816	0.4884	6.62	0.4529	0.5470	0.0603	0.4719	6.48
0.3517	0.6482	0.0589	0.5913	5.45	0.3524	0.6476	0.0451	0.5420	6.54
0.2190	0.7810	0.0473	0.6613	3.92	0.2329	0.7670	0.0429	0.5977	4.23
0.1403	0.8597	0.0282	0.6986	4.04	0.1451	0.8549	0.0184	0.6568	6.06
0.0595	0.9405	0.0099	0.7417	4.74	0.0607	0.9393	0.0058	0.7040	7.84
<b>T/K = 313.15</b>					<b>T/K = 313.15</b>				
0.9085	0.0915	0.1071	0.1189	11.03	0.9018	0.0982	0.0699	0.0972	12.78
0.8078	0.1922	0.1136	0.2246	8.31	0.7563	0.2437	0.0856	0.2120	7.69
0.6911	0.3088	0.0916	0.3422	8.36	0.6859	0.3141	0.0593	0.2952	10.87
0.5716	0.4283	0.0840	0.4337	6.89	0.5644	0.4356	0.0552	0.3865	9.07
0.5141	0.4859	0.0876	0.4699	5.68	0.4384	0.5616	0.0643	0.4529	5.50
0.3448	0.6552	0.0639	0.5755	4.74	0.3453	0.6547	0.0417	0.5271	6.67
0.2093	0.7907	0.0495	0.6486	3.47	0.2261	0.7739	0.0440	0.5804	3.85
0.1392	0.8607	0.0296	0.6890	3.76	0.1431	0.8569	0.0195	0.6409	5.49
0.0596	0.9403	0.0105	0.7341	4.43	0.0652	0.9348	0.0057	0.6864	8.39
<b>T/K = 333.15</b>					<b>T/K = 333.15</b>				
0.9036	0.0964	0.1184	0.1105	8.75	0.8976	0.1024	0.0787	0.0921	10.26
0.7906	0.2093	0.1192	0.2110	6.69	0.7501	0.2499	0.0882	0.2035	6.93
0.6835	0.3165	0.1005	0.3259	7.00	0.6788	0.3212	0.0672	0.2834	8.91
0.5610	0.4389	0.0878	0.4178	6.08	0.5560	0.4440	0.0622	0.3688	7.43
0.5054	0.4946	0.0909	0.4489	5.05	0.4302	0.5698	0.0678	0.4367	4.86
0.3334	0.6666	0.0661	0.5693	4.31	0.3333	0.6667	0.0579	0.5085	4.39
0.2026	0.7973	0.0497	0.6354	3.25	0.2220	0.7780	0.0459	0.5690	3.54
0.1389	0.8611	0.0308	0.6789	3.55	0.1437	0.8563	0.0334	0.6193	3.11
0.0668	0.9332	0.0107	0.7236	4.84	0.0654	0.9346	0.0252	0.6656	1.85



## 4. Vapor-liquid equilibrium for the system ethanol (1) + water (2) + ionic liquids (3)

### Abstract

The present chapter focuses on parameter determination to describe the vapor-liquid equilibrium (VLE) of the ternary mixtures ethanol(1) + water(2) + [EMIM][OAc](3) and [EMIM][DCA](3). Ternary VLE data were collected at 0.1 MPa and multiple liquid compositions by varying the ionic liquid (IL) content. The NRTL and UNIQUAC parameters are regressed and analyzed in this chapter for both ILs. The experimental data were well correlated by both thermodynamic models; however NRTL represents more accurate the experimental data, with a value for the root mean square error below 0.02. The increase in the relative volatility achieved by the ILs makes them suitable solvents for the separation of ethanol/water mixture by extractive distillation.

### 4.1 Introduction

Ethanol is an important base chemical which is produced from petrochemical streams or bioprocesses. It has been used as solvent, in cosmetic and food industry, among others. However, ethanol as a (partial) replacement of gasoline has influenced its worldwide demand. Just in USA,  $42 \times 10^6 \text{ m}^3$  ( $33 \times 10^6$  tons) of ethanol were added to gasoline in 2009 accounting for about 8% of gasoline consumption by volume [1, 2]. Water is involved in the ethanol production chain. This mixture forms an azeotrope with an ethanol mass composition of 0.956 and its challenging energy-efficient separation has been widely reported [3]. The separation of ethanol and water can be done by several technologies, e.g. azeotropic distillation, extractive distillation, extractive fermentation, adsorption, membrane separations [3], among others. Extractive distillation has several advantages over other technologies: it is operated like conventional distillation process, uses two key variables such as polarity and boiling point differences, it does not require additional steps to purify products [4]. This process makes use of polar solvents such as ethylene glycol (EG) [3, 5]. The solvent should interact with the mixture and make the separation easier. The easiness of separation is measured by the relative volatility (equation 4.1), the higher the relative volatility the better the solvent.

$$\alpha_{12} = \frac{y_1/x_1}{y_2/x_2} \quad 4.1$$

Ionic liquids (ILs) are a new class of components with high potential to replace existing solvents in extractive distillation and achieve energy/capital savings >20 % [6]. They are organic salts which are liquid at low temperature (< 100 °C) and consist of large organic cations and organic or inorganic anions. Therefore, it is possible to design an IL for a particular application by combining the ions to obtain the desired melting point, viscosity, density, hydrophobicity, miscibility, etc. This is the reason why the ILs are also referred as “designer solvents”. Their unique properties, such as negligible vapor pressure, thermal and chemical stability, wide liquidus range, lower corrosiveness than conventional salts,

make the ILs suitable candidates to replace conventional solvents [7-10]. ILs are being studied for several years; however, the information about their properties is still scarce. Experimental phase equilibrium data are required to develop thermodynamic models which can describe the systems containing these components.

Wilson, NRTL (Non Random Two Liquid), UNIQUAC and UNIFAC equations have been used for the correlation of systems involving ILs in several studies [11-13]. Even some equations of state have been adapted to predict the thermodynamic behavior of the ILs and their mixtures with organic components [14-16]. However, NRTL and UNIQUAC give the best description of activity coefficients, being the most commonly used models [16]. Although these models have been theoretically developed for non-electrolyte systems, it usually leads to good correlations for systems containing ILs [17].

In this work, the feasibility of using 1-ethyl-3-methyl-imidazolium acetate [EMIM][OAc] and 1-ethyl-3-methyl-imidazolium dicyanamide [EMIM][DCA] for the separation of ethanol and water using extractive distillation process is studied. Ternary vapor-liquid equilibrium data are taken for both ILs. For the mixture containing [EMIM][OAc], binary interaction parameters for NRTL and UNIQUAC models are regressed and compared with the experimental data. For the system using [EMIM][DCA] the experimental data are compared with the predicted values using the NRTL parameters reported by Ge Y. et.al. [18].

## 4.2 Theory

There are several thermodynamic models to describe phase equilibrium, some of them are empirical, e.g. Margules and van Laar models, and others are based on local composition theory, e.g. Wilson, NRTL models. The UNIQUAC model is also derived from local composition theory but has a more theoretical background. There are also models which use the group contribution concept (e.g. UNIFAC and ASOG). However, the NRTL and UNIQUAC models have been applied to highly non-ideal and azeotropic systems [19]. The equations of the NRTL model for the computation of activity coefficients in multicomponent systems are:

$$\ln(\gamma_i) = \frac{\sum_j x_j \tau_{ji} G_{ji}}{\sum_k x_k G_{ki}} + \sum_j \frac{x_j G_{ij}}{\sum_k x_k G_{kj}} \left( \tau_{ij} - \frac{\sum_m x_m \tau_{mj} G_{mj}}{\sum_k x_k G_{kj}} \right) \quad 4.2$$

where:

$$G_{ij} = \exp(-\alpha_{ij} \tau_{ij})$$

$$\tau_{ij} = a_{ij} + b_{ij}/T \quad 4.3$$

$$\tau_{ii} = 0; \quad G_{ii} = 1$$

As can be seen in equations 4.2 and 4.3, the model consists of three parameters; however,  $a_{ij}$  and  $b_{ij}$  are unsymmetrical, i.e.  $ij \neq ji$ .  $\alpha_{ij}$  is user-defined (commonly fixed) and it can be chosen according to the polarity, immiscibility and characteristics of the components and system [20]. In this work, a value of 0.4 was set in the regressions for the polar system ethanol + water + [EMIM][OAc]. Then, for each binary system there are four parameters in total to be regressed.

The equations of the UNIQUAC model for the computation of activity coefficients in multicomponent systems are [19]:

$$\begin{aligned} \ln(\gamma_i) = & \ln \frac{\Phi_i}{x_i} + \frac{z}{2} q_i \ln \frac{\theta_i}{\Phi_i} + l_i - \frac{\Phi_i}{x_i} \sum_j x_j l_j \\ & - q_i \ln \left( \sum_j \theta_j \tau_{ji} \right) + q_i \\ & - q_i \sum_j \frac{\theta_j \tau_{ij}}{\sum_k \theta_k \tau_{kj}} \end{aligned} \quad 4.4$$

where

$$\begin{aligned} \Phi_i &= \frac{r_i x_i}{\sum_k r_k x_k}; \quad \theta_i = \frac{q_i x_i}{\sum_k q_k x_k} \\ l_i &= \frac{z}{2} (r_i - q_i) + 1 - r_i; \quad z = 10 \\ \tau_{ij} &= \exp \left( a_{ij} + \frac{b_{ij}}{T} \right) \end{aligned} \quad 4.5$$

As can be seen in equations 4.4 and 4.5, the UNIQUAC model consists of two pure-component molecular structure constants ( $r_i$  and  $q_i$ , which represent the van der Waals volume and surface area parameter, respectively) and two binary parameters ( $a_{ij}$  and  $b_{ij}$ ); however, they are unsymmetrical. Then, for each binary system there are four parameters in total to be regressed and two constants to be specified. In this work, the vapor was considered as an ideal phase and the deviation of ideality in the liquid phase was treated with a gamma-model.

$$y_i P = x_i \gamma_i P_i^{sat} \quad 4.6$$

In equation 4.6,  $y$  and  $x$  refers to the vapor and liquid molar composition of the component  $i$ , respectively,  $P$  to the total pressure,  $\gamma$  to the activity coefficient and  $P^{sat}$  to the vapor pressure, calculated with Antoine's equation.

$$\ln(P_i^{sat}/kPa) = A_i + B_i/(T/K + C_i) \quad 4.7$$

The Antoine's parameters were taken from the literature [21] and are reported in Table 4.1. It should be mentioned that the IL was treated as a non-volatile component, thus its vapor pressure was set to zero.

**Table 4.1: Antoine parameters for ethanol and water.  
Taken from [21]**

Constant	Ethanol	Water
A	16.7808	16.5699
B	-3737.602	-3984.923
C	-44.170	-39.724

## 4.3 Experimental section

### 4.3.1 Materials

In the following, mass fraction purity is given. The ILs [EMIM][OAc] (>0.99) and [EMIM][DCA] (>0.98) were purchased from Iolitec. Methanol (>0.998), 1-butanol (>0.99) and acetone (>0.99) were purchased from Sigma-Aldrich. Ethylene glycol (EG; >0.9999) was purchased from VWR and ethanol (>0.995) from Merck. It should be mentioned that 1-butanol was used as internal standard in the gas chromatography (GC) analysis. Besides, methanol was used as diluent. After every experiment, the ILs were purified under vacuum (<1.0 kPa) at  $T = 333$  K for minimum 5 h in a rotary evaporator (Büchi Rotavapour R-200 equipped with a Büchi heating bath B-490).

### 4.3.2 Experimental method and procedure

Vapor-liquid equilibrium data were obtained by ebulliometric measurements using a Fischer technology Labodest unit (VLE 602D). The equilibrium apparatus is a dynamic recirculating still that ensures intimate contact of the liquid and vapor phase. A more detailed description of the procedure and experimental method is presented in Chapter 2. For all the measurements, the uncertainty for the vapor and liquid compositions is estimated at  $\pm 0.001$ , and for the temperature and pressure measurements are estimated at  $\pm 0.01$  K and  $\pm 0.001$  kPa, according to the manufacturer.

## 4.4 Results and discussion

### 4.4.1 Vapor-liquid equilibrium experiments

Vapor-liquid equilibrium data for the ILs and ethanol + water were determined experimentally by the ebulliometric technique. The mass composition of the feed, expressed in a solvent-free basis, used in the experiments was 0.80 and 0.20, for ethanol and water, respectively (set 1), and 0.88 and 0.12, for ethanol and water, respectively (set 2). The solvent to feed mass ratio was varied from 0 until 1.67 and a constant pressure (0.1 MPa) was set for all of the experiments. The experimental data are reported in Table 4.2, where  $w$  and  $y$  hold for mass composition in the liquid phase and molar composition in the vapor phase, respectively. The superscript  $sf$  refers to solvent free basis compositions and  $\alpha_{12}$  represents the relative volatility, defined in equation 4.1.

**Table 4.2: Experimental VLE data for the ternary system ethanol (1) + water (2) + [EMIM][OAc] (3)**

$S/F$	$T$ (K)	$w_1^{sf}$	$w_2^{sf}$	$y_1$	$y_2$	$\alpha_{12}$
0.00	351.35	0.8818	0.1182	0.7835	0.2165	1.24
0.33	354.95	0.8000	0.2000	0.7598	0.2402	2.02
0.49	357.75	0.8774	0.1226	0.8535	0.1465	2.08
0.70	362.35	0.8798	0.1202	0.8704	0.1296	2.35
1.11	371.55	0.8846	0.1154	0.8924	0.1076	2.77
1.47	377.35	0.8000	0.2000	0.8219	0.1781	2.95
1.67	381.75	0.8000	0.2000	0.8246	0.1754	3.01

The results of the experimental relative volatility and bubble temperature for the system containing [EMIM][OAc] are shown in Figure 4.1. It can be seen in Figure 4.1(a) that the relative volatility increases with the solvent to feed ratio reaching values of 3 for a solvent to feed mass ratio of 1.67. In Figure 4.1(b), the bubble temperature shows the same dependence on the solvent to feed ratio. In these figures it can be seen the calculations with the regressed parameters for the NRTL and UNIQUAC models for a constant ethanol mass fraction composition in solvent free basis of 0.8405 (averaged value taken from Table 4.2). The Figure 4.1(c) shows the comparison of the experimental data and the regressed values with NRTL and UNIQUAC models. These results will be analyzed in following sections in this chapter.

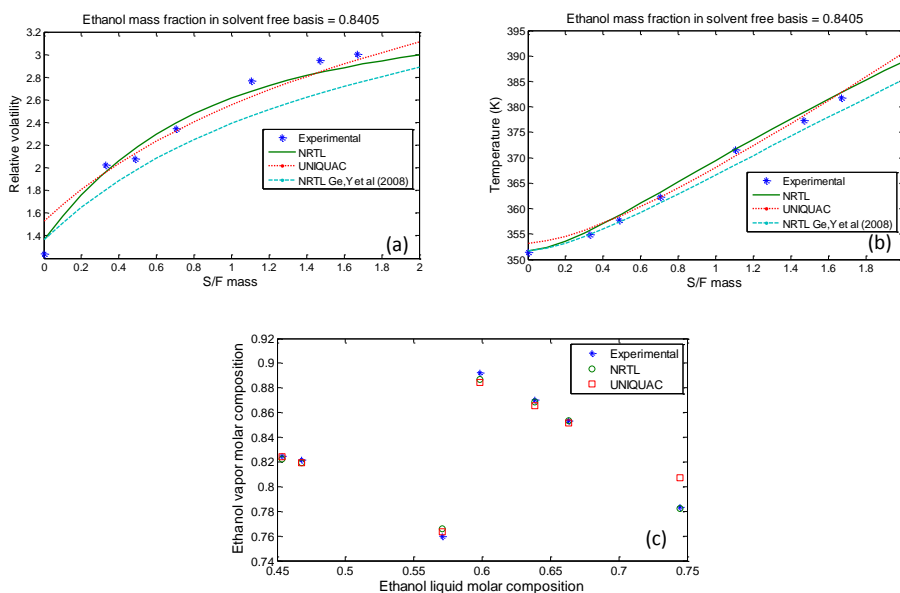


**Figure 4.1: Experimental and correlated data for the ternary system ethanol (1) + water (2) + [EMIM][OAc] (3). Relative volatility (a), bubble temperature (b) and ethanol compositions (c)**

Experimental results for the system containing [EMIM][DCA] are shown in Table 4.3 and represented in Figure 4.2. The line in this figure represents the predicted relative volatility with the NRTL model using the parameters reported by Ge Y. et al. [18]. These results will be analyzed in following sections in this chapter.



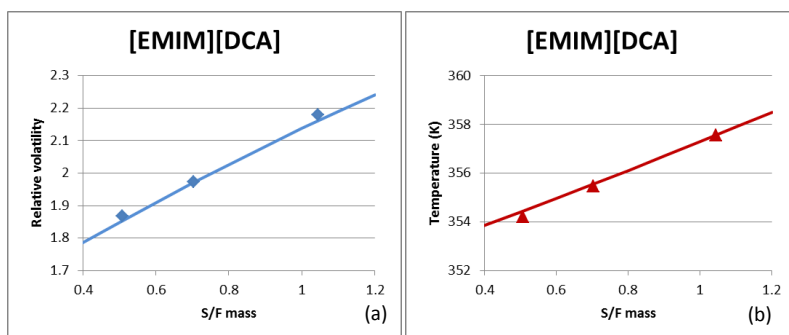


Figure 4.2: Experimental (symbols) and predicted (lines) relative volatility (a) and temperature (b) for the ternary system ethanol (1) + water (2) + [EMIM][DCA]

Table 4.3: Experimental VLE data for the ternary system ethanol (1) + water (2) + [EMIM][DCA]

$S/F$	$T$ (K)	$w_1^{sf}$	$w_2^{sf}$	$\gamma_1$	$\gamma_2$	$\alpha_{12}$
<b>0.51</b>	354.22	0.7976	0.2024	0.7421	0.2579	1.87
<b>0.70</b>	355.45	0.7990	0.2010	0.7542	0.2458	1.97
<b>1.05</b>	357.55	0.8006	0.1994	0.7734	0.2262	2.18

In this case, only three experiments were done to test the reliability of the predictions using the NRTL parameters reported by Ge Y. et.al. [18]. An initial mixture was prepared and used for all the experiments. It contained a mass composition, in a solvent free basis, of 0.80 and 0.20 of ethanol and water, respectively. The experimental data was taken at constant pressure (0.1 MPa) and the solvent to feed mass ratio used in the experiments was 0.51, 0.70 and 1.05. From the experimental data, it can be concluded that the relative volatility increases with the solvent to feed ratio. Comparing the results shown in Table 4.2 and Table 4.3, [EMIM][OAc] shows higher relative volatility than [EMIM][DCA] making the former IL more suitable for the extractive distillation of ethanol and water and confirming the behavior predicted with COSMOtherm, which was shown in Chapter 2.

#### 4.4.2 Comparison of experimental, regressed and predicted data

NRTL binary interaction parameters for the ternary mixture ethanol + water + [EMIM][OAc] were published by Ge, Y. et al. [18]. These parameters showed high deviations from our experimental data, as can be seen in Figure 4.1(a) and (b). The IL used in this work has a purity higher than 0.99 (mass basis) and were purchased from lolitec; however, Ge, Y. et al. synthesized their ILs and did not report their purity. This might be the reason why their experimental data and regression exhibit deviation from the data presented in this work.

For the correlation of the experimental data for the ternary system ethanol (1) + water (2) + [EMIM][OAc], the NRTL and UNIQUAC models were used. In order to consider temperature dependency in both models, linear temperature-dependent binary interaction parameters ( $\tau_{ij}$ ) were taken into account. The parameters for the models were regressed with a minimization procedure implemented in *MATLAB R2010b*. The function to minimize is shown in equation 4.8.

$$\begin{aligned} & \min F \\ & = \sqrt{\frac{1}{NE - 4} \sum_k^{NE} \left( 100 \sum_i (y_{i,k}^{exp} - y_{i,k}^{pred})^2 + (T_k^{exp} - T_k^{pred})^2 \right)} \end{aligned} \quad 4.8$$

In this equation, the subscript  $k$  stands for the number of the experiment and  $NE$ ,  $exp$  and  $pred$  refers to total number of experiments, experimental and predicted value, respectively. For the regressions, the IL was treated as a non-volatile component, thus its vapor pressure was set to zero. The binary parameters for ethanol and water were taken from *Aspen Plus V7.2* database VLE-LIT, which are based on literature values. As mentioned above, a value of 0.4 was chosen for the non-randomness NRTL parameter,  $\alpha_{ij}$ , for the binary parameters containing IL.

The UNIQUAC's van der Waals parameters  $r_i$  and  $q_i$  for ethanol and water were estimated using the Bondi method [19]. For the IL, they were estimated with the correlation proposed by Domanska [22, 23].

$$\begin{aligned} r_i &= 0.029281V_i \\ q_i &= \frac{(z - 2)r_i}{z} + \frac{2}{z} \end{aligned} \quad 4.9$$

Where  $V_i$  is the molar volume in  $cm^3 mol^{-1}$  of the IL at  $T/K = 298.15$  and  $z$  is the coordination number assumed to be equal to 10. The van der Waals volume and surface area parameters for the components involved in the mixture are listed in Table 4.4.

**Table 4.4: van der Waals volume and surface parameters for UNIQUAC model**

	Ethanol	Water	[EMIM][OAc] <sup>3</sup>
$r_i$	2.5755	0.9200	4.6496
$q_i$	2.5880	1.4000	3.9197

It should be noted that the values of  $r_i$  and  $q_i$  estimated for the IL in this work are in accordance with the values reported for other ILs [23-25]. The NRTL and UNIQUAC parameters obtained after the regression of the experimental data are listed in Table 4.5.

As can be seen in the results depicted in Figure 4.1, the experimental relative volatility, temperature and ethanol compositions are well correlated by both thermodynamic models. The goodness of fit was calculated with the root mean square error (RMS), shown in equation 4.10. The UNIQUAC model gives a RMS of 0.0139. However, the NRTL model exhibited a better accuracy with a RMS value of 0.0055. It should be noticed that in Figure 4.1(a) and (b), the predicted values with NRTL and UNIQUAC models using a constant ethanol composition of 0.8405 are shown to illustrate the ability of the parameters to predict the tendency in the relative volatility and bubble temperature.

<sup>3</sup> The molecular weight of [EMIM][OAc] and its molar volume are 170.21 and 158.79  $cm^3/mol$ , respectively. The molar volume of was predicted with the software package *COSMOtherm* version C2.1 release 01.11a).

Table 4.5: NRTL and UNIQUAC interaction parameters for the mixture ethanol + water + [EMIM][OAc]

	Ethanol (i) Water (j)		Ethanol (i) [EMIM][OAc] (j)		Water (i) [EMIM][OAc] (j)	
	NRTL	UNIQUAC	NRTL	UNIQUAC	NRTL	UNIQUAC
$\alpha_{ij}$	0	0	0	1.5614	0	2.3230
$\alpha_{ji}$	0	0	0	0.7474	0	0.8848
$b_{ij}$	-55.1698	-25.6061	-1426.4	0.9754	-1505.8	-1.0193
$b_{ji}$	670.4442	-116.7512	-965.94	-1.0219	-1109.3	-2.0240
$\alpha_{ij}$	0.3031	0	0.4	0	0.4	0

In Figure 4.1(c), the experimental and correlated data with both models is shown. From these figures it can be concluded that, especially the NRTL model and the regressed parameters can be used to accurately estimate the vapor-liquid equilibrium of this ternary mixture.

$$RMS = \sqrt{\frac{1}{NE} \sum_k \left( \left( \frac{T_k^{exp} - T_k^{pred}}{T_k^{exp}} \right)^2 + \sum_i (y_{i,k}^{exp} - y_{i,k}^{pred})^2 \right)} \quad 4.10$$

The parameters shown in Table 4.5 for the ternary mixture ethanol + water + [EMIM][OAc] will be used in following chapters to calculate the VLE of this ternary mixture and its behavior in an equilibrium-based unit such as an extractive distillation column.

For the system containing [EMIM][DCA] the deviation between our experimental data and the values calculated with the NRTL parameters shown in Table 4.6 and taken from Ge Y. et.al. [18] was obtained with equation 4.11.

$$RMS = \sqrt{\frac{1}{NE} \sum_k \left( (\alpha_k^{exp} - \alpha_k^{pred})^2 + \left( \frac{T_k^{exp} - T_k^{pred}}{T_k^{exp}} \right)^2 \right)} \quad 4.11$$

Table 4.6: NRTL interaction parameters for the ternary system ethanol + water + [EMIM][DCA]. Taken from [18]

	Ethanol (i) Water (j)	Ethanol (i) [EMIM][DCA] (j)	Water (i) [EMIM][DCA] (j)
	$\alpha_{ij}$	0.8065	0
$\alpha_{ji}$	0.5143	0	0
$b_{ij}$	-266.538	350.132	-289.933
$b_{ji}$	444.888	-415.384	-222.997
$\alpha_{ij}$	0.4	0.3	0.3

As can be seen in Figure 4.2, the parameters are in good agreement with the experimental data and this is confirmed by the low value of the root mean square error of 0.0196.

From these results it can be concluded that the NRTL model and the parameters reported in the literature for the system ethanol + water + [EMIM][DCA] [18] are in good agreement with our experimental data. The parameters shown in Table 4.6 and the NRTL model will be used for estimations and simulations of the vapor - liquid equilibrium for this ternary system.

## 4.5 Conclusions

Ternary vapor-liquid equilibrium for the systems ethanol + water + [EMIM][OAc] and ethanol + water + [EMIM][DCA] were collected at several solvent to feed ratios and pressure of 0.1 MPa.

For the ternary system containing [EMIM][OAc] there were found parameters reported in the literature for the NRTL model [18]. However, these parameters were unable to represent the experimental data taken in our laboratory. Therefore, binary interaction parameters for NRTL and UNIQUAC models were regressed with the obtained experimental data. The comparison between the experimental and correlated data, and the root mean square deviation showed that the NRTL model and its parameters give more accurate results than UNIQUAC. NRTL is able to accurately compute the relative volatility, bubble temperature and equilibrium compositions. This model is used to calculate the VLE behavior of this ternary system.

For the ternary system using [EMIM][DCA], few experimental data points were taken in order to be able to compare the values computed with the NRTL model and the parameters reported by Ge Y. et.al. [18]. These parameters accurately estimated the relative volatility and temperatures obtained in the experiments, giving a deviation of 0.0196. NRTL model and the parameters reported by Ge Y. can be used to calculate the VLE of the system ethanol + water + [EMIM][DCA].

The selected ILs are able to increase the relative volatility of ethanol + water mixture making them potential and suitable solvents for extractive distillation applications. However, it should be noticed that the IL [EMIM][OAc] gives higher relative volatilities than [EMIM][DCA]. In the Chapter 6, extractive distillation processes using these ILs will be designed and simulated, using the parameters obtained and shown in the present chapter.

## 4.6 References

1. Kumar, S., N. Singh and R. Prasad, *Anhydrous ethanol: A renewable source of energy*. Renewable & Sustainable Energy Reviews, 2010. **14**(7): p. 1830-1844.
2. McPhail, L.L., *Assessing the impact of US ethanol on fossil fuel markets: A structural VAR approach*. Energy Economics. **In Press, Corrected Proof**.
3. Huang, H.-J., S. Ramaswamy, U.W. Tschirner and B.V. Ramarao, *A review of separation technologies in current and future biorefineries*. Separation and Purification Technology, 2008. **62**(1): p. 1-21.

4. Lee, F.M. and J.C. Gentry, *Don't Overlook Extractive Distillation*. Chemical Engineering Progress, 1997. **93**(10): p. 56-64.
5. Doherty, M.F. and J.P. Knapp, *Distillation, Azeotropic and Extractive*, in *Kirk-Othmer Encyclopedia of Chemical Technology* 2004, John Wiley & Sons, Inc.
6. Seiler, M., C. Jork, A. Kavarnou, W. Arlt and R. Hirsch, *Separation of azeotropic mixtures using hyperbranched polymers or ionic liquids*. AIChE Journal, 2004. **50**(10): p. 2439-2454.
7. Meindersma, G.W., A. Podt, M.G. Meseguer and A.B. de Haan, *Ionic liquids as alternatives to organic solvents in liquid-liquid extraction of aromatics*. Ionic Liquids IIIB: Fundamentals, Progress, Challenges and Opportunities: Transformations and Processes, 2005. **902**: p. 57-71.
8. Verma, V.K. and T. Banerjee, *Ionic liquids as entrainers for water + ethanol, water + 2-propanol, and water + THF systems: A quantum chemical approach*. The Journal of Chemical Thermodynamics, 2010. **42**(7): p. 909-919.
9. Orchilles, A.V., P.J. Miguel, E. Vercher and A. Martinez-Andreu, *Ionic Liquids as Entrainers in Extractive Distillation: Isobaric Vapor-Liquid Equilibria for Acetone + Methanol + 1-Ethyl-3-methylimidazolium Trifluoromethanesulfonate*. J. Chem. Eng. Data, 2007. **52**(1): p. 141-147.
10. Wasserscheid, P. and T. Welton, *Ionic liquids in synthesis* 2003, Weinheim: Wiley-VCH. xvi, 364 p.
11. Simoni, L.D., L.E. Ficke, C.A. Lambert, M.A. Stadtherr and J.F. Brennecke, *Measurement and Prediction of Vapor-Liquid Equilibrium of Aqueous 1-Ethyl-3-methylimidazolium-Based Ionic Liquid Systems*. Industrial & Engineering Chemistry Research, 2010. **49**(8): p. 3893-3901.
12. Deenadayalu, N., S.H. Thango, T.M. Letcher and D. Ramjugernath, *Measurement of activity coefficients at infinite dilution using polar and non-polar solutes in the ionic liquid 1-methyl-3-octyl-imidazolium diethyleneglycolmonomethylethersulfate at T = (288.15, 298.15, and 313.15) K*. The Journal of Chemical Thermodynamics, 2006. **38**(5): p. 542-546.
13. Domanska, U. and A. Marciniak, *Measurements of activity coefficients at infinite dilution of aromatic and aliphatic hydrocarbons, alcohols, and water in the new ionic liquid [EMIM][SCN] using GLC*. The Journal of Chemical Thermodynamics, 2008. **40**(5): p. 860-866.
14. Li, J., Q. He, C. He, C. Peng and H. Liu, *Representation of Phase Behavior of Ionic Liquids Using the Equation of State for Square-well Chain Fluids with Variable Range*. Chinese Journal of Chemical Engineering, 2009. **17**(6): p. 983-989.
15. Tsiptsias, C., I. Tsvintzelis and C. Panayiotou, *Equation-of-state modeling of mixtures with ionic liquids*. Physical Chemistry Chemical Physics, 2010. **12**(18): p. 4843-4851.
16. Döker, M. and J. Gmehling, *Measurement and prediction of vapor-liquid equilibria of ternary systems containing ionic liquids*. Fluid Phase Equilibria, 2005. **227**(2): p. 255-266.
17. Meindersma, G.W., A. Podt and A.B. de Haan, *Selection of ionic liquids for the extraction of aromatic hydrocarbons from aromatic/aliphatic mixtures*. Fuel Processing Technology, 2005. **87**(1): p. 59-70.

18. Ge, Y., L. Zhang, X. Yuan, W. Geng and J. Ji, *Selection of ionic liquids as entrainers for separation of (water + ethanol)*. The Journal of Chemical Thermodynamics, 2008. **40**(8): p. 1248-1252.
19. Poling, B.E., J.M. Prausnitz and J.P. O'Connell, *The properties of gases and liquids*. 5th ed2001, New York: McGraw-Hill. 1 v. (various pagings).
20. Sandler, S.I., *Chemical, biochemical, and engineering thermodynamics*. 4th ed2006, Hoboken, N.J.: John Wiley. xiv, 945 p.
21. Kurihara, K., M. Nakamichi and K. Kojima, *Isobaric vapor-liquid equilibria for methanol + ethanol + water and the three constituent binary systems*. Journal of Chemical & Engineering Data, 1993. **38**(3): p. 446-449.
22. Domanska, U., *Solubility of n-alkanols (C16,C18,C20) in binary solvent mixtures*. Fluid Phase Equilibria, 1989. **46**(2-3): p. 223-248.
23. Gutierrez, J.P., W. Meindersma and A.B. de Haan, *Binary and ternary (liquid-liquid) equilibrium for {methylcyclohexane (1)+toluene (2)+1-hexyl-3-methylimidazolium tetracyanoborate (3)/1-butyl-3-methylimidazolium tetracyanoborate (3)}*. The Journal of Chemical Thermodynamics, 2011. **43**(11): p. 1672-1677.
24. Lei, Z., J. Zhang, Q. Li and B. Chen, *UNIFAC Model for Ionic Liquids*. Industrial & Engineering Chemistry Research, 2009. **48**(5): p. 2697-2704.
25. Kato, R., M. Krummen and J. Gmehling, *Measurement and correlation of vapor-liquid equilibria and excess enthalpies of binary systems containing ionic liquids and hydrocarbons*. Fluid Phase Equilibria, 2004. **224**(1): p. 47-54.



## 5. Extractive distillation process design for the separation of toluene + methylcyclohexane using ionic liquids

### Abstract

This chapter presents the results of the extractive distillation (ED) process design and simulation for the separation of the mixture methylcyclohexane (MCH) + toluene using the ionic liquid (IL) [HMIM][TCB] (1-hexyl-3-methyl-imidazolium tetracyanoborate) and the conventional solvent (N-methyl-2-pyrrolidone – NMP). The thermodynamic model and data used in the simulation are presented. The reflux and the solvent to feed ratio of the ED columns are obtained such that the energy requirements of the column are minimized. Different concepts for the recovery of the solvents are also proposed, simulated and analyzed. The conventional solvent can be recovered by conventional distillation. However, due to the non-volatility of the ILs, they need to be recovered by other technologies. For each technology, the overall energy requirements are compared with the conventional process duties and the ones yielding the better results are selected. Heat integration analysis of these processes is done and heat exchanger networks are proposed. Recovering the IL in a stripping column, using part of the distillate product of the extractive distillation column as the stripping gas, yields the most promising results. The use of this process results in a total energy saving of 50% compared to the conventional process using NMP. ILs are promising solvents to be used in extractive distillation processes for the separation of MCH and toluene, yielding large energy savings, not only in the ED column but in the whole process.

### 5.1 Introduction

Aromatics are a key compound in the petrochemical industry as raw materials for the production of polymers, solvents, dyes, drugs herbicides, etc. [1]. The current commercial source of aromatics is petroleum which is catalytically and thermally treated to produce reformates and the so-called pyrolysis gasoline. The pyrolysis gasoline produced in naphtha cracking has a higher aromatic content than the reformat and is the preferred source of aromatics in Western Europe [2]. A typical composition of pyrolysis gasoline is 70 wt. % of aromatics and 30 wt. % of non-aromatics [1, 2].

The isolation of aromatics consists essentially of stages for the separation of non-aromatics with low boiling points followed by the separation of the aromatics. Due to the close boiling points, presence of azeotropes and economic reasons, conventional distillation is unsuitable [2]. Therefore, the separation of these compounds is carried out by means of special separation processes: azeotropic distillation, extractive distillation (ED), liquid-liquid extraction, crystallization and adsorption. For medium aromatic content (65 – 90%), ED is the preferred technology for economic isolation of aromatics [2].

In ED, an extra component (solvent) is added to increase the relative volatility of the mixture enhancing the separation. Thermally stable, non-corrosive substances, such as N-methyl-2-pyrrolidone (NMP), are suitable and widely used solvents for aromatic



separation [2]. In this case, the solvent acts mainly on the aromatic fraction to decrease its volatility; the non-aromatics are distilled overhead of the ED column, and the aromatics remain with the solvent in the bottom stream, which are then separated in a solvent recovery column. The solvent is recovered in the bottom; meanwhile the aromatics are obtained overhead.

The more selective the solvent, the more efficient the separation is. In this chapter, the performance of the selected ionic liquid (IL) 1-hexyl-3-methyl-imidazolium tetracyanoborate (Chapter 3) is evaluated in an ED process. This IL has been selected over the 1-butyl-3-methyl-imidazolium tetracyanoborate ([BMIM][TCB]) because of its slightly higher solubility (especially with toluene, as it was shown in Figure 3.2 and Figure 3.3) maintaining similar selectivity. As in the conventional case, the solvent is added in the top of the ED column, the non-aromatics are obtained overhead and the solvent should be recovered from the aromatic compounds. Due to their non-volatility, conventional distillation cannot be used to recover the ILs. Several technologies have been proposed to recover and recycle the ILs; however, technical feasibility studies are not performed in this work. Evaporation (at high temperature and low pressure) and stripping are potential technologies to recover ILs from volatile compounds [3]. It should be mentioned that none of these technologies have been described and simulated in detail in the literature. Haerens et al. [4] discussed the use of pressure driven membrane processes to recover ILs. It was shown that the performance of these processes is not satisfactory and large membrane areas are required. In their work, separation technologies using supercritical carbon dioxide (SCCO<sub>2</sub>) is suggested. In this Chapter, several recovery technologies are analyzed, considering the energy requirements of the whole process and comparing them with the conventional process.

## 5.2 Thermodynamic and simulation data

In this work, a model feed mixture composed by 700 kmol/h of toluene (as representative of aromatics) and 300 kmol/h of methylcyclohexane (MCH – as representative of non-aromatics) at 35 °C and 100 kPa is taken. These values are based on representative plant capacities for aromatic production [5]. The separation processes simulated in this work are subject to the constraints that the final recovered products should have a molar purity  $\geq 99.5\%$  [6-8]. The condenser and the reboiler are taken into account as equilibrium stages, the condenser being the first stage. The results are based on thermodynamic equilibrium stage modeling using *Aspen Plus V7.2*. It should be mentioned that, due to the degradation temperatures, the IL is not allowed to be at temperatures higher than 150 °C. The thermodynamic and physical properties for the components involved in the simulations are presented in appendix 5.1.

## 5.3 Conventional extractive distillation process using NMP

The minimum number of stages of the extractive distillation column (EDC) was calculated with the Fenske equation [5], using the desired purity of MCH in the distillate and a relative volatility ( $\alpha$ ) of 2.8. This value is obtained when a solvent to feed molar ratio of unity (arbitrary) at 100 kPa is selected. It has been standard practice to use from 2 to 4 times the minimum number of stages predicted with the Fenske equation [6]. In this work, the total number of stages for the distillation column is taken as thrice the minimum

number of stages, i.e. the actual number of stages for the ED column using NMP is 30. An optimization procedure was implemented to determine the optimal feed stage ( $n_f$ ), solvent feed stage ( $n_s$ ), molar reflux ratio ( $RR$ ) and solvent to feed molar ratio ( $S/F$ ).

$$\min Q_R = f(S/F, RR, n_f, n_s)$$

5.1

$$s. t. \quad x_{MCH}^D \geq 0.995$$

In equation 5.1,  $Q_R$  and  $x_{MCH}^D$  refers to the reboiler heat duty and MCH molar composition in the distillate. The optimized column conditions and results are shown in Figure 5.1 and Table 5.1. The feed is fed at stage ( $n_f$ ) 19 and the solvent is fed ( $n_s$ ) at the 7<sup>th</sup> stage to avoid solvent losses in the overhead of the column. The column profiles can be seen in Figure 5.18 in appendix 5.2.

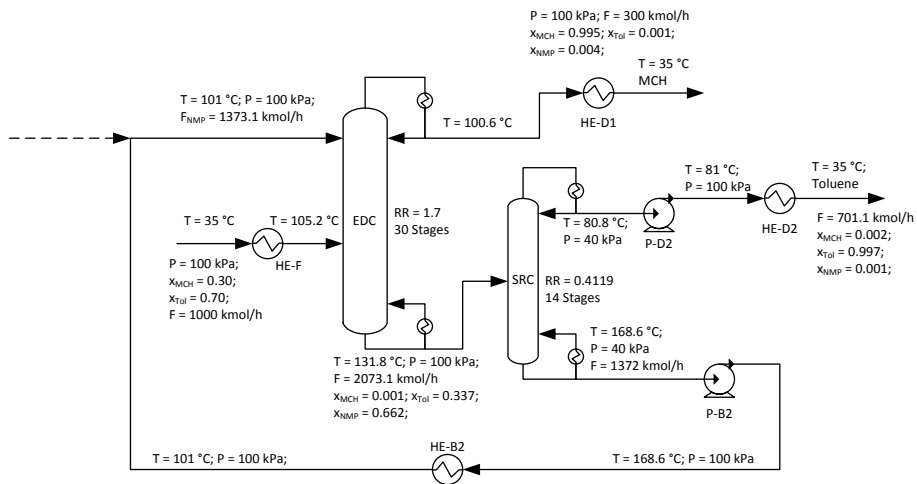


Figure 5.1: Conventional extractive distillation process using NMP

For the solvent recovery column (SRC) a similar procedure was applied, resulting in 14 actual stages. For this column, the feed stage, reflux ratio and pressure were determined by the optimization shown in equation 5.2.

$$\min Q_R = f(n_f, RR, P)$$

5.2

$$s. t. \quad x_{NMP}^D \leq 0.0005$$

To avoid solvent losses in the SRC, a constraint which limits the NMP molar composition in the distillate ( $x_{NMP}^D$ ) to be less than 500 ppm was taken into account. In equation 5.2,  $P$  refers to the total pressure of the distillation column. The results are shown in Figure 5.1. The feed of this column is located at the 9<sup>th</sup> stage. It should be mentioned that the lower the pressure in the SRC the lower the energy requirements (the vacuum pump needed to create the low pressure is not taken into account). However, if the pressure is decreased below 40 kPa, the NMP composition constraint in the distillate is not satisfied. Due to the

low pressure, the NMP becomes more volatile and its composition in the vapor phase increases until values higher than 500 ppm (molar composition of 0.0005). The energy requirements for the whole ED process using NMP as solvent are given in Table 5.1.

**Table 5.1: Energy requirements of the conventional ED process**

Unit	Energy requirements (MW)	
EDC-Condenser	-7.2	
EDC-Reboiler		13.1
SRC-Condenser	-9.7	
SRC-Reboiler		14.0
HE-D1	-1.1	
HE-D2	-1.5	
HE-B2	-11.1	
HE-F		3.5
P-D2		$1.9 \times 10^{-3}$
P-B2		$3.4 \times 10^{-3}$
<b>Total</b>	<b>-30.6</b>	<b>30.6</b>

From Figure 5.1, it can be seen that the solvent to feed molar ratio of the process is 1.37 (which results in a solvent to feed mass ratio of 1.45) and the reflux ratio of the EDC and SRC are 1.7 and 0.4, respectively. It should be noticed that through the overhead of both columns, 1.1 kmol/h of solvent is lost.

#### 5.4 Extractive distillation column using ionic liquids

As in the previous case, the Fenske equation was used to calculate the minimum number of stages using an arbitrary solvent to feed molar ratio of unity (in order to perform the first estimations) which gives a relative volatility of 4.5. Taking thrice the minimum, the actual number of stages of the EDC using the IL is 22. It should be noticed that the relative volatility for the IL is 1.6 times larger than for the conventional solvent. Besides, the higher selectivity (or volatilities) is expected to decrease the energy requirements of the EDC.

The solvent to feed ratio ( $S/F$ ), reflux ratio ( $RR$ ) and feed stage ( $n_f$ ) were determined using a minimization procedure subject to two constraints (equation 5.3).

$$\min Q_R = f(S/F, RR, n_f) \tag{5.3}$$

$$s. t. \quad x_{MCH}^D \geq 0.995 \text{ and } x_{IL}^2 \geq 0.85$$

It should be mentioned that the IL can be fed into the column combined with the reflux flow without losing the solvent in the overhead due to its non-volatility. In equation 5.3, the first constraint refers to the purity of MCH in the overhead product and the second constraint refers to the IL composition in the second stage of the EDC. This is a necessary condition to avoid formation of two liquid phases inside the column, and can be deduced from the ternary diagrams shown in Chapter 3. This value corresponds to the immiscibility boundary concentration of IL in MCH; compositions lower than this value lead to formation of two liquid phases. The feed is located at the 13<sup>th</sup> stage. The results for the EDC are shown in Figure 5.2. The column profiles can be seen in Figure 5.19 and Figure 5.20 in appendix 5.2.

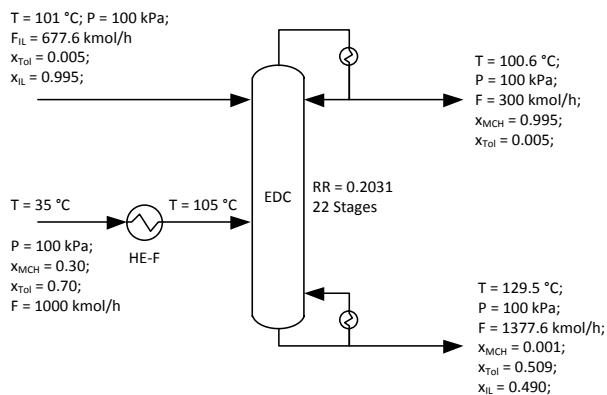


Figure 5.2: Extractive distillation column using ILs as solvent

In Figure 5.2, it should be noticed that the IL fed to the EDC has a molar purity of 99.5%. A lower purity will result in violation of the purity constraint in the overhead product and a higher purity will influence the IL recovery technology in terms of energy requirements (the higher the required purity of the IL the higher the cost involved in the recovery process). The solvent to feed molar ratio is around 0.68; resulting in a solvent to feed mass ratio of 2.03. Notice that the molar ratio is 0.5 times lower and the mass ratio is 1.4 times larger than for the EDC using the conventional solvent NMP. It should be mentioned that for systems where the differences in molecular weights are considerable (i.e. systems using ILs), especial attention should be paid to the solvent to feed mass ratios.

The energy requirements in the condenser and reboiler of the EDC using ILs are -3.3 MW and 7.4 MW, respectively. As a result, the energy savings in the EDC are 55% and 43% for the condenser and reboiler, respectively. The higher selectivity of the IL is reflected in the lower reflux ratio and, at the same time, gives lower energy requirements in the condenser. Besides, the solvent is being heated up in the reboiler and not (partially) evaporated (like in the NMP case) which results in lower energy input to this unit.

In the following section, several recovery technologies for the ILs are proposed and analyzed. So far, the ILs perform more efficiently than the conventional solvent, however, the recovery technology influences the energy requirements involved in the whole process.

## 5.5 Ionic liquid recovery techniques

Several recovery technologies are studied in this section to recover the IL. Processes like flash vaporization, stripping, combination of both technologies, and  $\text{SSCO}_2$  are taken into account. The energy requirements of the recovery technologies combined with the extractive distillation column are presented, summarized and analyzed at the end of the current section.

### 5.5.1 Recovery using flash evaporation

This process consists of a simple evaporation flash drum which will remove the toluene from the IL due to the decrease in pressure (and increase of temperature). The toluene is

obtained in the vapor outlet of the flash with a high purity and the IL is obtained in the liquid outlet of the drum with the desired purity, which will be influenced by the pressure and temperature used in this unit. Three conditions were analyzed: adiabatic, isothermal and operation at 150 °C (maximum temperature allowed to avoid degradation of the IL).

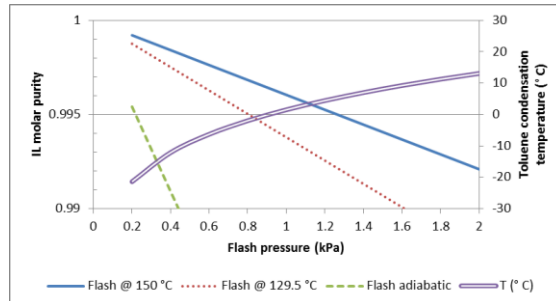


Figure 5.3: Flash pressure influence on the IL purity and toluene condensation temperature

In Figure 5.3, the results of the three processes are shown. It should be mentioned that the IL should be recycled to the EDC with a molar purity of 0.995. From Figure 5.3, it can be concluded that if the flash is operated until the desired purity, pressures of 0.22, 0.80 and 1.26 kPa are needed in the adiabatic, isothermal and 150 °C flash, respectively. Furthermore, the toluene in the vapor phase needs to be condensed and re-compressed by a liquid pump. Temperatures of -20.3, -1.9 and 5.3 °C are needed to condense the vapor stream for adiabatic, isothermal and 150 °C operation. In any case, a refrigeration system needs to be used, implying extra energy and equipment requirements.

To avoid the use of refrigeration systems, a compressor can be used. However, there are several disadvantages:

- Due to the large amount of gas to be compressed (between  $2 \times 10^6$  and  $10 \times 10^6$  m<sup>3</sup>/h depending on the flash pressure, which corresponds to a toluene mole flow of 700 kmol/h) several compressors in parallel need to be used [5];
- Due to the compression, there is an increase in temperature (reaching between 200 and 300 °C) which make necessary the use of at least one extra heat exchanger to cool this stream down (if several stages during the compression are used the temperature can be decreased in between stages by heat exchangers).

Due to these reasons, the use of compressors after the flash drums is not considered a viable option to recover the toluene.

$$COP = \frac{Q_{cooling}}{W_{refri}} = 0.6 \times COP^{ideal} = \frac{0.6 \times T^{evap}}{T^{cond} - T^{evap}} \quad 5.4$$

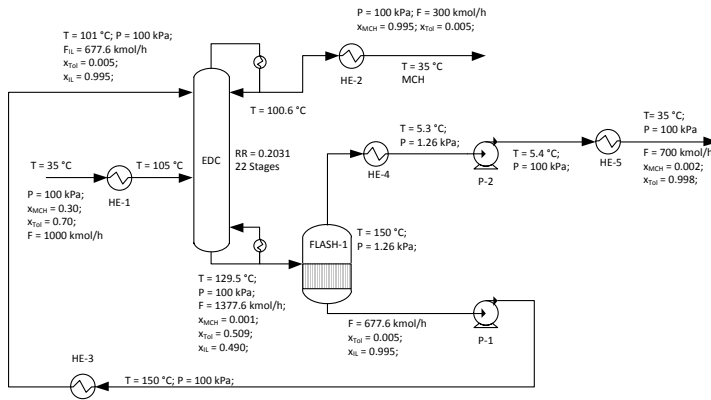


Figure 5.4: ED process using ILs. Recovery with flash drum at 150 °C

Considering these options, the recovery process using a flash drum operating at 150 °C and a refrigeration system to condense the toluene at 5.3 °C is selected for further studies. This process is shown in Figure 5.4. The energy requirements of this process are listed in Table 5.2 and the analysis will be given in the summary at the end of this section. However, it is appropriate to mention that the duty of the refrigeration system was obtained taken 60% of the its ideal coefficient of performance ( $COP$ ) as recommended by Smith [9] (equation 5.4).

In equation 5.4, the evaporation and condensation temperatures ( $T^{evap}$  and  $T^{cond}$ ) are from the refrigeration fluid (expressed in K). In this case, the temperature of the stream (5.3 °C) and the temperature of evaporation of the refrigeration fluid should have a temperature difference of 10 K. Thus, the evaporation temperature of the refrigerant is -4.7 °C. The condensation temperature of the refrigerant is taken as 35 °C (to be able to use cooling water as condenser fluid). In the present case, the cooling duty ( $Q_{cooling}$ ) is taken as the energy required to decrease the temperature of the stream (high purity toluene in vapor phase) from 35 °C to 5.3 °C (liquid phase). In this case  $Q_{cooling}$  is -8.3 MW.

### 5.5.2 Recovery using stripping with hot nitrogen

In this process, the bottom stream from the EDC enters to a stripping column. The number of stages was calculated with a simplified algebraic method [10] with a constant toluene partition coefficient of 1.85 (value obtained with Raoult's law at an arbitrary total pressure of 40 kPa, pressure at which the SRC for the conventional process is operating) which gives a minimum stripping gas flow of 371 kmol/h. Besides, it was assumed that the gas and IL remain in their original vapor and liquid phase, respectively. It is common practice to use 1.5 times the minimum flow [10]. Therefore, the stripper is fed with 556 kmol/h. Using only material balances per stage, a total of 10 equilibrium stages are necessary to get the desired IL purity. It should be mentioned that the procedure described above was only applied to obtain the number of equilibrium stages. The following simulations and results are done using rigorous methods such as *RadFrac* (*Aspen Plus V7.2*).

Nitrogen at 150 °C is used as stripping gas. The gas removes the toluene from the liquid phase, purifying the IL. It should be mentioned that the desired molar purity of the IL exiting the stripping column is 0.995. This stream is recycled back to the EDC. Hot nitrogen and toluene in vapor phase are obtained at the top of the stripping column; however, the toluene needs to be removed from this stream. This can be done by decreasing the temperature (like in the previous case, compression after flash is not considered as an economically feasible process). The nitrogen can be re-heated and recycled back to the stripping column.

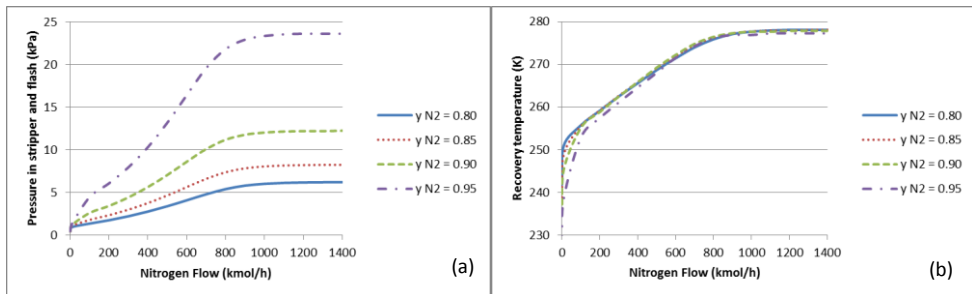


Figure 5.5: Influence of nitrogen flow in the (a) maximum flash and stripper pressure, and (b) toluene recovery temperature. Recovery using nitrogen stripping

The nitrogen flow was varied until the desired purity of the IL was reached. Figure 5.5(a) shows how the pressure in the units can be increased with the nitrogen flow. In this figure, the influence of the nitrogen purity can be seen. For a given pressure in the stripper, the nitrogen flow can be drastically decreased if the nitrogen has a high purity. However, there is a region where the pressure and the nitrogen flow are not sufficient to reach the desired IL purity. In Figure 5.5(b) it can be seen that low temperatures in the flash are necessary to recover the nitrogen and condense the toluene. The purity of the stream does not have a remarkable influence on the recovery temperature; however, the larger the flow the easier the recovery (higher temperature can be used). A nitrogen purity of 0.95 and a pressure in the stripper of 20 kPa (which gives a nitrogen flow of 714.2 kmol/h and a condensation temperature of 1.5 °C) are chosen to analyze this technology in more detail. This process is shown in Figure 5.6.

The duty of the refrigeration system was obtained as in the previous process; however, in this case, the stream has a temperature of 1.5 °C which results in an evaporation temperature of -8.5 °C. In this case, the cooling duty (energy required to decrease the temperature of the vapor stream exiting the stripper from 35 °C to 1.5 °C) is -6.6 MW. The energy requirements of this process are listed in Table 5.2. As the previous case, the analysis is done in the following sections.

### 5.5.3 Recovery using flash and stripping with hot nitrogen

In this case, a flash drum operating at 6.22 kPa (pressure at which the toluene in the vapor outlet can be condensed with cooling water) is located immediately after the EDC. Toluene is obtained in the vapor outlet of the flash and is condensed. The remaining toluene is recovered from the IL by a stripping column operating at pressures higher than 6.22 kPa. Because the amount of toluene is lower, the nitrogen flow needed to remove

the toluene decreases in comparison with the previous case. However, the toluene needs to be recovered again from the nitrogen. The reason why this technology is studied is the expected increase of the temperature at which this recovery is taking place. The flow diagram of this technology and its results are shown in Figure 5.7.

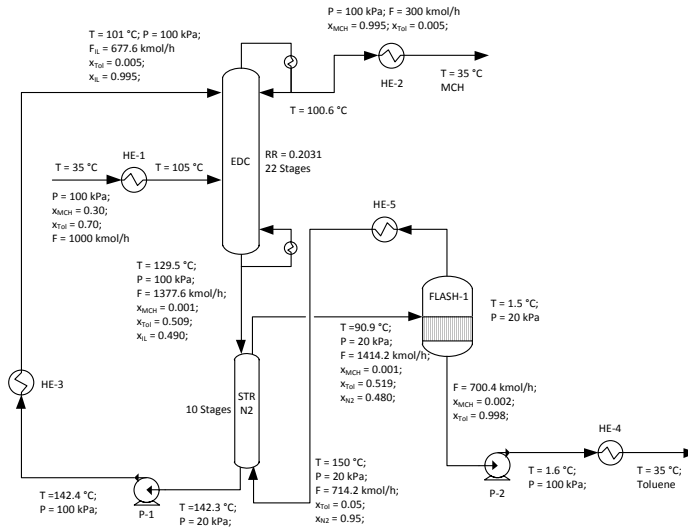


Figure 5.6: ED process using ILs. Recovery using stripping with hot nitrogen

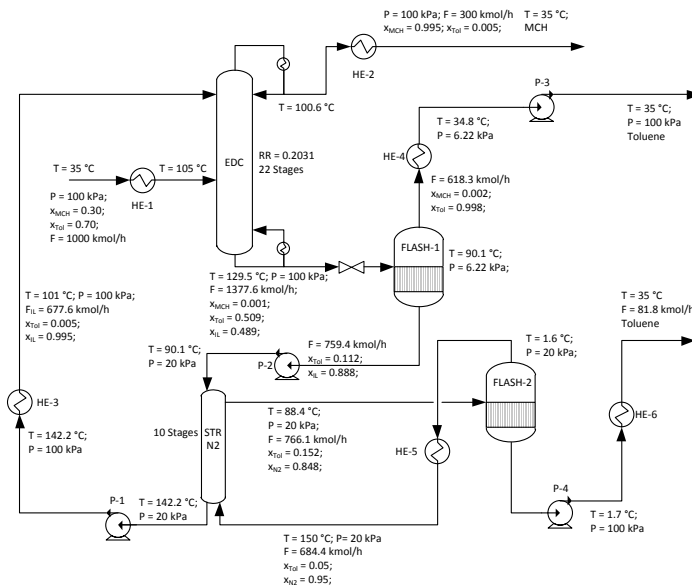


Figure 5.7: ED process using ILs. Recovery with flash + stripping with hot nitrogen

Taking the same nitrogen purity and stripping pressure as in the previous case, the nitrogen flow needed to remove the toluene is 684.4 kmol/h. A reduction of only 4.2 % is



achieved. Besides, the temperature at which the toluene needs to be recovered from the nitrogen is hardly affected by such a small reduction in the flow (only an increase of 0.1 K is obtained). Due to the small reduction in the nitrogen flow, the total energy requirements of the process are hardly affected, as can be seen in Table 5.2. Besides, this process does not look more promising in terms of capital costs than the previous technology (more units need to be used). Due to these reasons, the combination of flash drum and stripping with hot nitrogen is not further studied in this work.

#### 5.5.4 Recovery using stripping with hot methylcyclohexane

This technology consists of an EDC in which MCH with the desired purity is obtained overhead as described by Beste et al. [3]. The IL together with the toluene exits the EDC in the bottom stream, which is fed to a flash drum operating at 6.22 kPa. Toluene is obtained as a vapor and is condensed with cooling water. The liquid stream obtained in the flash drum is fed to a stripping column operating with hot MCH vapor as stripping agent. This stream is obtained from the vapor outlet of the partial condenser of the EDC. It removes the remaining toluene from the IL. The IL reaches the desired purity and is recycled back to the extractive distillation column. The outlet vapor obtained in the stripping column contains toluene and MCH. This stream is condensed, re-pressurized (by a pump) and sent back to the EDC.

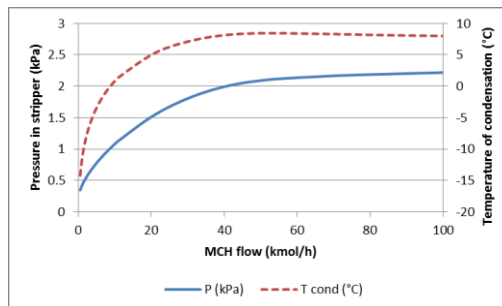


Figure 5.8: Influence of the MCH flow on the maximum stripper pressure and toluene condensation temperature

Figure 5.8 shows how the MCH flow influences the maximum stripper pressure (needed to reach the desired IL purity) and the temperature to condense the vapor outlet of the stripper, which is recycled back to the EDC. As can be seen, the higher the pressure in the stripper, the larger the flow needed in the stripping column and the easier the condensation of the vapor stream containing MCH and toluene. In this case, the highest value of the condensation temperature is reached when the flow of MCH is greater than 40 kmol/h. To avoid the use of higher vacuum, a pressure of 2 kPa in the stripper is chosen, which gives a flow of 46.1 kmol/h of stripping agent (representing 15% of the MCH entering the ED process) and a condensation temperature of 8.2 °C.

The process and its results can be seen in Figure 5.9. It should be noticed that in this case, the pressure in the flash drum is 6.22 kPa which allows condensing the toluene with cooling water. The pressure in the stripper should be decreased until 2 kPa. In this unit, the IL is recovered at the desired purity and the MCH mixed with recovered toluene is

condensed at 8.2 °C and 2 kPa. This stream is then re-pressurized, heated up and recycled back to the EDC. Due to its composition, the stream was fed in the 13<sup>th</sup> stage of the EDC.

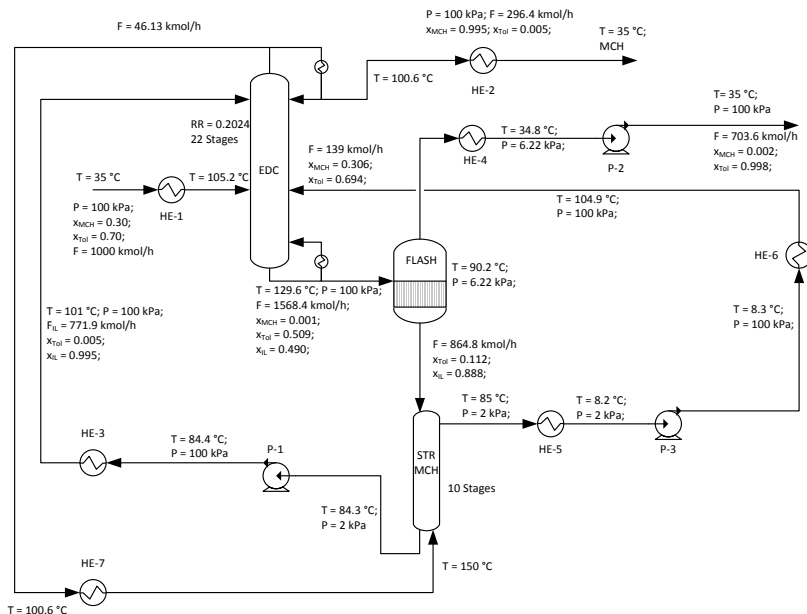


Figure 5.9: ED process using ILs. Recovery using stripping with hot MCH

The duty of the refrigeration system was obtained as in the previous processes; however, in this case, the duty of the refrigerant system is estimated with a stream temperature of 8.2 °C which results in an evaporation temperature of the refrigerant of -1.8 °C. Thus, the cooling duty (energy required to decrease the temperature and condense the vapor exiting the stripper from 35 °C to 8.2 °C) is -1.6 MW. The energy requirements of this process are listed in Table 5.2. The results are analyzed in the coming sections.

### 5.5.5 Recovery using supercritical CO<sub>2</sub> extraction

It has been proposed to use supercritical CO<sub>2</sub> (SCCO<sub>2</sub>) to extract organic compounds from ILs [4, 11, 12]. This technology makes use of the capabilities of SCCO<sub>2</sub> to solubilize the organic compounds. At supercritical conditions, the CO<sub>2</sub> is soluble in ILs (to some extent) but they are not soluble in SCCO<sub>2</sub>. Then, the supercritical phase will be composed by CO<sub>2</sub> and the recovered volatile compound and the liquid phase will contain IL and SCCO<sub>2</sub>.

The critical pressure and temperature for the CO<sub>2</sub> are 7.38 MPa and 30.9 °C [10]. Ng and Robinson [13] had reported equilibrium phase properties for the mixture toluene and CO<sub>2</sub>. From their data, the distribution coefficient at 8.4 MPa and 120.6 °C of the toluene is 0.0742. CO<sub>2</sub> solubilities in different ILs had been reported at different conditions [14-17]. A representative value of the solubility of CO<sub>2</sub> in imidazolium-based ILs at the conditions mentioned above is 1.07 kmol CO<sub>2</sub>/kmol IL. With the help of mass balances, the minimum CO<sub>2</sub> flow can be calculated, and the inlet and outlet conditions can be obtained [10]. It should be mentioned that, as in stripping, the actual CO<sub>2</sub> flow was taken as 1.5 times the minimum flow. The results and the flow sheet of the process can be seen in Figure 5.10.

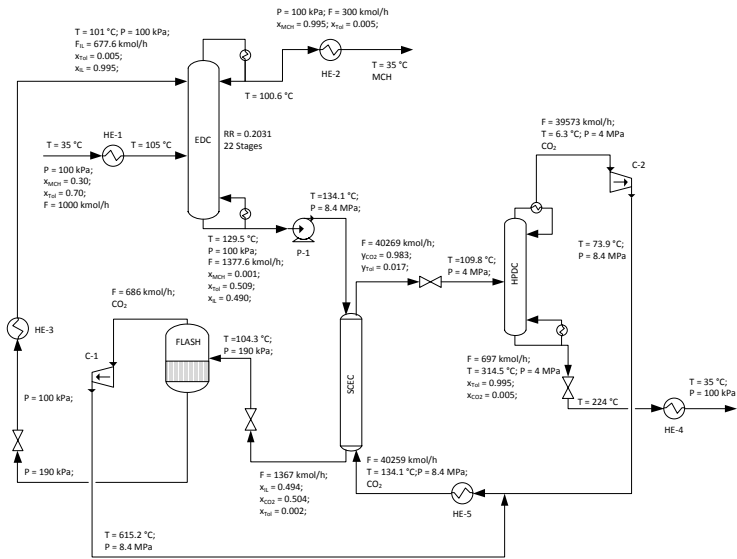


Figure 5.10: ED process using ILs. Recovery using extraction with supercritical CO<sub>2</sub>

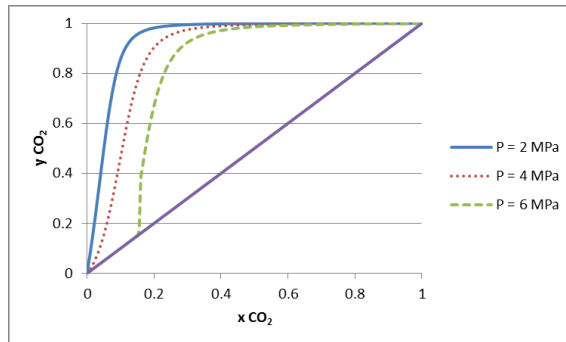


Figure 5.11: Equilibrium composition diagram for the VLE of CO<sub>2</sub> + toluene at three different pressures

The carbon dioxide dissolved in the liquid phase (689 kmol/h) needs to be recovered by depressurization of the liquid stream until 190 kPa [14]. Then, the dissolved CO<sub>2</sub>, which after decompression is in vapor phase, needs to be re-compressed to 8.4 MPa. If this is done in a single compressor (unit C-1 in Figure 5.10), the work required is 4.6 MW. The outlet temperature of this stream will be 615.2 °C. The gas exiting the supercritical extraction column (SEEC) contains the recovered toluene diluted in CO<sub>2</sub>. At higher pressures than 6 MPa, highly pure toluene cannot be obtained by simple condensation, as can be seen in Figure 5.11.

Figure 5.11 was obtained with Soave-Redlich-Kwong equation of state (SRK EOS) as suggested by Raal and Mühlbauer [18] for this binary system. The pressure needs to be decreased; however, to obtain toluene at the desired purity, several equilibrium stages need to be used. One of the most efficient technologies to remove volatiles from CO<sub>2</sub> are the so called high pressure distillation columns (HPDCs) [10, 19, 20] which make use of

partial condensers to reflux some of the CO<sub>2</sub>. The overhead product is obtained in vapor phase. In this work, the mixture exiting the SCEC is expanded until 4 MPa and fed to the HPDC. In this column, the CO<sub>2</sub> is obtained overhead and the toluene is recovered at the bottom. The carbon dioxide needs to be re-compressed using 19.9 MW. The temperature of this streams increases from 6.3 to 73.9 °C. This stream can be mixed with the CO<sub>2</sub> that was dissolved in the IL and recovered by decompression. Due to the mixing, the final temperature of the recovered CO<sub>2</sub> is 81 °C. This mixed stream needs to be heated up until 134.1 °C to be able to reuse it in the SCEC. However, due to the large flow, the energy duty of the heat exchanger (HE-5) is 35.3 MW.

There are more units which require energy supply/removal; however, merely the re-compression and re-heating of the CO<sub>2</sub> leads to a total energy requirement of 59.8 MW. Only these units require two times more energy than the whole conventional process using NMP. The total energy requirement of this process (extractive distillation column and the recovery technology) is 98 MW (Table 5.2). The recovery and recycling of the supercritical CO<sub>2</sub> requires 88% of the total energy duty of this process. Besides, due to its solubility in the ILs, extra units are necessary to remove the dissolved CO<sub>2</sub>. According to these results, it can be concluded that the extraction with supercritical CO<sub>2</sub> is not a suitable technology to recover ILs. This technology is no longer study in this work.

#### 5.5.6 Summary

The energy requirements of each unit of every process (including the EDC and the solvent recovery process) are shown in Table 5.2. In Figure 5.12, the energy requirements of each process are compared. As mentioned before, due to the re-heating and re-compression (in the case of the recovery using SCCO<sub>2</sub>), the technologies using nitrogen and CO<sub>2</sub> showed the higher energy duties than the other recovery technologies. Using a combination of flash and nitrogen stripping, 14% less energy is required in the process. However, other technologies shown in this work give greater energy savings. For these reason, processes using stripping with nitrogen and extraction with supercritical CO<sub>2</sub> are not further analyzed in this work.

The ED process using a flash operating at 150 °C to recover the IL, presented energy savings of 25% compared with the conventional ED process using NMP. It should be mentioned that the energy required in the refrigeration system of this process (W-REFRI in Table 5.2) represents 9% of the total energy input due to the large quantity of toluene that needs to be cooled down and condensed (all the toluene fed to the process need to be treated in this way), and to the temperature at which this process is taking place (5.3 °C).

In the process where the IL is recovered by stripping with MCH, the refrigeration energy only represents 3% of its total energy duties. In this case, only 20% of the total amount of toluene fed to the process is treated by the refrigeration system. The recovery using MCH as stripping agent looks the most promising technology to purify the IL, giving total energy savings of 50%. In the following section, the heat integration for the conventional ED process and the processes where the IL is recovered with a flash drum and stripping with MCH is presented.

Table 5.2: Energy requirements of the ED process with ILs using five different recovery technologies

Unit	Energy requirements (MW)									
	Flash @ 150 °C		Stripping with N2		Flash + Stripping		Stripping with MCH		SCCO2	
	Output	Input	Output	Input	Output	Input	Output	Input	Output	Input
EDC-Cond	-3.3		-3.3		-3.3		-3.3		-3.3	
EDC-Reb		7.4		7.4		7.4		8.4		7.4
HE-1		3.5		3.5		3.5		3.5		3.5
HE-2	-1.1		-1.1		-1.1		-1.1		-1.1	
HE-3	-5.8		-4.8		-4.8		2.2		-0.4	
HE-4	-10.9			1.0	-7.6		-8.6		-11.9	
HE-5		0.9		14.9		14.3		-1.8		35.3
HE-6						0.1		0.7		
HE-7								0.1		
Q-FLASH1		9.2		-17.6		0	0		0	
Q-FLASH2						-8.6				
P-1		$5.8 \times 10^{-3}$		$4.7 \times 10^{-3}$		$4.7 \times 10^{-3}$		$6.3 \times 10^{-3}$		0.7
P-2		$3.0 \times 10^{-3}$		$2.4 \times 10^{-3}$		$0.8 \times 10^{-3}$		$2.9 \times 10^{-3}$		
P-3						$2.6 \times 10^{-3}$		$0.9 \times 10^{-3}$		
P-4						$0.5 \times 10^{-3}$				
SCEC-Cond										-65.6
SCEC-Reb										10.9
C-1										4.6
C-2										19.9
W-REFRI		(2.0)		(1.8)		(1.0)		(0.4)		(15.7)
<b>Total</b>	<b>-21.1</b>	<b>21.0</b> <b>(23.0)</b>	<b>-26.8</b>	<b>26.8</b> <b>(28.6)</b>	<b>-25.4</b>	<b>25.3</b> <b>(26.3)</b>	<b>-14.8</b>	<b>14.9</b> <b>(15.3)</b>	<b>-82.3</b>	<b>82.3</b> <b>(98.0)</b>

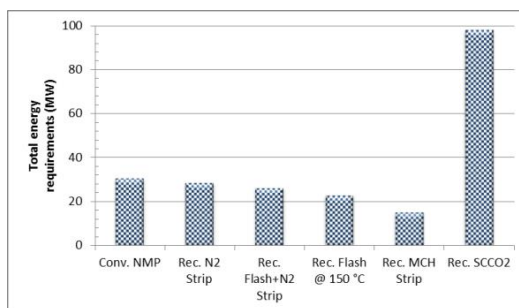


Figure 5.12: Total energy requirements for the ED process (ED column + recovery technologies)

## 5.6 Energy analysis

In this section, the heat integration analysis is done for the conventional ED and the two selected processes using IL (recovery of the IL with a flash drum and MCH stripping). The composite curves are used to determine the maximum energy that can be recovered using process-to-process heat exchangers. It also gives information about the minimum energy requirements (minimum usage of heating and cooling utilities, also called targets, when exchanging heat between hot and cold streams within a process). The composite curves and the heat integration were created with methods proposed in literature [5, 9] and using *Aspen Energy Analyzer V7.2*, taking a minimum temperature difference ( $\Delta T_{min}$ ) of 10 K. It was assumed that the heat-capacity flow rate (product of the heat capacity and the flow rate of the stream) does not vary with temperature, except for the cases where phase changes are present (in those cases, the enthalpy of the stream is discretized into several segments and linearized with respect to the temperature following the procedure reported in the literature [5, 9]).

Figure 5.13 shows the composite curve for the conventional process using NMP. It can be seen that the heating and cooling targets (minimum energy input and output to the process) are 20.7 and 20.8 MW, respectively. Performing the heat integration, a maximum of 9.8 MW can be recovered. In such a case where all of the recoverable energy is transfer within the process, the total energy requirements of the conventional ED process are reduced until 20.7 MW. This implies an energy reduction of 32% in comparison with the process without heat integration.

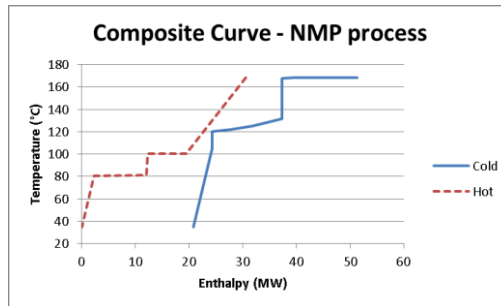


Figure 5.13: Composite curve for the conventional ED process

The same methodology was applied for the processes using IL. The composite curves were obtained and they are shown in Figure 5.14(a) for the process using a flash drum at 150 °C to recover the IL and Figure 5.14(b) for the process using stripping with MCH.

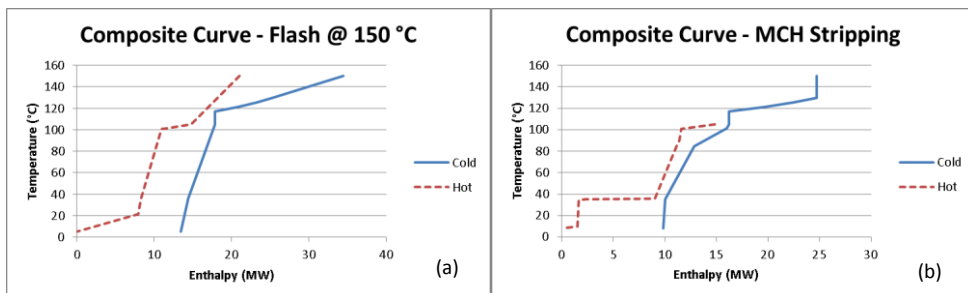


Figure 5.14: Composite curves for the ED processes using ILs. (a) Recovery with flash at 150 °C and (b) Recovery using stripping with hot MCH

The composite curve for the process using the flash drum (Figure 5.14(a)) shows that the heating and cooling targets are 13.4 MW. It should be noticed that some of the energy should be removed with a refrigerant due to the low temperatures reached in this process. Performing the heat integration, a maximum of 7.6 MW can be recovered which results in a total energy requirement of 15.5 MW (33% lower than the process without heat integration). Compared with the heat-integrated conventional ED process, a maximum energy saving of 25 % can be obtained using IL as solvents and recovering it with a flash drum.

In Figure 5.14(b), the composite curve for the process using MCH to recover the IL is shown. It can be seen that the heating and cooling targets are 9.9 MW. Like in the previous case, some of the energy should be removed with a refrigerant. A maximum of 5

MW can be recovered carrying out the heat integration which gives a total energy requirement of 10.2 MW saving 33 % of the energy. Compared with the conventional process, a maximum of 51 % of the energy can be saved when the IL is recovered with stripping with MCH and when the process is completely heat-integrated.

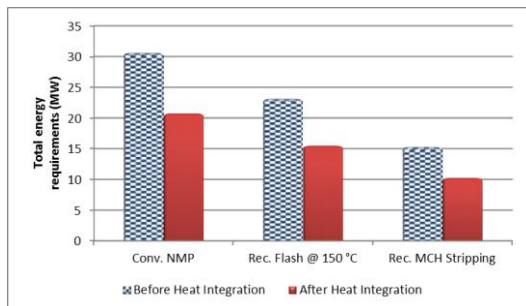


Figure 5.15: Energy requirements before and after heat integration

Figure 5.15 gives a summary of the energy requirements of the three processes. Heat integration of any of these processes can give 33 % of energy savings. This means that before and after heat integration similar energy savings (expressed in percentage) are achieved. This is mainly due to the energy content of the solvent which is recycled back to the EDC. Its available energy can be transferred back to a process stream in a process-to-process heat exchanger. The large amount of energy that can be saved shows the importance of performing heat integration during the design of sustainable processes.

As supplementary information, the heat exchanger networks for the selected processes are proposed and shown in appendix 5.3. The heat exchanger duties and areas are shown in Table 5.11 in the same appendix.

## 5.7 Conclusions

In this chapter, the design of the ED process using NMP (conventional solvent) and the IL 1-hexyl-3-methyl-imidazolium tetracyanoborate ([HMIM][TCB]) was shown. For the conventional process, the EDC uses 30 stages with a solvent to feed (S/F) mass ratio of 1.45. Due to the larger selectivity of the IL, the number of stages in the distillation column is decreased to 22 stages. However, due to its high molecular weight, this process uses a solvent to feed mass ratio of 2.03.

Comparing the conventional and IL EDCs, a total of 43 % of the energy in the reboiler can be saved due to the non-volatility of the IL and its selectivity. The most promising IL recovery technologies according to the energy requirements were: recovery using flash evaporation at 150 °C and stripping with hot MCH as stripping agent.

Heat integration (HI) analysis showed that 33% of energy can be saved in every process (including the conventional ED using NMP). After HI, a total of 25% and 51% of the energy can be saved when the IL is used and recovered with flash and MCH stripping, respectively. The large energy savings achieved by recovering the IL with hot MCH in a

stripping column makes this technology the most suitable process to recover, purify and recycle the solvent.

From the heat exchanger network, it can be concluded that the selected technology utilizes 1.7 times more heat exchangers and 7 times more transfer area than the conventional process using NMP.

## 5.8 References

1. Folkins, H.O., *Benzene*, in *Ullmann's Encyclopedia of Industrial Chemistry* 2005, WILEY-VCH.
2. Weissermel, K. and H.J. Arpe, *Industrial Organic Chemistry*. 4 ed 2003: WILEY-VCH. 491.
3. Beste, Y.A., H. Shoenmakers, W. Arlt, M. Seiler, and C. Jork, *Recycling of Ionic Liquids Produced in Extractive Distillation*, BASF, Editor 2006.
4. Haerens, K., S. Van Deuren, E. Matthijs, and B. Van der Bruggen, *Challenges for recycling ionic liquids by using pressure driven membrane processes*. *Green Chemistry*, 2010. **12**(12): p. 2182-2188.
5. Seider, W.D., J.D. Seader, and D.R. Lewin, *Product and process design principles : synthesis, analysis, and evaluation*. 2nd ed 2004, New York: Wiley. xviii, 802 p.
6. Tiverios, P.G. and V. Van Brunt, *Extractive Distillation Solvent Characterization and Shortcut Design Procedure for Methylcyclohexane-Toluene Mixtures*. *Ind. Eng. Chem. Res.*, 2000. **39**(6): p. 1614-1623.
7. Chen, B., Z. Lei, and J. Li, *Separation on Aromatics and Non-aromatics by extractive distillation with NMP*. *Journal of Chemical Engineering of Japan*, 2003. **36**(1): p. 20-24.
8. Ko, M., S. Na, J. Cho, and H. Kim, *Simulation of the aromatic recovery process by extractive distillation*. *Korean Journal of Chemical Engineering*, 2002. **19**(6): p. 996-1000.
9. Smith, R., *Chemical process design and integration* 2005, Chichester, West Sussex, England ; Hoboken, NJ: Wiley. xxiii, 687 p.
10. Seader, J.D. and E.J. Henley, *Separation Process Principles*. 2 ed 2005: Wiley. 800.
11. Blanchard, L.A. and J.F. Brennecke, *Recovery of Organic Products from Ionic Liquids Using Supercritical Carbon Dioxide*. *Ind. Eng. Chem. Res.*, 2001. **40**(1): p. 287-292.
12. Aki, S.N.V.K., A.M. Scurto, and J.F. Brennecke, *Ternary Phase Behavior of Ionic Liquid (IL)-Organic-CO<sub>2</sub> Systems*. *Ind. Eng. Chem. Res.*, 2006. **45**(16): p. 5574-5585.
13. Ng, H.-J. and D.B. Robinson, *Equilibrium-phase properties of the toluene-carbon dioxide system*. *Journal of Chemical & Engineering Data*, 1978. **23**(4): p. 325-327.
14. Kumetan, J., Á. Pérez-Salado Kamps, D. Tuma, and G. Maurer, *Solubility of CO<sub>2</sub> in the ionic liquid [hmim][Tf<sub>2</sub>N]*. *The Journal of Chemical Thermodynamics*, 2006. **38**(11): p. 1396-1401.
15. Lim, B.-H., W.-H. Choe, J.-J. Shim, C. Ra, D. Tuma, H. Lee, and C. Lee, *High-pressure solubility of carbon dioxide in imidazolium-based ionic liquids with anions [PF<sub>6</sub>]<sup>-</sup> and [BF<sub>4</sub>]<sup>-</sup>*. *Korean Journal of Chemical Engineering*, 2009. **26**(4): p. 1130-1136.



16. Shariati, A. and C.J. Peters, *High-pressure phase equilibria of systems with ionic liquids*. The Journal of Supercritical Fluids, 2005. **34**(2): p. 171-176.
17. Aki, S.N.V.K., B.R. Mellein, E.M. Saurer, and J.F. Brennecke, *High-Pressure Phase Behavior of Carbon Dioxide with Imidazolium-Based Ionic Liquids*. The Journal of Physical Chemistry B, 2004. **108**(52): p. 20355-20365.
18. Raal, J.D. and A.L. Mühlbauer, *Phase equilibria : measurement and computation*. Series in chemical and mechanical engineering 1998, Washington, D.C.: Taylor & Francis. xxiii, 461 p.
19. DeFilippi, R.P. and J.E. Vivian, *Process for separating organic liquid solutes from their solvent mixtures*, 1982.
20. Martinez, J.L., *Supercritical fluid extraction of nutraceuticals and bioactive compounds* 2008, Boca Raton, FL: CRC Press. xv, 402 p.
21. Stephan, K. and H. Hildwein, *Recommended data of selected compounds and binary mixtures*. Chemistry data series 1987, Frankfurt am Main: DECHEMA. I, 661 p.
22. Gutierrez, J.P., W. Meindersma, and A.B. de Haan, *Binary and ternary (liquid-liquid) equilibrium for {methylcyclohexane (1)+toluene (2)+1-hexyl-3-methylimidazolium tetracyanoborate (3)}/1-butyl-3-methylimidazolium tetracyanoborate (3)}*. The Journal of Chemical Thermodynamics, 2011. **43**(11): p. 1672-1677.
23. Yaws, C.L., *The Yaws handbook of thermodynamic properties for hydrocarbons and chemicals* 2006, Houston, Tex.: Gulf Pub. iv, 777 p.
24. Yaws, C.L., *Thermophysical properties of chemicals and hydrocarbons* 2008, Norwich, NY: William Andrew. x, 809 p.
25. Green, D.W. and R.H. Perry, *Perry's Chemical Engineers' Handbook (8th Edition)*, 2008, McGraw-Hill.
26. Yaws, C.L., *Transport properties of chemicals and hydrocarbons : viscosity, thermal conductivity, and diffusivity of C1 to C100 organics and Ac to Zr inorganics* 2009, Norwich, NY: William Andrew.
27. Poling, B.E., J.M. Prausnitz, and J.P. O'Connell, *The properties of gases and liquids*. 5th ed 2001, New York: McGraw-Hill. 1 v. (various pagings).

## Appendix 5.1: Thermodynamic and physical properties

The fugacity of the compounds in the vapor and liquid phase were predicted with the Raoult's law and an activity coefficient model, respectively, following the equation 5.5.

$$y_i P = x_i \gamma_i P_i^{sat} \quad 5.5$$

Where,  $P$  holds for the total pressure,  $\gamma_i$ ,  $P_i^{sat}$ ,  $y_i$  and  $x_i$  are the activity coefficient, vapor pressure, vapor and liquid composition of the compound  $i$ , respectively. The vapor pressure of the volatile compounds was calculated with the Antoine equation (5.6).

$$\ln(P_i^{sat} / kPa) = A_i + \frac{B_i}{T/K + C_i} \quad 5.6$$

with the parameters shown in Table 5.3.

Table 5.3: Antoine constants for MCH, toluene and NMP

Constant	MCH [1]	Toluene [1]	NMP <sup>4</sup>
A	13.6063	14.0701	15.0743
B	-2878.74	-3141.17	-4405.898
C	-53.8723	-51.4554	-54.9298

In literature, the ternary vapor-liquid equilibrium experimental data for the system MCH + toluene + NMP was not found. Therefore, ternary experiments to determine the relative volatility were performed in our laboratory with headspace technique (described in Chapter 2) at temperatures of 30 and 35 °C (the data is shown in Figure 5.16). The NRTL thermodynamic model was selected and its parameters are reported in Table 5.4.

Table 5.4: NRTL parameters for the ternary system MCH, toluene and NMP

$i$	MCH	MCH	Toluene
$j$	Toluene	NMP	NMP
$a_{ij}$	0	0	0
$a_{ji}$	0	0	0
$b_{ij}$	-43.2404	834.8067	923.7569
$b_{ji}$	134.0625	330.3512	-256.3133
$\alpha_{ij}$	0.3	0.3	0.3

The Figure 5.16 compares the experimental and regressed data with the values predicted with the default parameters reported *Aspen plus v7.2* for the NRTL model. It can be seen that the regressed and reported parameters are able to represent the ternary system at solvent to feed mass ratios lower than 1. From this figure it can be concluded that the regressed NRTL parameters are able to represent the experimental data yielding a root mean square error of 0.0842.

<sup>4</sup> Regressed from our experimental data. RMS = 0.0990.

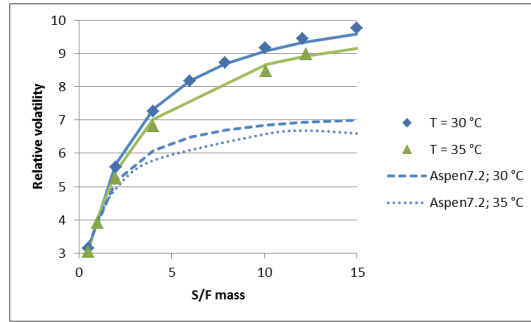


Figure 5.16: Comparison of experimental (symbols) and calculated (lines) relative volatilities for the ternary mixture MCH + Toluene + NMP. The solid and dashed lines represent the regressed data and the calculated data with Aspen parameters, respectively.

For the mixture with the ionic liquid, the UNIQUAC model using the parameters obtained in Chapter 3 and reported in Table 5.5 were selected [2].

Table 5.5: UNIQUAC parameters for the ternary system MCH, toluene and ILs

i	MCH	MCH	Toluene	MCH	Toluene
j	Toluene	[HMIM][TCB]	[HMIM][TCB]	[BMIM][TCB]	[BMIM][TCB]
$a_{ij}$	0	-3.5766	2.5666	6.9708	8.5816
$a_{ji}$	0	0.8286	0.2403	-0.8646	-0.7278
$b_{ij}$	-25.3041	378.549	-1733.290	-2804.825	-3515.548
$b_{ji}$	-2.312	-166.264	220.374	310.424	488.981

The van der Waals volume and surface parameters for UNIQUAC model are listed in Table 5.6 [2].

Table 5.6: van der Waals volume and surface parameters for MCH, toluene and ILs

	MCH	Toluene	[HMIM][TCB]	[BMIM][TCB]
$r_i$	4.7200	3.9228	8.1611	7.1645
$q_i$	3.7760	2.9680	6.7289	5.9316

The liquid heat capacities were calculated with a polynomial equation (5.7) and the parameters used in the simulations are shown in Table 5.7. The volatile compound heat capacity parameters were obtained from literature [3]; the parameters for the ILs were obtained by differential scanning calorimetric measurements in our laboratory.

$$C_p / \text{Jmol}^{-1} \text{K}^{-1} = A + BT/K + CT/K^2 + DT/K^3 + ET/K^4 \quad 5.7$$

For the enthalpy calculations, the liquid phase at 298.15 K and 100 kPa was taken as the reference state. The heats of vaporization for the volatile compounds were predicted with the equation 5.8. The parameters for this equation are shown in Table 5.8, which are reported in literature [4]. It should be noticed that due to the non-volatility of the ionic liquid, their enthalpy of vaporization and vapor pressure were set to zero.

Table 5.7: Heat capacity constants for MCH, toluene, NMP and ILs

Compound	MW	A	B	C	D	E
MCH	98.19	159.2841	-0.17606	-7.27075E-4	9.64300E-6	-1.41539E-8
Toluene	92.14	256.5334	-1.66009	7.521110E-3	-1.27973E-5	8.35574E-9
NMP	99.13	362.0696	0.277024	-5.98452E-4	7.89863E-7	0
[HMIM][TCB]	282.2	419.3142	0.5171	0	0	0
[BMIM][TCB]	254.1	377.3544	0.4040	0	0	0

$$\Delta H^{vap} / kJ mol^{-1} = A \left( 1 - \frac{T/K}{T_c/K} \right)^n \quad 5.8$$

Table 5.8: Heat of vaporization parameters for MCH, toluene and NMP

Compound	A	$T_c/K$	n
MCH	49.4195	572.2	0.415
Toluene	50.139	591.8	0.383
NMP	63.7494	724.0	0.332

The vapor pure component enthalpy was calculated from liquid enthalpy and enthalpy of vaporization. In the enthalpy predictions, deviations from ideality were neglected in the liquid and vapor phase and the enthalpy of mixtures was calculated with the mole fraction average of the pure component enthalpies.

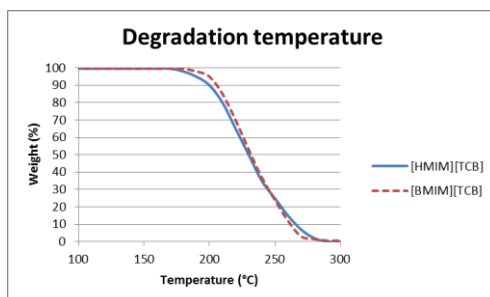


Figure 5.17: Degradation temperature of the ILs determined by TGA under  $N_2$  atmosphere

In Figure 5.17, the degradation temperatures of the ILs studied in this chapter are shown. The experiments were done in a TGA (Thermogravimetric Analyzer) TA instruments model Q500 under nitrogen atmosphere. The temperature was varied from 30 °C till 250 °C with a ramp of 2 °C/min. It can be seen that the IL starts to decompose at 170 °C. In this work and for safety reasons, a maximum process temperature of 150 °C is selected.



## Appendix 5.2: Extractive distillation column (EDC) profiles for the separation of MCH and toluene

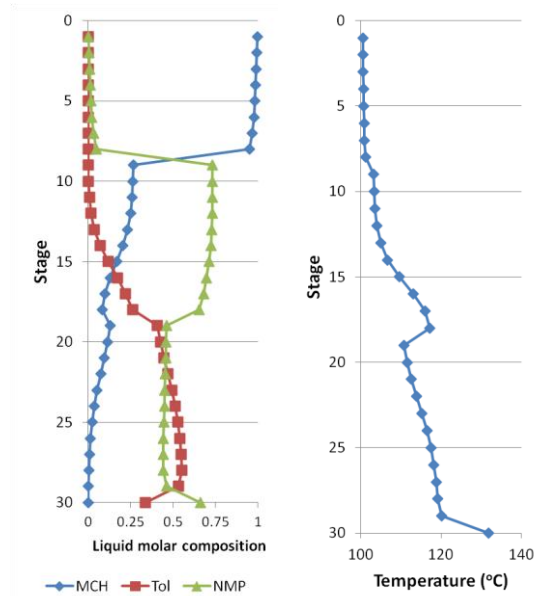


Figure 5.18: Liquid molar composition (left) and temperature (right) profiles for the EDC using the conventional solvent NMP

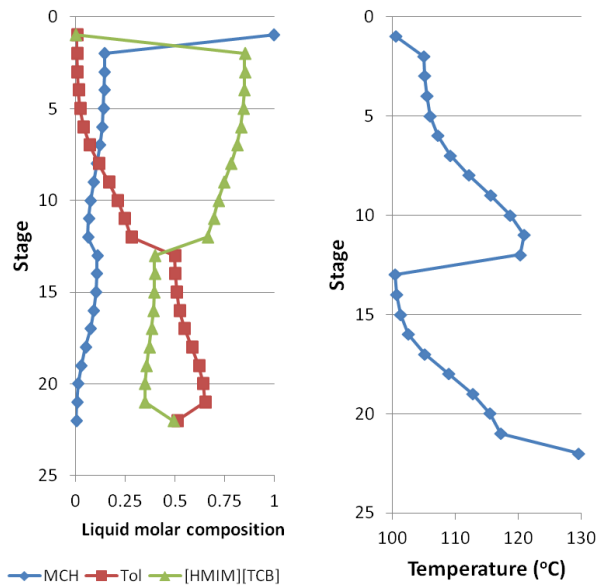


Figure 5.19: Liquid molar composition (left) and temperature (right) profiles for the EDC using the IL [HMIM][TCB]

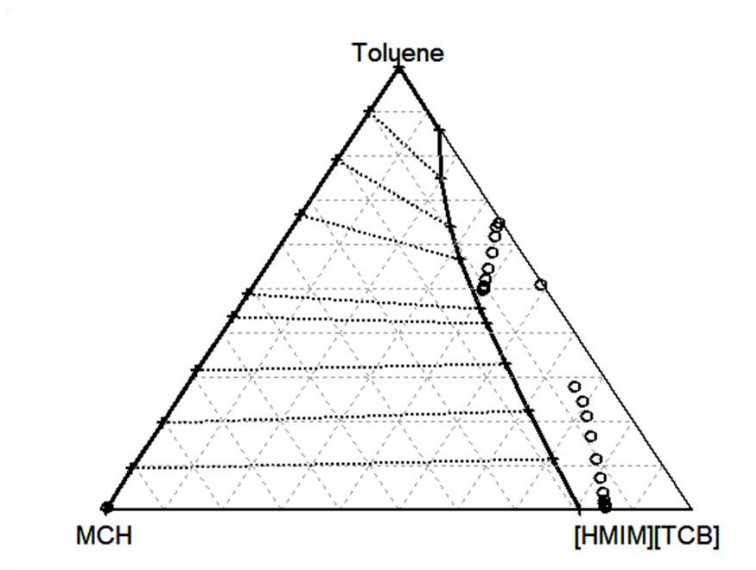


Figure 5.20: Liquid molar composition profile inside the EDC using [HMIM][TCB] as solvent. Envelope estimated with the UNIQUAC model at 100°C

### Appendix 5.3: Heat exchanger networks (HEN's)

In this section, the design of the heat exchanger network (HEN) is done. It should be mentioned that the designs proposed in this work are not the most optimal. They are done in such a way that all of the available energy is recovered in the most logical way. High pressure steam at 250 °C and cooling water at 20 °C are chosen as utility streams. If necessary, a refrigerant is used to decrease the temperature until values lower than 30 °C. In this work, the refrigerant is not defined; however, according to the temperatures reached in the processes propylene, propane, ammonia, tetrafluoroethane, among others, can be used [1, 2].

HEN designs are done to have an idea on how the actual process would look like and to make a comparison of the HEN, transfer areas and number of heat exchangers needed in the processes. A minimum temperature difference of 10 K was fixed and average values for the film heat transfer coefficients were taken (Table 5.9). These values were obtained with the equation 5.9 for multiple conditions of temperatures and pressures and for multiple concentrations.

$$\frac{h \times D}{k} = 0.023Re^{0.80}Pr^{1/3} \quad 5.9$$

Where  $h$ ,  $D$  and  $k$  hold for the film heat transfer coefficient (HTC), flow area diameter (taken as 2.54 cm) and thermal conductivity, respectively. The Reynolds ( $Re$ ) and Prandtl ( $Pr$ ) numbers are defined in equation 5.10.

$$Re = \frac{D \times \rho \times v}{\mu} \quad 5.10$$
$$Pr = \frac{C_p^{ef} \times \mu}{k}$$

Where  $\rho$ ,  $v$ ,  $\mu$  and  $C_p^{ef}$  refer to the stream density, velocity (taken as 1 m/s), viscosity and the effective heat capacity, respectively. The effective heat capacity comes from a simple energy balance of a heat exchanger where the heat load ( $Q$ ), mass flow ( $m$ ) and temperature difference ( $\Delta T$ ) are known (equation 5.11).

$$C_p^{ef} = \frac{Q}{m \times \Delta T} \quad 5.11$$

The properties of the pure components were calculated with the correlations presented by Yaws [3-5] and the properties of mixtures were obtained with the mole (or mass) fraction average of the pure component properties as reported in literature [6]. In this work an approximate design of the network is done; however, it should be mentioned that the detailed design of heat exchangers should be done with more specific correlations. The HTC values listed in Table 5.9 are in agreement with the ones reported in the literature for general conditions and fluids [2, 7].



Table 5.9: Average film heat transfer coefficients

Fluid	$h(W/m^2K)$
Liquid (no solvent)	1250
Liquid (solvent)	1550
Vapor	20
Vapor (LP)	10
Condensation	1050
Condensation (LP)	500
Evaporation	700
Evaporation (LP)	300
HP Steam	8500
Cooling water	3500
Refrigerant	1300

All the hot and cold stream's inlet and outlet temperatures, and heat load (duty) of every process were known from the simulations; the conditions can be seen in Table 5.10. In the last column of this table, the HTC are shown (necessary to determine the transfer area of the heat exchangers). The streams 6 of every process and 7 from the NMP process were discretized due to their phase change. It must be noticed that they represent the reboilers of the distillation columns. These streams are segmented into several parts as a linear approximation to the actual curved behavior of the temperature-enthalpy diagrams when a phase change occurs.

There are more segmented streams in which phase changes are happening (cooling down and condensation of the fluid). The stream number 1 from the second process represents the cooling down and condensation of the toluene after the flash drum. The streams number 3 and 4 from the third process represent the cooling down and condensation of the toluene (coming from the flash drum) and the mixture toluene + MCH (recycled back to the EDC), respectively. These streams are segmented in two parts, one for the cooling down and the other for the condensation.

With the information presented in Table 5.10 and the composite curves (Figure 5.13 and Figure 5.14) the HENs for every process are proposed. In Figure 5.21, the HEN for the process using NMP as solvent is presented. In the following figures, H, C, HE and R refer to hot utility, cold utility, process-to-process and refrigeration heat exchangers, respectively. The hot stream number 1 in the NMP process, representing the cooling down of the solvent after being recovered in the solvent recovery column, has enough energy to exchange with the cold streams. As can be seen in Figure 5.21, a total of 9.848 MW from stream 1 can be used to heat up the streams number 7 and 8, through the heat exchanger HE1 and HE2, respectively. The cold utility heat exchangers (C1 – C5) are used to cool down the streams 1 – 5. In total, 20.750 MW need to be removed using a cool utility (cooling water). The hot utility heat exchangers (H1 and H2) are used to heat up the streams number 6 and 7, using in total 20.733 MW. In this figure, it can be seen that the pinch temperatures are 130.1 and 120.1 °C. As can be seen, there is not heat transfer across the pinch temperatures. In total 9 heat exchangers are necessary, according to the network proposed in Figure 5.21.

Table 5.10: Hot and cold streams conditions for the selected processes

Stream	Description	Inlet T(°C)	Outlet T(°C)	Duty (MW)	$h(W/m^2K)$
<b>1. NMP Process</b>					
1	NMP being recycled	168.6	101.0	11.060	1550
2	Condenser EDC	100.6	100.6	7.182	1050
3	MCH from EDC	100.6	35.0	1.127	1250
4	Condenser SRC	80.9	80.4	9.728	1050
5	Toluene from SRC	80.8	34.9	1.498	1250
6	Reboiler SRC	167.6	168.2	1.989	700
		168.2	168.5	5.046	700
		168.5	168.6	6.920	700
7	Reboiler EDC	120.1	122.2	3.554	700
		122.2	125.3	3.797	700
		125.3	128.1	2.741	700
		128.1	131.8	2.981	700
8	Feed to EDC	35.0	105.2	3.548	1250
<b>2. Recovery with flash @ 150</b>					
1	Condensation of toluene from flash	150.0	21.4	2.964	10
		21.4	5.3	7.971	500
2	IL being recycled	150.0	101.0	5.755	1550
3	Condenser EDC	105.0	100.5	3.263	1050
4	MCH from EDC	100.6	35.0	1.121	1250
5	Bottoms from EDC entering the flash	129.5	150.0	9.234	300
6	Reboiler EDC	117.2	121.3	3.024	700
		121.3	125.4	2.420	700
		125.4	129.5	1.954	700
7	Feed to EDC	35.0	105.0	3.534	1250
8	Toluene after being condensed	5.3	35.0	0.8963	1250
<b>3. Recovery with MCH Stripping</b>					
1	Condenser EDC	105.0	100.6	3.315	1050
2	MCH from EDC	100.6	35.0	1.108	1250
3	Toluene from flash (cooling down and condensation)	90.2	35.9	1.246	10
		35.9	34.9	7.366	500
4	Cooling down and condensation of vapor from stripper	85.0	9.8	0.3469	10
		9.8	8.2	1.499	500
5	Heating of vapor distillate going to stripper	100.6	150.0	0.0976	20
6	Reboiler EDC	117.2	121.3	3.449	700
		121.3	125.4	2.760	700
		125.4	129.6	2.228	700
7	Feed to EDC	35.0	105.0	3.534	1250
8	Heating up of second feed of EDC	8.2	104.8	0.6612	1250
9	IL being recycled	84.3	101.0	2.162	1550

The HEN for the ED process using IL and recovering it with a flash drum is shown in Figure 5.22. In this case, there are 5 process-to-process heat exchangers (HE1 – HE5). A total of 7.631 MW can be recovered by these heat exchangers. There are 2 and 3 heat exchangers for the hot utility (H1 and H2) and for the cold utility (C1 – C3), respectively. A total of 13.431 MW need to be provided by the hot utility and 13.443 MW need to be removed for the cold utility. The use of a refrigerant is necessary to remove 8.170 MW from the hot stream number 1 to be able to decrease the temperature from 35 °C to 5.3 °C. In the proposed HEN, 11 heat exchangers are used. In this case, the pinch temperatures are 127.2 °C – 117.2 °C.

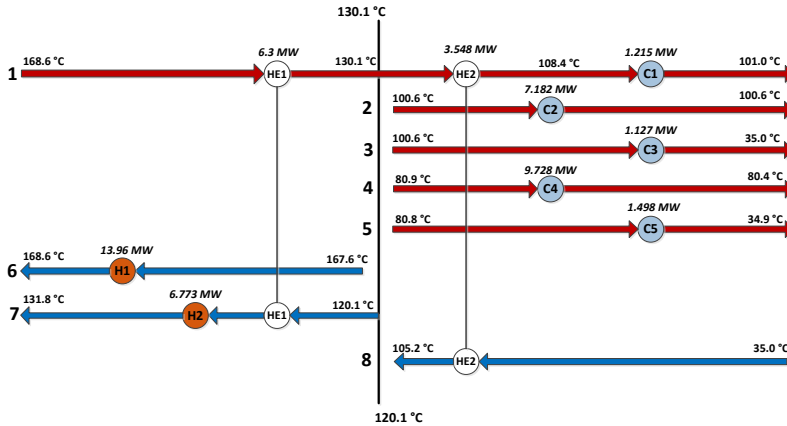


Figure 5.21: Heat exchanger network for the conventional extractive distillation process

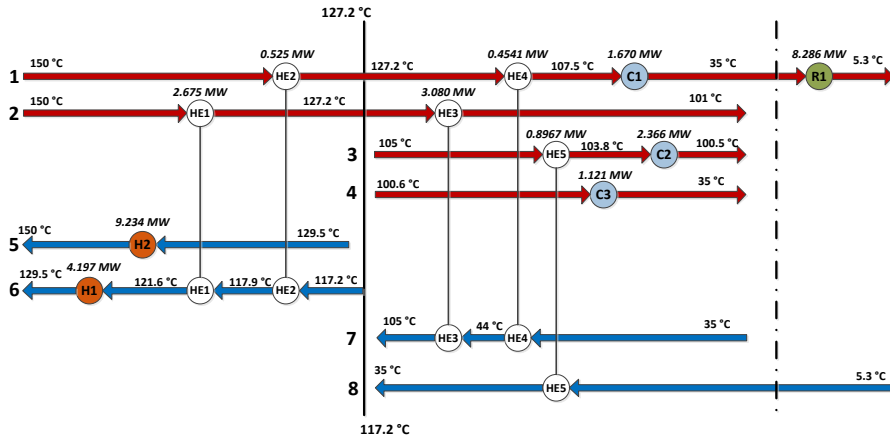


Figure 5.22: Heat exchanger network for the ED process using IIs. Recovery with flash drum at 150 °C

In Figure 5.23, the HEN for the process using hot MCH as a stripping agent to recover the IL used in the ED is shown. As can be seen, there are 6 process-to-process heat exchangers (HE1 – HE6) where 5.013 MW can be recovered. There are 5 and 3 heat exchangers for the hot utility (H1 – H5) and for the cold utility (C1 – C3), respectively. A total of 9.877 MW need to be provided by the hot utility and 13.443 MW need to be removed for the cold utility. Like in the previous case, a refrigerant is necessary to remove 1.615 MW from the hot stream number 4 to be able to decrease its temperature from 35 °C to 8.2 °C. In this process, 15 heat exchangers are used having pinch temperatures of 105 °C – 95 °C. It should be noticed that in this case the stream 1 was divided in 3 sub-streams to be able to bring closer the cold streams to the pinch temperature. Thus, 17.9% of the mass flow of the stream 1 is used to heat up the cold stream 8 from 8.2 to 95 °C; 41.9% of the mass flow of the stream 1 is used to heat up the cold stream 9 from 84.3 to 95 °C and the remaining (40.2% of the mass flow of stream 1) is used to heat up the cold stream 7 from 68.6 to 95 °C.

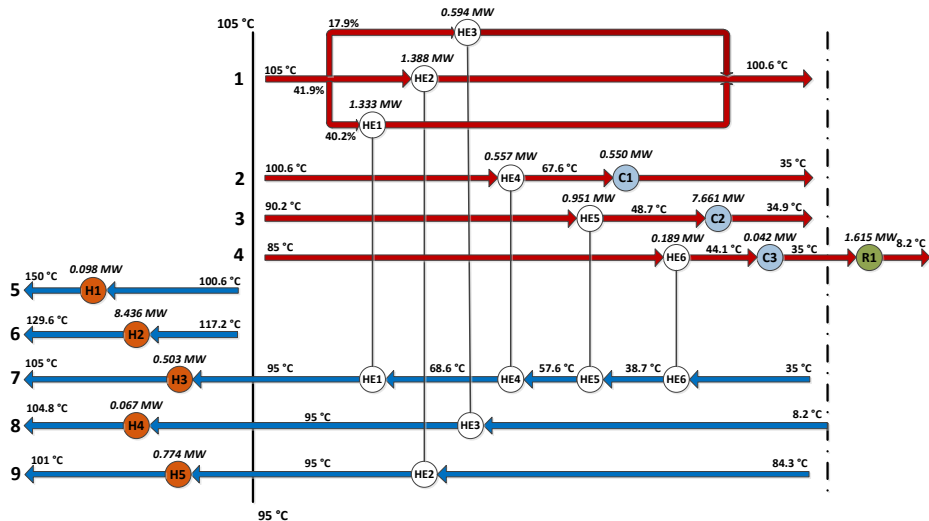


Figure 5.23: Heat exchanger network for the ED process using ILs. Recovery using stripping with hot MCH

The areas of the heat exchangers are obtained using the equation 5.12.

$$A = \frac{Q}{\Delta T_{LM}} \left( \frac{1}{h_c} + \frac{1}{h_h} \right) \quad 5.12$$

Where  $A$  is the transfer area of the heat exchanger,  $Q$  is the duty of the heat exchanger,  $h_c$  and  $h_h$  are the film heat transfer coefficients of the cold and hot stream, respectively, and  $\Delta T_{LM}$  is the log mean temperature difference, defined in equation 5.13.

$$\Delta T_{LM} = \frac{\Delta T_H - \Delta T_C}{\ln(\Delta T_H / \Delta T_C)} \quad 5.13$$

where the subscripts  $H$  and  $C$  refers to the hot and cold side of a countercurrent heat exchanger.

The heat transfer areas for the heat exchangers in every process are shown in Table 5.11. It can be seen that the largest areas are needed when a gas or vapor at low pressure is involved, due to the low HTC's. The heat exchangers for the condensation of toluene at low pressure in the process recovering the IL with a flash drum (C1, R1, HE2 and HE4) need a total area of 9349.7 m<sup>2</sup>. This area represents 91.2 % of the total transfer area needed in the whole ED process. In the case where the IL is recovered with hot MCH as stripping gas, there are two process streams which are at low pressure, the toluene recovered in the flash and the MCH/toluene mixture exiting the stripper in vapor phase (streams number 3 and 4, respectively). For the toluene condensation (C2 and HE5), 8676 m<sup>2</sup> are needed, meanwhile 1489.4 m<sup>2</sup> are needed for the condensation of the vapor outlet of the stripper (C3, R1 and HE6). The condensation of both streams represents 94.6 % of the total transfer area used in the process.

Table 5.11: Heat exchanger areas for the extractive distillation processes

NMP Process			Recovering with flash @ 150 °C			Recovering with MCH stripping		
Heat exchanger	Duty (MW)	Area (m <sup>2</sup> )	Heat exchanger	Duty (MW)	Area (m <sup>2</sup> )	Heat exchanger	Duty (MW)	Area (m <sup>2</sup> )
H1	13.96	273.9	H1	4.197	52.16	H1	0.098	39.79
H2	6.773	89.09	H2	9.234	291.7	H2	8.436	106.2
C1	1.215	13.89	C1	1.670	4719	H3	0.503	3.262
C2	7.182	114.4	C2	2.366	36.15	H4	0.067	0.433
C3	1.127	34	C3	1.121	34.36	H5	0.774	4.160
C4	9.728	200.6	R1	8.286	1205	C1	0.550	25.88
C5	1.498	49.20	HE1	2.675	342.7	C2	7.661	3115
HE1	6.300	601.8	HE2	0.525	2834	C3	0.042	218.9
HE2	3.548	135.1	HE3	3.080	127.1	R1	1.615	383.1
			HE4	0.4541	591.7	HE1	1.333	131.6
			HE5	0.8967	18.83	HE2	1.388	181.2
						HE3	0.594	29.59
						HE4	0.557	49.37
						HE5	0.951	5561
						HE6	0.189	887.4
<b>Total</b>	<b>1512.0</b>		<b>Total</b>	<b>10252.7</b>		<b>Total</b>	<b>10736.9</b>	

Due to the low pressures involved in the recovery, the heat transfer area of the processes using IL as solvents are 7 times higher than for the conventional process. The transfer area needed in both process using IL are similar; however, according to the network proposed in this work, the process where the recovery is done using stripping with MCH uses 6 heat exchangers more than the conventional ED process.

Just as an example, if the shell and tubes heat exchangers are used, for an area of 5000 m<sup>2</sup> (approximate value for HE5 in the case of recovering the IL with MCH stripping) 10000 pipes of 25 mm diameter and 6 m long are necessary (therefore, each pipe will have a heat transfer area of 0.5 m<sup>2</sup>). Compact heat exchangers are suggested in these cases.

## 6. Extractive distillation process design for the separation of ethanol + water using ionic liquids

### Abstract

In this chapter, the feasibility of using ionic liquids (ILs) for the separation of ethanol – water by extractive distillation (ED) is analyzed. In total three solvents were studied: the conventional solvent (ethylene glycol – EG), and the ILs 1-ethyl-3-methyl-imidazolium acetate ([EMIM][OAc]) and 1-ethyl-3-methyl-imidazolium dicyanamide ([EMIM][DCA]). The energy requirements of the ED processes (including recovery of the solvent) are compared, taking as a benchmark the conventional EG-based process. The ILs cannot be recovered by ordinary distillation. In this work, several recovery technologies were studied for both ILs (e.g. simple evaporation, stripping and supercritical extraction). Only after heat integration, the use of ILs appeared to be more attractive, yielding 16% of energy savings compared to the heat integrated conventional process. The strong interactions between water and [EMIM][OAc] make this IL unsuitable due to the difficulties in the recovery and purification of the IL. As a result of their non-volatility and high selectivity, ILs seem to be promising ED solvents for the separation of ethanol – water; however, their recovery conditions and the relatively low energy savings might limit their applicability in industrial scale.

### 6.1 Introduction

Ethanol is an important base chemical which is produced from petrochemical streams or bioprocesses. It has been used as solvent, in cosmetic and food industry, among others. However, ethanol as a (partial) replacement of gasoline has influenced its worldwide demand. Just in the USA,  $42 \times 10^6 \text{ m}^3$  ( $33 \times 10^6$  tons) of ethanol were added to gasoline in 2009, accounting for about 8% of gasoline consumption by volume [1, 2]. Water is involved in the ethanol production chain. This mixture forms an azeotrope with an ethanol content of 95.6 wt.% and its challenging energy-efficient separation has been widely reported [3]

In this work, bio-refinery production data is taken as a model process. Typical plants have an ethanol production capacity of 150-200 kmol/h, with a molar purity  $\geq 99.8\%$  [4]. The fermenter (reactor) produces an aqueous solution containing about 5-12 wt% ethanol. This solution is introduced to an ordinary distillation column (also called pre-concentrator) where the ethanol is purified until 60-90 wt%. Due to the azeotropic composition (95.6 wt% of ethanol), further purification by ordinary distillation becomes unfeasible.

Extractive distillation (ED) has been used to separate and purify the ethanol leaving the pre-concentrator. Anhydrous ethanol is obtained in the overhead of the extractive distillation column (EDC) and the solvent mixed with the water exits the column in the bottom [3]. Ethylene glycol (EG) is one of the most commonly used extractive solvents for ethanol dehydration [3, 5, 6]. This solvent increases the relative volatility of the mixture

and enhances the separation. The EG is recovered by ordinary distillation, and then it is recycled back to the EDC [7, 8].

The more selective the solvent, the more efficient the separation is [8]. Ionic liquids (ILs) can increase the relative volatility of the mixture ethanol-water interacting with both components [1, 9]. The application of ILs to the separation of mixtures of ethanol-water has been reported [3, 10]. However, most of the ILs studied were composed of fluorinated anions, which can react with water, decomposing the ILs and forming the highly corrosive and toxic hydrofluoric acid (HF) [10, 11]. In this work (Chapter 2 and 4) non-fluorinated ILs 1-ethyl-3-methyl-imidazolium acetate [EMIM][OAc] and 1-ethyl-3-methyl-imidazolium dicyanamide [EMIM][DCA] were selected. In this chapter, these ILs are evaluated in an ED process for the separation of ethanol-water taking into account the recovery of the solvent and energy requirements (heat integration).

## 6.2 Thermodynamic and simulation data

In this work, a model feed mixture of 200 kmol/h composed of 160 kmol/h of ethanol and 40 kmol/h of water (which corresponds to the outlet concentration of the pre-concentrator, 90 wt%) at 35 °C and 100 kPa is taken. These values are based on representative plant capacities for bio-ethanol production [3, 10, 12]. The separation processes simulated in this work are subject to the constraints that the recovered ethanol should have a molar purity  $\geq 99.8\%$  [10, 12]. The condenser and the reboiler are taken into account as equilibrium stages, the condenser being the first stage. The results are based on thermodynamic equilibrium stage modeling using *Aspen Plus V7.2*. It should be mentioned that, due to the degradation temperatures, the ILs are not allowed to be at temperatures higher than 240 °C for [EMIM][DCA] [13] and 160 °C for [EMIM][OAc] (Appendix 6.1). The thermodynamic and physical properties for the components involved in the simulations are presented in Appendix 6.1.

The relative volatility ( $\alpha$ ) is the property which defines the suitability of distillation processes and is shown in equation 6.1.

$$\alpha = \frac{y_{eth}/x_{eth}}{y_{wat}/x_{wat}} = \frac{K_{eth}}{K_{wat}} \quad 6.1$$

where  $K$ ,  $y$  and  $x$  hold for distribution coefficient, vapor and liquid molar composition, respectively, and the subscripts *eth* and *wat* for water and ethanol.

In Figure 6.1, the relative volatility (equation 6.1) of the model mixture ethanol/water using EG, [EMIM][OAc] and [EMIM][DCA] are shown. It should be noticed that the relative volatility of ethanol/water with the ILs fall over and under the relative volatility with the solvent benchmark (EG). According to its relative volatility, [EMIM][OAc] is the most promising IL to use as a solvent in the EDC. However, the solvent selection should be based in the performance on the overall process and not only on the EDC.

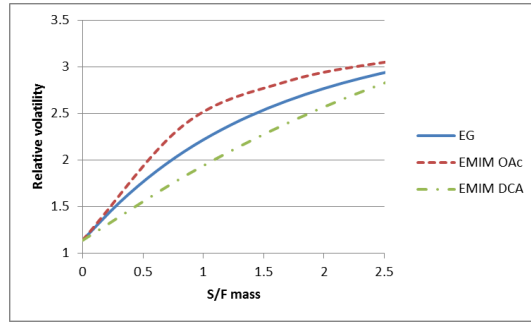


Figure 6.1: Relative volatility for ethylene glycol and ionic liquids

Beside the avoidance of solvent losses in the overhead of the EDC, the higher selectivity with [EMIM][OAc] is expected to decrease the energy requirements of the EDC.

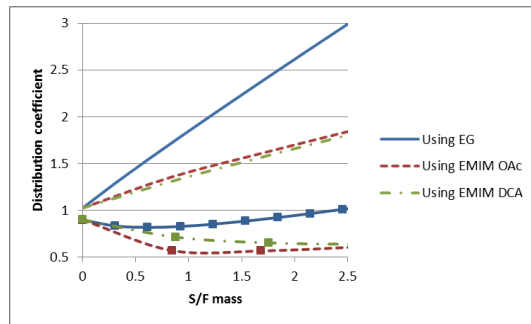


Figure 6.2: Distribution coefficients for ethanol (lines) and water (symbols) using three different solvents

In Figure 6.2, the distribution coefficients for ethanol and water are presented. It should be noticed that, compared to EG, the ILs studied in this work decrease the distribution coefficient of ethanol. However, only [EMIM][OAc] gives a higher relative volatility than EG (Figure 6.1). The ILs are also interacting with the water making it “less volatile”. Thus, the ILs are able to modify the relative volatility of the binary mixture ethanol + water by *attracting* and *retaining* the water and not by repelling the ethanol. This will influence the removal of water from the IL (the more attracted the water is, the more difficult its evaporation) affecting the EDC (specifically the reboiler, where high concentration of water and IL will occur) and the recovery of the IL.

### 6.3 Conventional extractive distillation process using EG

The Fenske equation [14] was used to calculate the minimum number of stages of the EDC, using the desired ethanol purity in the distillate and a relative volatility ( $\alpha$ ) calculated at a solvent to feed molar ratio of unity (arbitrary) at 100 kPa. As in the design of the EDC for the separation of methylcyclohexane from toluene (Chapter 5), the total number of stages for the distillation column is taken as thrice the minimum number of stages [15], i.e. the actual number of stages for the EDC using EG is 30. An optimization procedure was implemented in order to determine the optimal feed stage ( $n_f$ ), solvent feed stage ( $n_s$ ), molar reflux ratio ( $RR$ ) and solvent to feed molar ratio ( $S/F$ ).



$$\min Q_R = f(S/F, RR, n_f, n_s)$$

6.2

$$s. t. \quad x_{Eth}^D \geq 0.998$$

In equation 6.2,  $Q_R$  and  $x_{Eth}^D$  refers to the reboiler heat duty and ethanol molar composition in the distillate, respectively. The optimized column conditions and results are presented in Figure 6.3 and Table 6.1. The column profiles can be seen in Figure 6.15 in appendix 6.2. The main feed is located at stage ( $n_f$ ) 23 and the solvent is fed ( $n_s$ ) at the 4<sup>th</sup> stage avoiding solvent losses in the overhead of the column.

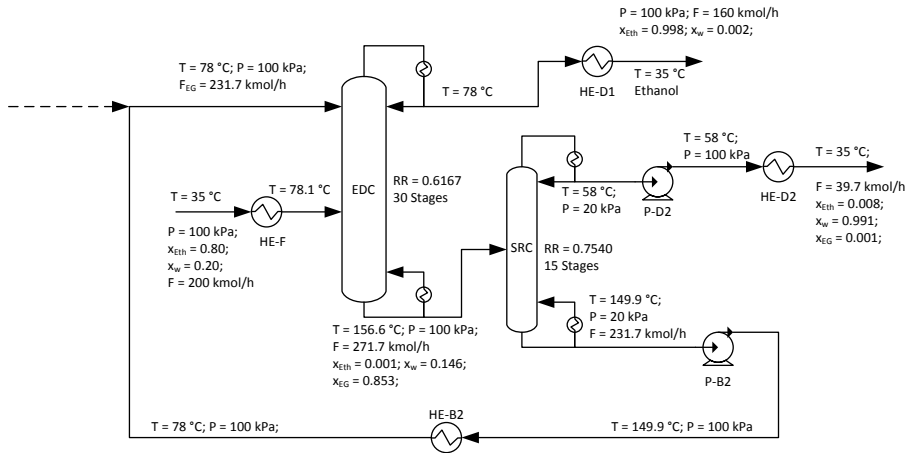


Figure 6.3: Conventional extractive distillation process using ethylene glycol (EG)

An analogous procedure was applied for the solvent recovery column (SRC), resulting in 15 actual stages. For this column, the feed stage, reflux ratio and pressure were determined by the optimization shown in equation 6.3. The results of the SRC are also presented in Figure 6.3 and Table 6.1.

$$\min Q_R = f(n_f, RR, P)$$

6.3

To avoid solvent losses in the SRC, the maximum EG composition allowed in the overhead of the SRC ( $x_{EG}^D$ ) was limited to less than 500 ppm. In equation 6.3,  $P$  refers to the total pressure of the distillation column. The feed is located at the 8<sup>th</sup> stage. The lower the pressure in the SRC the lower the energy requirements (the vacuum pump needed to create the low pressure is not taken into account). However, if the pressure is lower than 20 kPa, the constraint for the EG in the overhead is not satisfied (due to the low pressure, the solvent becomes more volatile). In this work, a pressure in the SRC of 20 kPa is chosen which gives a temperature in the condenser 58 °C. The energy requirements for the whole ED process using EG as solvent are presented in Table 6.1.

Table 6.1: Energy requirements of the conventional ED process

Unit	Energy Requirements (MW)	
	Output	Input
EDC-Cond	-2.83	
EDC-Reb		3.80
SRC-Cond	-0.82	
SRC-Reb		0.66
HE-F		0.36
HE-D1	-0.33	
HE-D2	-0.02	
HE-S	-0.82	
P-D2		$0.60 \times 10^{-4}$
P-B2		$6.50 \times 10^{-4}$
<b>Total</b>	<b>-4.82</b>	<b>4.82</b>

The solvent to feed molar ratio of the process is 1.16 (which gives a solvent to feed mass ratio of 1.8) and the reflux ratio of the EDC and SRC are 0.6 and 0.8, respectively (Figure 6.3). It should be mentioned that 0.02 kmol/h of EG is lost through the overhead of both columns (90% through the SRC).

#### 6.4 Extractive distillation column using ionic liquids

As in the previous case, the minimum number of stages was calculated with the Fenske equation using an arbitrary solvent to feed molar ratio of unity to calculate the relative volatility. Thus, the actual number of stages of the EDC using ILs is 30. The solvent to feed ratio ( $S/F$ ), reflux ratio ( $RR$ ) and feed stage ( $n_f$ ) were determined using a minimization procedure (equation 6.4).

$$\min Q_R = f(S/F, RR, n_f) \tag{6.4}$$

$$s. t. \quad x_{Eth}^D \geq 0.998$$

It should be mentioned that the IL can be fed into the column combined with the reflux flow without losing the solvent in the overhead due to its non-volatility. The constraint in equation 6.4 refers to the required purity of ethanol in the overhead product. According to the results, the feed should be located at the 23<sup>th</sup> stage.

According to the simulations, if the EDC using [EMIM][OAc] is operated at 100 kPa, the bottom temperature reaches 212.5 °C. This temperature is required to evaporate the water retained by the IL. Despite of its higher selectivity, no energy savings are achieved due to the heating up of this IL in the reboiler. To avoid its degradation, the temperature of any stream in the process should be lower than 160 °C. Therefore, the pressure in the EDC using [EMIM][OAc] should be decreased to 25 kPa. In this case, the bottom temperature is 154.2 °C. For the EDC using [EMIM][DCA] operating at 100 kPa, the bottom temperature is 164.8 °C (lower than its degradation temperature). The results of both ED columns are shown in Figure 6.4.

It should be noticed in Figure 6.4 that the ILs fed to the EDCs have a molar purity of 99.8%. A lower purity results in an increase of the reflux ratio (and consequently an increase of the energy requirements) or a violation of the purity constraint in the overhead product. The energy requirements of the IL recovery technology will be also affected by the purity of the IL fed to the EDC (the higher the required purity of the IL, the higher the cost involved in the recovery process).

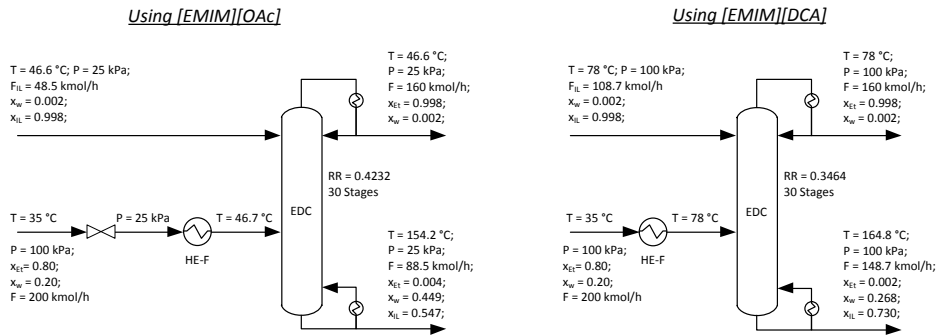


Figure 6.4: Extractive distillation column using ILs as solvent

The extractive distillation column (EDC) profiles can be seen in Figure 6.16 for [EMIM][OAc] and Figure 6.17 for [EMIM][DCA] in appendix 6.2. The solvent to feed molar ratios are 0.25 and 0.54 for the processes using [EMIM][OAc] and [EMIM][DCA], respectively. Both molar ratios are lower than the one obtained for EG (molar ratio of 1.16). However, when the solvent to feed mass ratios are analyzed (1.02, 2.38 and 1.8 for [EMIM][OAc], [EMIM][DCA] and EG, respectively) it can be seen that the most promising solvent is [EMIM][OAc] followed by EG. In this work, the energy requirements are taken as the main criteria for the definite solvent selection. They are shown in Table 6.2.

Table 6.2: Energy requirements in the reboiler for an EDC using three solvents

EDC using	Energy Requirements (MW) in the reboiler
[EMIM][OAc]	3.49
[EMIM][DCA]	3.55
EG	3.80

As it can be concluded from Table 6.2, a maximum of 8.2 % of the energy of the EDC can be saved when the conventional solvent (EG) is replaced by [EMIM][OAc]. The higher selectivity (and its lower solvent to feed mass ratio) is reflected in the lower energy duty in the reboiler. It should be noticed that, despite of the lower relative volatility and higher solvent to feed mass ratio, using [EMIM][DCA] can save 6.6% of the energy input in the reboiler in comparison with the conventional solvent. This is caused by some evaporation of EG in the reboiler, while the non-volatile ILs are only heated up.

In the following section, several recovery technologies for the ILs are proposed and analyzed. The recovery of [EMIM][DCA] is expected to be easier than [EMIM][OAc] due to the weaker interaction with water (larger distribution coefficients in Figure 6.2). So far, the ILs perform slightly more efficiently than the conventional solvent, however, significant energy savings in the recovery technology need to be achieved (> 25% compared to the conventional technology [16]) to make these solvents attractive and suitable for the separation of ethanol and water by ED.

## 6.5 Ionic liquid recovery techniques

Ordinary distillation is not a suitable technology to recover ILs due to their non-volatility. Several technologies have been proposed to recover and recycle the ILs. Evaporation (at high temperature and low pressure) and stripping are potential technologies to recover ILs from volatile compounds [17]. Membrane-based processes have been analyzed; however, due to their large membrane area needed, this process is not feasible for IL recovery [18]. Extraction with supercritical carbon dioxide (SCCO<sub>2</sub>) of the volatile compounds had been suggested [18]. In this section, several recovery technologies are studied. Processes like flash vaporization, stripping, combination of both technologies, and SSCO<sub>2</sub> are taken into account. The energy requirements of the recovery technologies combined with the EDC are presented, summarized and analyzed at the end of the current section.

### 6.5.1 Recovery using flash evaporation

This process consists of a simple evaporation flash drum which will remove the water from the ILs due to the decrease in pressure and simultaneously increase of temperature. The water is obtained in the vapor outlet of the flash with a high purity and the IL is obtained in the liquid outlet of the drum with the desired purity, which will be influenced by the pressure and temperature used in this unit. Due to the interactions of the ILs and water, high temperatures need to be used. For both ILs, the flash evaporator was operated at their maximum tolerable temperature (160 and 240 °C for [EMIM][OAc] and [EMIM][DCA], respectively).

At the above mentioned conditions, the pressure required to obtain the IL with a molar purity of 0.998 are  $1 \times 10^{-7}$  and 2.3 kPa for [EMIM][OAc] and [EMIM][DCA], respectively. It can be concluded that the use of a flash drum to recover [EMIM][OAc] is unfeasible due to the extremely low pressures required to purify it and its relatively low degradation temperature, which limits the recovery conditions. The recovery of [EMIM][OAc] by evaporation in a flash drum is not further discussed. For the case using [EMIM][DCA], the process and its results are shown in Figure 6.5. It can be seen that after the water is removed from the IL, it needs to be condensed and re-pressurized. The condensation temperature of the water at 2.3 kPa is 18 °C, therefore a refrigeration system needs to be implemented.

To avoid the use of a refrigerator, a compressor can be used to increase the pressure of 40 kmol/h of water (which corresponds to  $7.4 \times 10^4$  m<sup>3</sup>/h). However, there are some disadvantages:

- *The large amount of gas to be compressed requires the use of several compressors in parallel [14].*

- The compression will increase the temperature of the gas stream (reaching 940 °C for compression to 100 kPa or 370 °C for compression to 6.5 kPa, a pressure at which the water can be condensed with cooling water). This requires the use of extra heat exchangers to cool down and condense the water vapor stream.

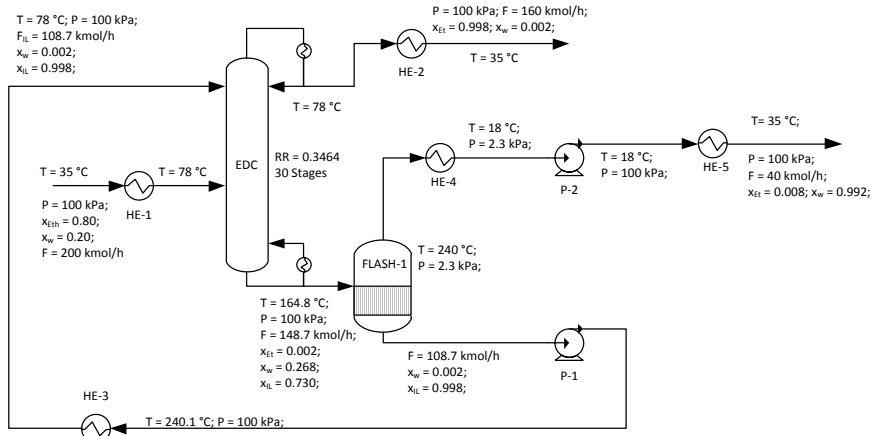


Figure 6.5: ED process using [EMIM][DCA]. Recovery of IL with flash drum at 240 °C

Due to these reasons, the use of compressors after the flash drums is not considered a viable option to re-pressurize and recover the water.

Considering these options, the recovery process using a flash drum operating at 240 °C and a refrigeration system to condense the water at 18 °C is selected for further studies. The energy requirements of this process are listed in Table 6.3 and the analysis will be given in the summary at the end of this section of the chapter.

As it was mentioned before, a refrigeration system is needed in this process to condense the recovered water. The duty of the refrigeration system was obtained taken 60% of the its ideal coefficient of performance ( $COP$ ) as recommended by Smith [16] (equation 6.5).

$$COP = \frac{Q_{cooling}}{W_{refri}} = 0.6 \times COP^{ideal} = \frac{0.6 \times T^{evap}}{T^{cond} - T^{evap}} \quad 6.5$$

The evaporation and condensation temperatures ( $T^{evap}$  and  $T^{cond}$ ) are from the refrigeration fluid (expressed in K). In this case, the temperature of the stream (18 °C) and the temperature of evaporation of the refrigeration fluid should have a temperature difference of 10 K. Thus, the evaporation temperature of the refrigerant is 8 °C. The condensation temperature of the refrigerant is taken as 35 °C (to be able to use cooling water as condenser fluid). In the present case, the cooling duty ( $Q_{cooling}$ ) is taken as the energy required to decrease the temperature of the stream (water in vapor phase) from 35 °C to 18 °C at 2.3 kPa (liquid phase). In this case,  $Q_{cooling}$  is -0.50 MW which gives an energy requirement for the refrigeration system of 0.08 MW.

### 6.5.2 Recovery using stripping with hot nitrogen

The bottom stream of the EDC enters a stripping column which uses a hot gas as stripping agent. The number of stages was calculated with a simplified algebraic method [19] with a constant distribution coefficient of 3.7 (value obtained with the concentration in the bottom stream at an arbitrary pressure of 50 kPa). The method requires the calculation of the minimum stripping gas flow (29.3 kmol/h). In this work, 1.5 times the minimum flow was taken as the actual flow entering the stripping column [19]. The method gives 11 stages as a result. It should be mentioned that only water is being transferred between the vapor and liquid phases. The procedure described above was only applied to obtain the number of equilibrium stages. The following simulations and results are done using rigorous methods such as *RadFrac (Aspen Plus V7.2)*.

Nitrogen at the maximum allowed temperature is used as stripping gas which removes the water from the liquid phase, purifying the IL. It should be mentioned that the desired molar purity of the IL exiting the stripping column is 0.998. This stream is recycled back to the EDC. Hot nitrogen and water in vapor phase are obtained at the top of the stripping column; however, it is desirable to remove the water and recycle back the nitrogen to the stripping column. This can be done by decreasing the temperature of the stream and condensing the water (like in the previous case, compression after flash is not considered as an economically feasible process).

The nitrogen flow was varied until the desired purity of the IL was reached for a specified pressure in the stripper. According to the simulations for the recovery of [EMIM][OAc] at 2 kPa, a nitrogen flow of  $1 \times 10^6$  kmol/h at 160 °C is required. It should be noticed that this equals a gas-liquid molar flow ratio in the stripper larger than 10000. Due to these extreme conditions, the recovery of [EMIM][OAc] by stripping with hot nitrogen is considered unfeasible.

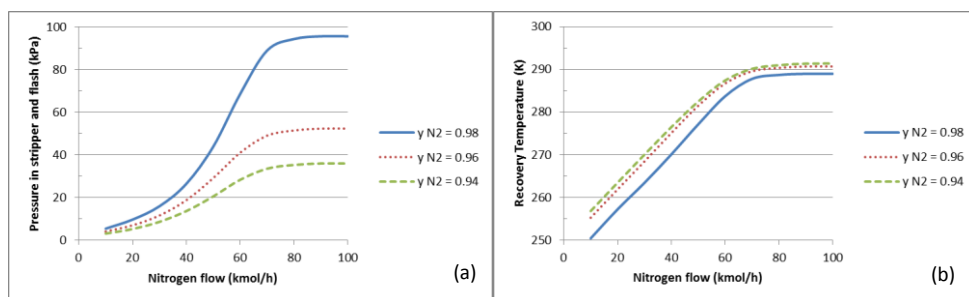


Figure 6.6: Influence of nitrogen flow in the (a) maximum flash and stripper pressure, and (b) water recovery temperature. Recovery using of [EMIM][DCA] nitrogen stripping

On the other hand, the IL [EMIM][DCA] can be recovered with the technology showed in this section. As can be seen in Figure 6.6(a), the pressure in the stripper and the purity of the nitrogen fed influence the required nitrogen flow to purify the IL. For a given pressure in the stripper, the nitrogen flow can be decreased if the purity is increased.

In Figure 6.6 (b) it can be seen that low temperatures in the flash are necessary to recover the nitrogen and condense the water. The nitrogen purity does not have a remarkable

influence on the recovery temperature in the flash; however, the recovery and condensation of water becomes easier when the column is operated at large nitrogen flows (higher temperature can be used). A nitrogen purity of 0.96 and a pressure in the stripper of 50 kPa are chosen to analyze this technology in more detail. This process is shown in Figure 6.18 (appendix 6.3).

As in the previous technology, a refrigeration system is required to condense the water recovered in the stripping column. The duty of the refrigeration system was obtained as in the previous process; however, in this case, the stream has a temperature of 16.7 °C which results in an evaporation temperature of 6.7 °C. In this case, the cooling duty (energy required to decrease the temperature of the vapor stream exiting the stripper from 35 °C to 16.7 °C at 50 kPa) is -0.24 MW. The energy requirements of this process are listed in Table 6.3. As the previous case, the analysis is done in the following sections.

### 6.5.3 Recovery using flash and stripping with hot nitrogen

It must be mentioned that this process would not be feasible for the recovery of the IL [EMIM][OAc], as the stripper is not able to recover efficiently the IL and remove the remaining water, which had been shown in the previous section.

This recovery technology is similar to the one shown in Figure 6.18. After the EDC, a flash drum is located. In Table 6.3, it can be seen that 25% of the total energy for the process using only a flash drum to recover the IL is required in the flash unit. In the current case, an adiabatic flash operating at 6.34 kPa (pressure at which the vapor outlet of the evaporator can be condensed with cooling water) is selected to save some of this energy. The required IL purity is not achieved by the flash only (the pressure in the evaporator is not low enough to remove the water from the IL stream – section 6.5.1). The evaporator's liquid outlet is fed to a stripping column using hot nitrogen (as in the previous case, the inlet nitrogen has the maximum temperature allowed to avoid IL degradation) to remove the water remaining in the IL. The purified IL is then recycled back to the EDC and the vapor exiting the stripping column is cooled down to condense the water and recover the nitrogen (which is then recycled back to the stripping column). Because some of the water is removed by the flash drum, the required nitrogen flow is expected to decrease compared to the previous technology (saving some energy in the heat exchanger to re-heat the nitrogen up).

The nitrogen flow necessary to purify the IL will vary accordingly to the pressure used in the stripper (Figure 6.7(a)). The nitrogen exiting the stripper is purified (purity 96 mol%) in another flash drum to be able to recycle it back into the stripper. It should be mentioned that the recovered nitrogen needs to be heated up until 240 °C before entering the stripping column. In Figure 6.7(a) it can be seen that the required temperature to reach the desired nitrogen purity in this separator will increase with the nitrogen flow (due to the increase of the pressure). Temperatures below 0 °C are discarded due to the freezing point of the water. As it is observed in this figure, a refrigeration unit is mandatory (the temperature in the separator reaches a maximum value of 17.5 °C). The lower the temperature required to recover the nitrogen, the higher the energy requirements in the refrigeration unit and the lower the energy requirements in the re-heating of the nitrogen which is recycled back to the stripper (Figure 6.7(b)). As it can be seen in this figure, the

energy duties of the refrigeration system are negligible compared to the energy needed to increase the temperature of the nitrogen, i.e. it is more convenient to use low nitrogen flows to avoid large energy requirements in the heat exchanger to heat up the nitrogen.

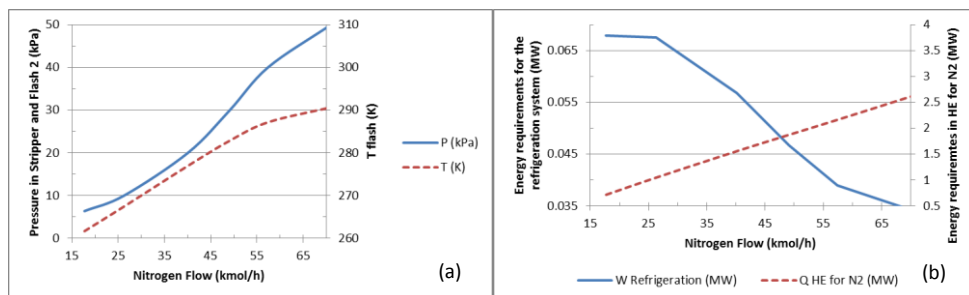


Figure 6.7: Influence of the nitrogen flow on the pressure of the stripper and the recovery temperature of the nitrogen

In this work, a pressure of 20 kPa was selected (to avoid temperatures below 0 °C in the flash drum) as the operation pressure of the stripper and the second flash. The flow diagram of the process and the results can be seen in Figure 6.19 (appendix 6.3). The energy requirements of the process are listed in Table 6.3.

In this case, the duty of the refrigerant system was obtained with a stream temperature of 3.8 °C which results in an evaporation temperature of the refrigerant of -6.2 °C. Thus, the cooling duty (energy required to decrease the temperature of the vapor exiting the stripper from 35 °C to 3.8 °C) is -0.2 MW. The energy requirements of this process are listed in Table 6.3. The results are analyzed in the coming sections.

#### 6.5.4 Recovery using stripping with hot ethanol vapor

This technology, described in the work of Beste et al. [17], makes use of an EDC using a partial condenser. Ethanol is obtained in the overhead of the column with the desired purity. The IL mixed with the water exits the EDC through the bottom of the column and is fed to a flash evaporator operating at 6.34 kPa (as in the previous technology). Water is obtained as a vapor and is condensed with cooling water. The liquid stream exiting the flash drum is then fed into a stripping column using hot ethanol vapor as stripping agent. This stream is obtained from the vapor outlet of the partial condenser of the EDC. It strips out the remaining water from the IL which is purified and recycled back to the EDC. The outlet vapor obtained in the stripping column contains water and ethanol. This stream is condensed, re-pressurized (by a pump) and sent back to the EDC.

Figure 6.8 shows how the ethanol flow used as stripping gas influences the needed pressure in the stripper and the condensation temperature of the vapor exiting this unit when [EMIM][DCA] is used in the EDC. As it can be seen, molar flows below 125 kmol/h will lead to a condensation temperature lower than the freezing point of water (273.15 K). To avoid operative issues and shorten the window of possible conditions, ethanol flows smaller than 125 kmol/h are discarded. Large flows imply large energy duties in the condensation process of the vapor exiting the stripper. An ethanol flow of 125 kmol/h is selected, which gives a pressure in the stripper of 1.7 kPa (this flow represents 78 % of the



total ethanol fed to the ED process). Notice that the required stripper pressure is lower than the pressure necessary when the IL is recovered in a flash evaporator, 2.3 kPa (Figure 6.5). In other words, lowering the pressure is more effective than the stripping gas to remove the water from the liquid phase. This can be explained by the small (but present) affinity of the IL for ethanol. The liquid stream entering the stripper contains mainly water and IL; however, the water is being replaced by the stripping gas as it can be seen in Figure 6.9.

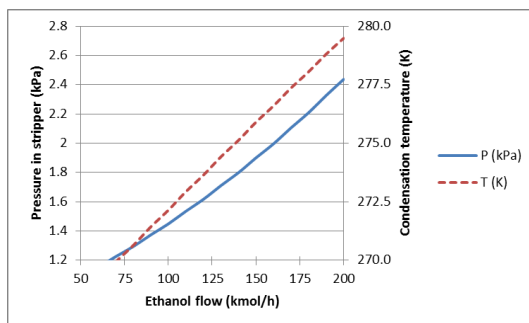


Figure 6.8: Influence of the ethanol flow on the needed pressure in the stripper and condensation temperature. IL used [EMIM][DCA]

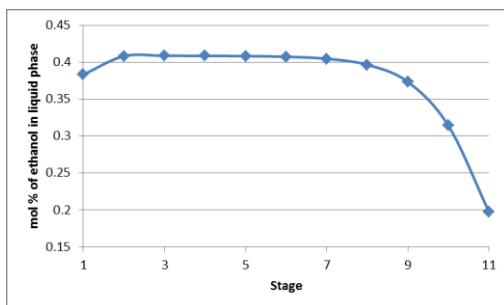


Figure 6.9: Ethanol liquid concentration profile in the stripper. IL used [EMIM][DCA]

Figure 6.9 shows the ethanol concentration profile in the stripping column. The water is being removed and replaced by ethanol. The liquid outlet of the stripping column has an ethanol molar composition of 0.002 (IL molar purity of 0.998). Due to the negligible effect of the ethanol as stripping gas and the affinity of the IL and ethanol, this technology is not a suitable recovery process for the removal of water from [EMIM][DCA].

The IL [EMIM][OAc] shows a similar affinity for ethanol but a higher affinity for water than [EMIM][DCA], as it can be seen in Figure 6.2. Due to this reason and according to the simulations, it is necessary an ethanol flow of  $1 \times 10^6$  kmol/h at 160 °C to be able to recover the IL to the desired purity.

According to these results, the recovery of the ILs by stripping with hot ethanol is unfeasible. This technology is not further studied in this work.

### 6.5.5 Recovery using supercritical CO<sub>2</sub> extraction

It has been proposed to use supercritical CO<sub>2</sub> (SCCO<sub>2</sub>) to recover volatile compounds from ILs [18, 20, 21]. This technology uses the capabilities of SCCO<sub>2</sub> to solubilize the volatiles. At supercritical conditions, the CO<sub>2</sub> is soluble in the ILs (to some extent) but the ILs are not soluble in SCCO<sub>2</sub>. Then, the supercritical phase will be composed by CO<sub>2</sub> and the recovered volatile compound, and the liquid phase will contain IL and dissolved CO<sub>2</sub>. In this section, a conceptual design for the recovery process using carbon dioxide is proposed and analyzed.

The critical pressure and temperature for the CO<sub>2</sub> are 7.38 MPa and 30.9 °C [19]. The solubility and phase equilibrium behavior of the mixture water + SCCO<sub>2</sub> and [EMIM][DCA] + SCCO<sub>2</sub> has been taken from the literature [22, 23] to perform the conceptual design of this recovery technology. With the help of mass balances, the minimum CO<sub>2</sub> flow can be calculated and the inlet and outlet conditions can be obtained [19]. It should be mentioned that, as in stripping, the actual CO<sub>2</sub> flow was taken as 1.5 times the minimum flow. The actual CO<sub>2</sub> flow entering the extraction column is 37200 kmol/h. However, due to the solubility of the CO<sub>2</sub> in the IL, 0.3% of this flow exits the column dissolved in the liquid phase. This yields a CO<sub>2</sub> molar composition in the liquid phase of 0.5. Therefore, the dissolved gas needs to be recovered by decompression (reaching pressures of 3.8 kPa) and recompressed again to be recycled back to the stripping column. This re-compression requires 2.7 MW and, according to the simulations, the outlet temperature of this stream is 1491 °C. This stream needs to be cooled down until the operative temperature of the extractive column (240 °C).

The gas exiting the supercritical extraction column (SCEC) contains the recovered water diluted in CO<sub>2</sub>. As in section 5.5.5 in Chapter 5, high pressure distillation at 4 MPa using a partial condenser is used to recover the water from this stream and purify the CO<sub>2</sub>. In this column, the CO<sub>2</sub> is obtained overhead and the water is recovered at the bottom. The carbon dioxide needs to be re-compressed using 22.2 MW. The temperature of this stream increases from 6.3 to 114.6 °C. This stream can be mixed with the CO<sub>2</sub> that was dissolved in the IL and recovered by decompression. Due to the mixing, the final temperature of the recovered CO<sub>2</sub> is 119.8 °C. This mixed stream needs to be heated up until 240 °C to be able to reuse it in the SCEC. However, due to the large flow, the energy duty of the heat exchanger (HE-5) is 63.9 MW. The process is shown in Figure 6.20 and the energy requirements of every unit are listed in Table 6.3. As it can be seen, only the re-compression and re-heating of the carbon dioxide represents more than 90% of the total energy requirements. Furthermore, this process requires 20 times more energy than the conventional process using ethylene glycol. According to these results, it can be concluded that the extraction with supercritical CO<sub>2</sub> is not a suitable technology to recover ILs. This technology is no longer studied in this work.

### 6.5.6 Summary

Due to the strong interactions between the water and [EMIM][OAc], the recovery and purification of this IL is challenging, energy intensive and unfeasible (very low pressures are needed). Even though the relative volatility of the mixture ethanol/water using [EMIM][DCA] is lower, this IL is better solvent than [EMIM][OAc]. Because of this reason,

[EMIM][OAc] is not further studied in this work due to the extreme conditions necessary for its recovery.

The energy requirements of each unit of every process (including the EDC and the solvent recovery process) are shown in Table 6.3. In Figure 6.10, the energy requirements of the whole process (ED column + recovery technology) are compared. Due to the re-heating and re-compression of the carbon dioxide, the energy requirements of this technology are by far the highest from the technologies analyzed in this work. This technology is not suitable to recover ILs.

**Table 6.3: Energy requirements of the ED process with ILs using five different recovery technologies**

Unit	Energy requirements (MW)							
	Flash @ 240 °C [EMIM][DCA]		Stripping with N2 [EMIM][DCA]		Flash + Stripping with N2 [EMIM][DCA]		SCCO2 [EMIM][DCA]	
	Output	Input	Output	Input	Output	Input	Output	Input
EDC-Cond	-2.51		-2.51		-2.51		-2.51	
EDC-Reb		3.55		3.55		3.55		3.55
HE-1		0.37		0.37		0.37		0.37
HE-2	-0.33		-0.33		-0.33		-0.33	
HE-3	-1.88		-1.85		-1.40		-0.57	
HE-4	-0.54			0.02	-0.42		-0.22	
HE-5		0.01		2.72		1.55		63.9
HE-6						0.01		
HE-7								
Q-FLASH1		1.33	-1.96		0	0		
Q-FLASH2					-0.81			
P-1		$1.3 \times 10^{-3}$		$6.7 \times 10^{-4}$		$1.1 \times 10^{-3}$		0.1
P-2		$6.7 \times 10^{-5}$		$3.4 \times 10^{-5}$		$5.4 \times 10^{-5}$		$1.2 \times 10^{-3}$
P-3						$9.8 \times 10^{-6}$		
P-4						$1.7 \times 10^{-4}$		
SCEC-Cond								-89.2
SCEC-Reb								0.13
C-1								2.69
C-2								22.17
W-REFRI		(0.08)		(0.04)		(0.06)		(21.4)
<b>Total</b>	<b>-5.26</b>	<b>5.26</b> <b>(5.34)</b>	<b>-6.65</b>	<b>6.66</b> <b>(6.70)</b>	<b>-5.47</b>	<b>5.48</b> <b>(5.54)</b>	<b>-92.83</b>	<b>92.91</b> <b>(114.3)</b>

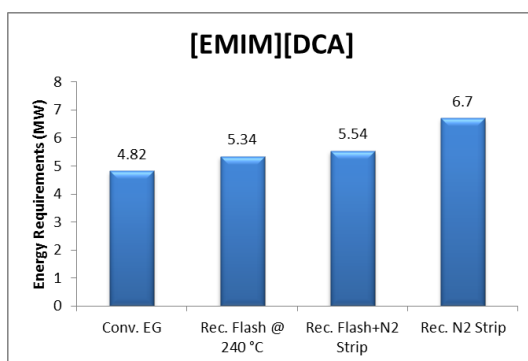


**Figure 6.10: Total energy requirements for the ED process using [EMIM][DCA] (ED column + recovery technology)**

All the technologies analyzed in this work yielded higher energy requirements than the process using EG. Replacing the conventional solvent for [EMIM][DCA] yields 6.6% less

energy duties in the EDC. However, the recovery of ILs is more energy intensive than the recovery of EG. No energy savings are achieved when the conventional solvent is replaced.

It should be mentioned that the combination of flash (adiabatic) with nitrogen stripping yields lower energy requirements than using nitrogen stripping only to recover the IL. The flash drum is able to remove some of the water contained in the IL, resulting in a lower nitrogen flow in the stripping column. This yields lower energy requirements in the re-heating of the nitrogen. As mentioned before, both technologies do not achieve reasonable energy savings compared to the conventional process. Neither of these two technologies is further analyzed in this work.

Recovering the IL with a flash drum operating at 240 °C is the least energy intensive IL recovery technology. This process requires 11 % more energy than the conventional ED process (which has a total energy requirement of 4.82 MW, as shown in Table 6.1). In the following section, the heat integration for the conventional ED process and the processes where the [EMIM][DCA] is recovered with a flash drum at 240 °C is presented.

## 6.6 Energy analysis

In this section, the heat integration analysis is done for the conventional ED process utilizing EG and [EMIM][DCA] using flash at 240 °C as the recovery technology.

The composite curves are used to determine the maximum energy that can be recovered using process-to-process heat exchangers. It also gives information about the minimum energy requirements (minimum usage of heating and cooling utilities, also called targets, when exchanging heat between hot and cold streams within a process). The composite curves and the heat integration were created with methods proposed in literature [14, 16] and using *Aspen Energy Analyzer V7.2*, taking a minimum temperature difference ( $\Delta T_{min}$ ) of 10 K. It was assumed that the heat-capacity flow rate (product of the heat capacity and the flow rate of the stream) does not vary with temperature, except for the cases where phase changes are present (in those cases, the enthalpy of the stream is discretized into several segments and linearized with respect to the temperature following the procedure reported in the literature [14, 16]).

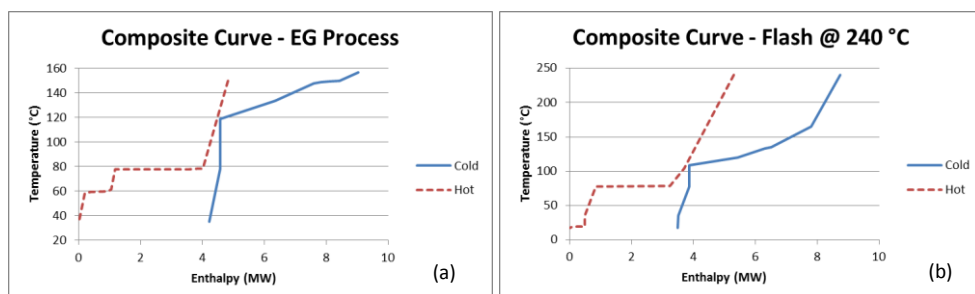


Figure 6.11: Composite curve for (a) the conventional ED process and (b) the process using [EMIM][DCA] utilizing a flash drum at 240 °C to recover the IL

Figure 6.11 shows the composite curves for the conventional process using EG and [EMIM][DCA]. In Figure 6.11(a) can be seen that the heating and cooling targets (minimum

energy input and output to the process) are 4.21 and 4.22 MW, respectively. Performing the heat integration, a maximum of 0.61 MW can be recovered with process-to-process heat exchangers, representing 13% of the energy requirements of the process without heat integration. The composite curve for the process using [EMIM][DCA] (Figure 6.11(b)) shows that the heating and cooling targets are 3.43 and 3.49 MW, respectively. Some of the energy should be removed with a refrigerant due to the low temperatures reached in this process. Performing the heat integration, a maximum of 1.82 MW can be recovered which results in a total energy requirement of 3.52 MW (34% lower than the process without heat integration). Compared to the heat-integrated conventional ED process, a maximum energy saving of 16 % can be obtained using IL as solvent and recovering it with a flash drum.

As supplementary information, the heat exchanger networks (HENs) for the selected processes are proposed and shown in Appendix 6.4. In this appendix (Table 6.12) it can be seen that the minimum heat transfer area for the heat integrated IL process (345 m<sup>2</sup>) is 93% larger than the heat transfer area of the integrated conventional process (179 m<sup>2</sup>).

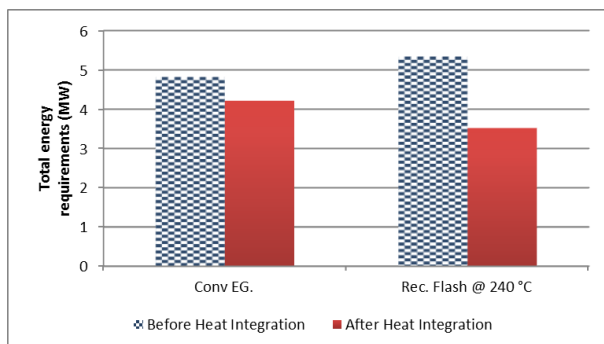


Figure 6.12: Energy requirements before and after heat integration

Figure 6.12 gives a summary of the energy requirements of the two processes. Without heat integration, the IL process requires 11% more energy than the conventional process using EG. However, after heat integration, the ED using [EMIM][DCA] and recovering it with a flash drum operating at 240 °C becomes more energy efficient. If both technologies are compared after heat integration, the ED process using [EMIM][DCA] requires 16% less energy than the conventional process (this shows the importance of performing the heat integration during the design of sustainable processes). However, the necessary heat transfer area in the IL process might increase the capital expenditures (CAPEX) and reduce the general benefits of using ILs.

## 6.7 Conclusions

In this chapter, the feasibility of implementing ILs as solvents in ED for the separation of ethanol – water was shown. Two ILs were compared with the conventional solvent EG. It was shown that the relative volatility of ethanol/water varies according to the following order [EMIM][OAc] > EG > [EMIM][DCA]. The ILs can increase the relative volatility by strongly *attracting* the water making it less volatile which makes more challenging its recovery.

Several technologies were analyzed to recover the ILs. However, due to the high hydrophilicity, the recovery of [EMIM][OAc] is unfeasible with the technologies studied in this work. As it was shown in this chapter, besides the performance in the ED column, the IL should be easily recoverable. All the recovery processes studied yielded to higher energy requirements than the benchmark (ED using EG). The recovery of the IL using flash evaporation at 240 °C was chosen for further studies regarding the heat integration (HI) of the process. Without HI, the ED process using the IL required 11% more energy than the benchmark. After HI, the total energy requirements of both processes can be decreased and the use of the IL becomes more energetically attractive, yielding 16% of energy savings compared to the heat integrated conventional process; From the energy analysis, it can be concluded that the IL process needs larger heat transfer area than the conventional ED process using EG. This might decrease the attractiveness of ILs for the separation of ethanol-water mixture.

## 6.8 References

1. Kumar, S., N. Singh and R. Prasad, *Anhydrous ethanol: A renewable source of energy*. Renewable & Sustainable Energy Reviews, 2010. **14**(7): p. 1830-1844.
2. McPhail, L.L., *Assessing the impact of US ethanol on fossil fuel markets: A structural VAR approach*. Energy Economics. **In Press, Corrected Proof**.
3. Huang, H.-J., S. Ramaswamy, U.W. Tschirner and B.V. Ramarao, *A review of separation technologies in current and future biorefineries*. Separation and Purification Technology, 2008. **62**(1): p. 1-21.
4. Mielenz, J.R., *Ethanol production from biomass: technology and commercialization status*. Current Opinion in Microbiology, 2001. **4**(3): p. 324-329.
5. Gil, I.D., A.M. Uyazan, J.L. Aguilar, G. Rodriguez and L.A. Caicedo, *Separation of ethanol and water by extractive distillation with salt and solvent as entrainer: Process simulation*. Brazilian Journal of Chemical Engineering, 2008. **25**(1): p. 207-215.
6. Ramanujam, M. and G.S. Laddha, *Vapour liquid equilibria for ethanol-water-ethylene glycol system*. Chemical Engineering Science, 1960. **12**(1): p. 65-68.
7. Seiler, M., D. Köhler and W. Arlt, *Hyperbranched polymers: new selective solvents for extractive distillation and solvent extraction*. Separation and Purification Technology, 2003. **30**(2): p. 179-197.
8. Stratula, C., F. Oprea and D. Mihaescu, *The obtaining of anhydrous ethanol by azeotropic distillation using a new entrainer*. Revista De Chimie, 2005. **56**(5): p. 544-548.
9. Lei, Z., C. Li and B. Chen, *Extractive Distillation: A Review*. Separation and Purification Reviews, 2003. **32**(2): p. 121 - 213.
10. Seiler, M., C. Jork, A. Kavarnou, W. Arlt and R. Hirsch, *Separation of azeotropic mixtures using hyperbranched polymers or ionic liquids*. AIChE Journal, 2004. **50**(10): p. 2439-2454.
11. Endres, F. and S. Zein El Abedin, *Air and water stable ionic liquids in physical chemistry*. Physical Chemistry Chemical Physics, 2006. **8**(18): p. 2101-2116.

12. Jonathan R, M., *Ethanol production from biomass: technology and commercialization status*. Current Opinion in Microbiology, 2001. **4**(3): p. 324-329.
13. Paraknowitsch, J.P., J. Zhang, D. Su, A. Thomas and M. Antonietti, *Ionic Liquids as Precursors for Nitrogen-Doped Graphitic Carbon*. Advanced Materials, 2010. **22**(1): p. 87-92.
14. Seider, W.D., J.D. Seader and D.R. Lewin, *Product and process design principles : synthesis, analysis, and evaluation*. 2nd ed2004, New York: Wiley. xviii, 802 p.
15. Tiverios, P.G. and V. Van Brunt, *Extractive Distillation Solvent Characterization and Shortcut Design Procedure for Methylcyclohexane-Toluene Mixtures*. Ind. Eng. Chem. Res., 2000. **39**(6): p. 1614-1623.
16. Smith, R., *Chemical process design and integration*2005, Chichester, West Sussex, England ; Hoboken, NJ: Wiley. xxiii, 687 p.
17. Beste, Y.A., H. Shoenmakers, W. Arlt, M. Seiler and C. Jork. *Recycling of Ionic Liquids Produced in Extractive Distillation*. 2006. Patent US 2006/0272934 A1.
18. Haerens, K., S. Van Deuren, E. Matthijs and B. Van der Bruggen, *Challenges for recycling ionic liquids by using pressure driven membrane processes*. Green Chemistry, 2010. **12**(12): p. 2182-2188.
19. Seader, J.D. and E.J. Henley, *Separation Process Principles*. 2 ed2005: Wiley. 800.
20. Blanchard, L.A. and J.F. Brennecke, *Recovery of Organic Products from Ionic Liquids Using Supercritical Carbon Dioxide*. Ind. Eng. Chem. Res., 2001. **40**(1): p. 287-292.
21. Aki, S.N.V.K., A.M. Scurto and J.F. Brennecke, *Ternary Phase Behavior of Ionic Liquid (IL)-Organic-CO<sub>2</sub> Systems*. Ind. Eng. Chem. Res., 2006. **45**(16): p. 5574-5585.
22. Vorholz, J., V.I. Harismiadis, B. Rumpf, A.Z. Panagiotopoulos and G. Maurer, *Vapor+liquid equilibrium of water, carbon dioxide, and the binary system, water+carbon dioxide, from molecular simulation*. Fluid Phase Equilibria, 2000. **170**(2): p. 203-234.
23. Scovazzo, P., D. Camper, J. Kieft, J. Poshusta, C. Koval and R. Noble, *Regular Solution Theory and CO<sub>2</sub> Gas Solubility in Room-Temperature Ionic Liquids*. Industrial & Engineering Chemistry Research, 2004. **43**(21): p. 6855-6860.

## Appendix 6.1: Thermodynamic and physical properties

The fugacity of the compounds in the vapor and liquid phase were predicted with the Raoult's law and an activity coefficient model, respectively, following the equation 6.6.

$$y_i P = x_i \gamma_i P_i^{sat} \quad 6.6$$

Where,  $P$  holds for the total pressure,  $\gamma_i$ ,  $P_i^{sat}$ ,  $y_i$  and  $x_i$  are the activity coefficient, vapor pressure, vapor and liquid composition of the compound  $i$ , respectively. The vapor pressure of the volatile compounds was calculated with the Antoine equation (6.7).

$$\ln(P_i^{sat} / kPa) = A_i + \frac{B_i}{T/K + C_i} \quad 6.7$$

with the parameters shown in Table 6.4.

Table 6.4: Antoine constants for ethanol, water and EG

Constant	Ethanol [1]	Water [1]	EG [2]
A	16.7808	16.5699	12.4723
B	-3737.602	-3984.923	-2491.574
C	-44.170	-39.724	-160.9176

Ternary vapor-liquid equilibrium experimental data for the system ethanol + water + ethylene glycol (EG) is available in literature [3]. In this work, the regression of the NRTL parameters was performed making use of these data. The obtained parameters of the NRTL model are reported in Table 6.5.

Table 6.5: NRTL parameters for the ternary system ethanol, water and EG

$i$	Ethanol	Ethanol	Water
$j$	Water	EG	EG
$a_{ij}$	0	0	0
$a_{ji}$	0	0	0
$b_{ij}$	-55.1698	365.3139	769.0499
$b_{ji}$	670.4442	-88.8285	-443.9649
$\alpha_{ij}$	0.3031	0.4	0.4

The Figure 6.13 compares the experimental and regressed data. From this figure, it can be concluded that the regressed NRTL parameters are able to represent the experimental data yielding a root mean square error of 0.04.



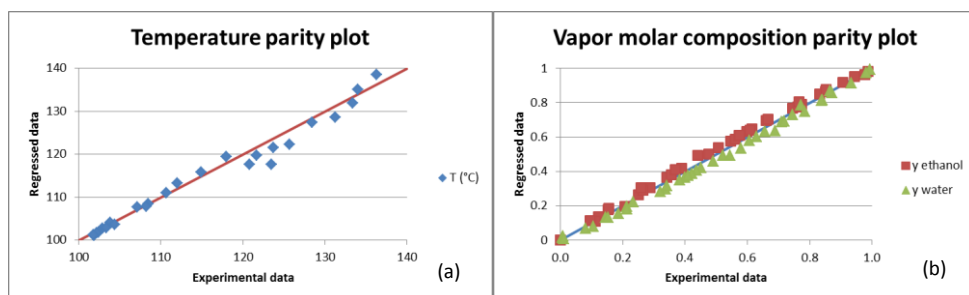


Figure 6.13: Parity plots for the ternary system ethanol + water + ethylene glycol. (a) Temperature and (b) vapor molar composition

For the mixture with the ILs, the NRTL model was selected using the parameters obtained in Chapter 4 and reported in Table 6.6 and Table 6.7 for the system containing [EMIM][OAc] and [EMIM][DCA], respectively.

Table 6.6: NRTL parameters for the ternary system ethanol, water and [EMIM][OAc]

<i>i</i>	Ethanol	Ethanol	Water
<i>j</i>	Water	[EMIM][OAc]	[EMIM][OAc]
$a_{ij}$	0	0	0
$a_{ji}$	0	0	0
$b_{ij}$	-55.1698	-1426.3862	-1505.8078
$b_{ji}$	670.4442	-965.9411	-1109.3131
$\alpha_{ij}$	0.3031	0.4	0.4

Table 6.7: NRTL parameters for the system ethanol, water and [EMIM][DCA]. Adapted from [4]

<i>i</i>	Ethanol	Ethanol	Water
<i>j</i>	Water	[EMIM][DCA]	[EMIM][DCA]
$a_{ij}$	0.8065	0	0
$a_{ji}$	0.5143	0	0
$b_{ij}$	-266.538	350.132	-289.933
$b_{ji}$	444.888	-415.384	-222.997
$\alpha_{ij}$	0.4	0.3	0.3

The liquid heat capacities were calculated with a polynomial equation (6.8) and the parameters used in the simulations are shown in Table 6.8. The volatile compound heat capacity parameters were obtained from literature [5]; the parameters for the ILs were obtained by differential scanning calorimetric measurements in our laboratory.

$$C_p / \text{Jmol}^{-1}\text{K}^{-1} = A + BT/K + CT/K^2 + DT/K^3 + ET/K^4 \quad 6.8$$

Table 6.8: Heat capacity constants for ethanol, water, EG and ILS

Compound	MW	A	B	C	D	E
Ethanol	46.07	283.308	-2.38064	1.331706E-2	-3.19962E-5	3.15051E-8
Water	18.02	-22.417	0.876972	-2.57039E-3	2.48383E-6	0
EG	62.07	-57.2437	1.45678	-4.32548E-3	7.35678E-6	-4.82842E-9
[EMIM][OAc]	170.2	128.1434	0.6434	0	0	0
[EMIM][DCA]	177.2	199.7438	0.4275	0	0	0

For the enthalpy calculations, the liquid phase at 298.15 K and 100 kPa was taken as the reference state. The heats of vaporization for the volatile compounds were predicted with the equation 6.9. The parameters for this equation are shown in Table 6.9, which were taken from literature [6]. It should be noticed that due to the non-volatility of the IL, their enthalpy of vaporization and vapor pressure were set as zero.

$$\Delta H^{vap} / kJ mol^{-1} = A \left( 1 - \frac{T/K}{T_c/K} \right)^n \quad 6.9$$

Table 6.9: Heat of vaporization parameters for MCH, toluene and NMP

Compound	A	$T_c/K$	n
Ethanol	60.8036	516.3	0.38
Water	54	647.1	0.34
EG	88.2	645	0.397

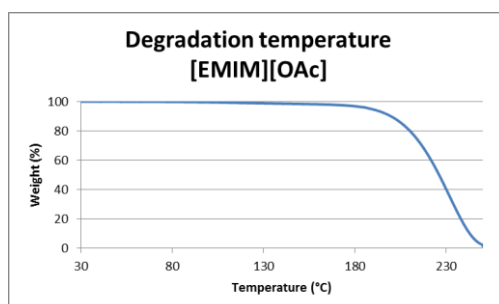


Figure 6.14: Degradation temperature of [EMIM][OAc] determined by TGA under  $N_2$  atmosphere

The vapor pure component enthalpy was calculated from liquid enthalpy and enthalpy of vaporization. In the enthalpy predictions, deviations from ideality were neglected in the liquid and vapor phase and the enthalpy of mixtures was calculated with the mole fraction average of the pure component enthalpies.

In Figure 6.14 the degradation temperature of [EMIM][OAc] under nitrogen atmosphere is shown. The experiments were done in a TGA (Thermogravimetric Analyzer) TA instruments model Q500. The temperature was varied from 30 °C till 250 °C with a ramp of 2 °C/min. It can be seen that the IL starts to decompose at 180 °C. In this work and for safety reasons, a maximum process temperature of 160 °C is selected.



## Appendix 6.2 Extractive distillation column (EDC) profiles for the separation of ethanol and water

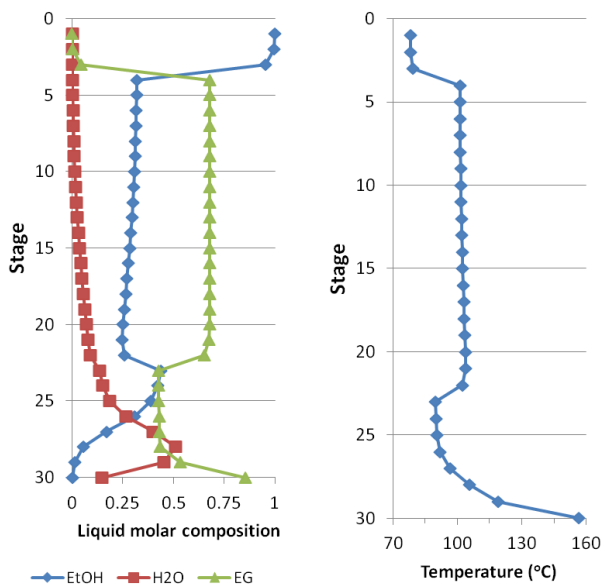


Figure 6.15: Liquid molar composition (left) and temperature (right) profiles for the EDC using ethylene glycol (EG) as solvent

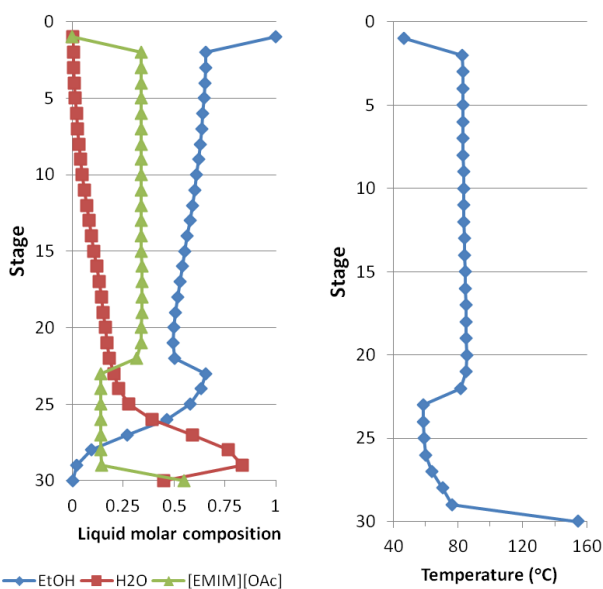


Figure 6.16: Liquid molar composition (left) and temperature (right) profiles for the EDC using the IL [EMIM][OAc]

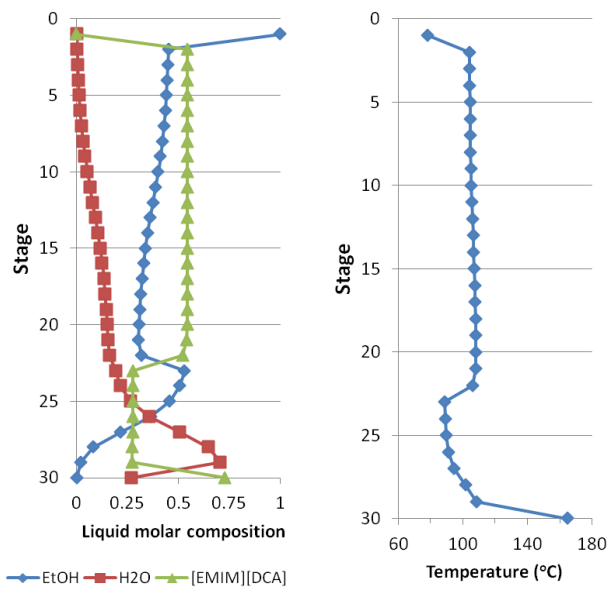


Figure 6.17: Liquid molar composition (left) and temperature (right) profiles for the EDC using the IL [EMIM][DCA]

## Appendix 6.3: Process flow diagrams

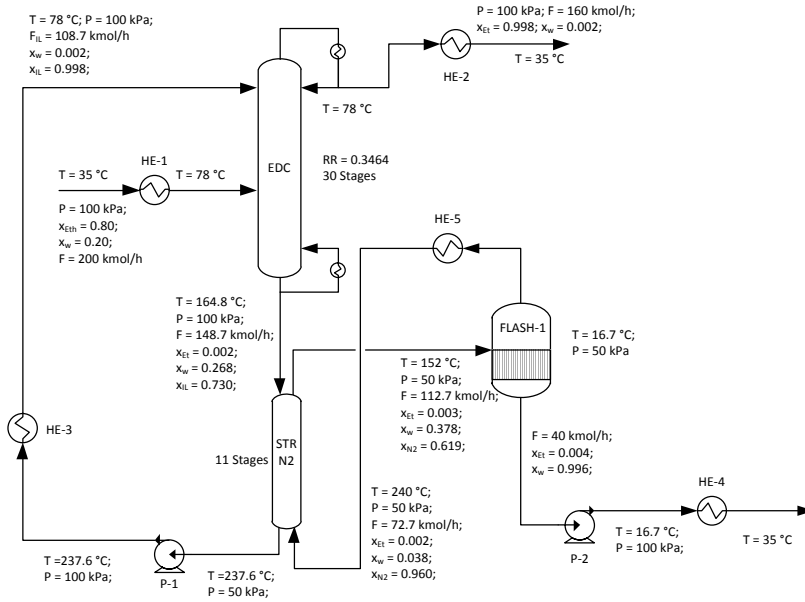


Figure 6.18: ED process using [EMIM][DCA]. Recovery of IL using stripping with nitrogen

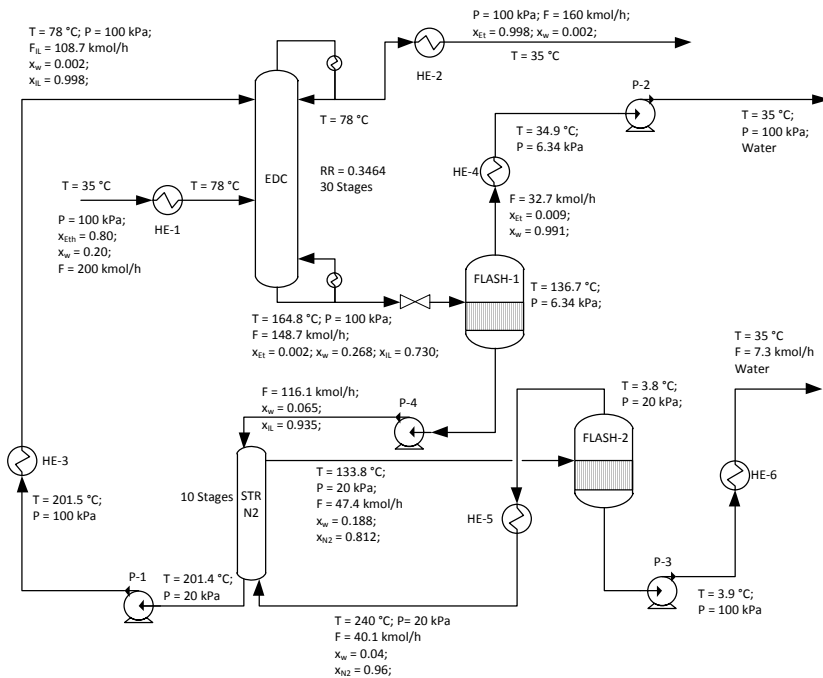


Figure 6.19: ED process using [EMIM][DCA]. Recovery of IL using flash + stripping with hot nitrogen

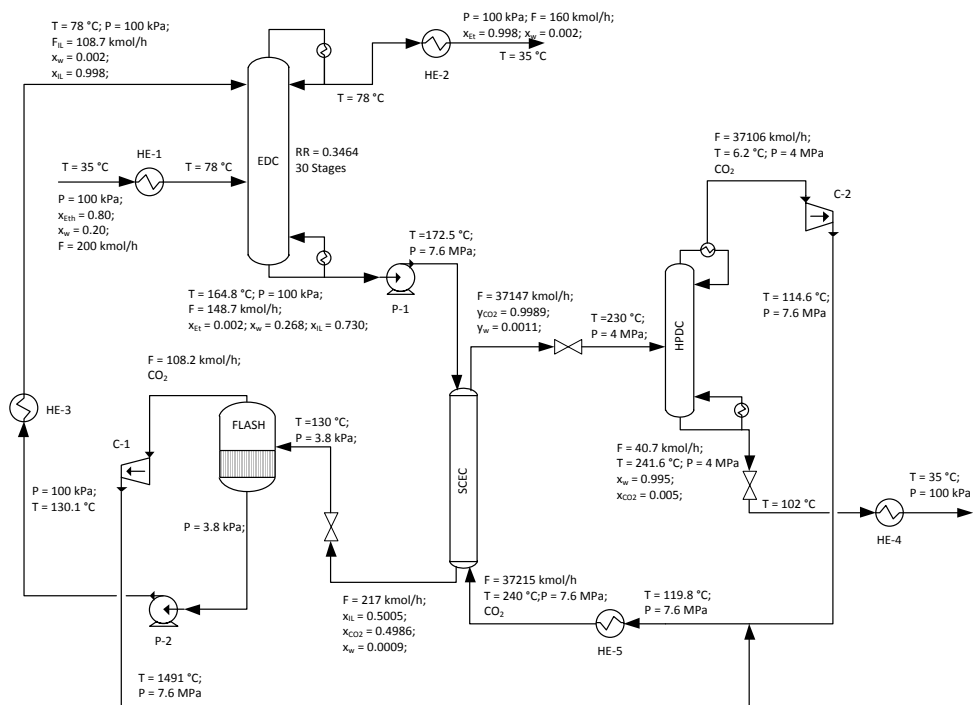


Figure 6.20: ED process using [EMIM][DCA]. Recovery of IL using SCCO<sub>2</sub>

## Appendix 6.4: Heat exchanger networks (HEN's)

In this section, the design of the heat exchanger network (HEN) is done. It should be mentioned that the designs proposed in this work are not the most optimal. They are done in such a way that all the available energy is recovered in the most logical way. High pressure steam at 250 °C and cooling water at 20 °C are chosen as utility streams. If necessary, a refrigerant is used to decrease the temperature until values lower than 30 °C. In this work the refrigerant is not defined; however, according to the temperatures reached in the processes propylene, propane, ammonia, tetrafluoroethane, among others, can be used [1, 2].

The heat exchanger network (HEN) designs are done to have an idea on how the actual process would look like and to make a comparison of the HEN, transfer areas and number of heat exchangers needed in the processes. A minimum temperature difference of 10 K was fixed and average values for the film heat transfer coefficients are taken (Table 6.10). These values were obtained with the equation 6.10 for multiple conditions of temperatures and pressures and for multiple concentrations.

$$\frac{h \times D}{k} = 0.023Re^{0.80}Pr^{1/3} \quad 6.10$$

where  $h$ ,  $D$  and  $k$  hold for the film heat transfer coefficient (HTC), flow area diameter (taken as 2.54 cm) and thermal conductivity, respectively. The Reynolds ( $Re$ ) and Prandtl ( $Pr$ ) numbers are defined in equation 6.11.

$$Re = \frac{D \times \rho \times v}{\mu} \quad 6.11$$
$$Pr = \frac{C_p^{ef} \times \mu}{k}$$

where  $\rho$ ,  $v$ ,  $\mu$  and  $C_p^{ef}$  refer to the stream density, velocity (taken as 1 m/s), viscosity and the effective heat capacity, respectively. The effective heat capacity comes from a simple energy balance of a heat exchanger where the heat load ( $Q$ ), mass flow ( $m$ ) and temperature difference ( $\Delta T$ ) are known (equation 6.12).

$$C_p^{ef} = \frac{Q}{m \times \Delta T} \quad 6.12$$

The properties of the pure components were calculated with the correlations presented by Yaws [3-5] and the properties of mixtures were obtained with the mole (or mass) fraction average of the pure component properties as reported in literature [6]. In this work, an approximate design of the network is done; however, it should be mentioned that the detailed design of heat exchangers should be done with more specific correlations. The HTC values listed in Table 6.10 are in agreement with the ones reported in the literature for general conditions and fluids [2, 7].



Table 6.10: Average film heat transfer coefficients

Fluid	$h(W/m^2K)$
Liquid (no solvent)	2500
Liquid (solvent)	3800
Vapor	30
Vapor (LP)	15
Condensation	1100
Condensation (LP)	500
Evaporation	1200
Evaporation (LP)	800
HP Steam	8500
Cooling water	3500
Refrigerant	1300

Table 6.11: Hot and cold streams conditions for the selected processes

Stream	Description	Inlet T(°C)	Outlet T(°C)	Duty (MW)	$h(W/m^2K)$
<b>4. EG Process</b>					
1	EG being recycled	149.9	77.9	0.819	3800
2	Condenser EDC	78.0	77.5	2.830	1100
3	Ethanol from EDC	78.0	35.0	0.328	2500
4	Condenser SRC	61.5	60.0	0.077	500
		60.0	59.5	0.577	500
		59.5	58.0	0.167	500
5	Water from SRC	58.0	34.9	0.020	2500
6	Reboiler EDC	118.8	133.6	1.759	1200
		133.6	156.6	2.041	1200
7	Reboiler SRC	147.8	148.8	0.138	800
		148.8	149.4	0.197	800
		149.4	149.9	0.320	800
8	Feed to EDC	35.0	78.1	0.366	2500
<b>5. Recovery with flash @ 240</b>					
1	Condensation of water from flash	240.0	19.7	0.054	15
		19.7	19.3	0.400	500
		19.3	18.0	0.090	500
2	IL being recycled	240.0	77.9	1.880	3800
3	Condenser EDC	104.2	78.5	0.154	30
		78.5	78.0	2.407	1100
4	Ethanol from EDC	78.0	35.0	0.328	2500
5	Bottoms from EDC entering the flash	132.8	240.0	1.322	1200
6	Reboiler EDC	108.3	119.7	1.557	1200
		119.7	135.4	1.048	1200
		135.4	164.8	0.944	1200
7	Feed to EDC	35.0	78.0	0.365	2500
8	Water after being condensed	18.0	34.9	0.015	2500

All the hot and cold stream's inlet and outlet temperatures, and heat load (duty) of every process were known from the simulations; the conditions can be seen in Table 6.11. In the last column of this table, the HTC are shown (necessary to determine the transfer area of the heat exchangers). Some streams were discretized due to their phase change. It must be noticed that they represent the reboilers and condensers of the processes. These

streams are segmented into several parts as a linear approximation to the actual curved behavior of the temperature-enthalpy diagrams when a phase change occurs.

With the information presented in Table 6.11 and the composite curves (Figure 6.11) the HENs for every process are proposed. In Figure 6.21, the HEN for the process using EG as solvent is presented.

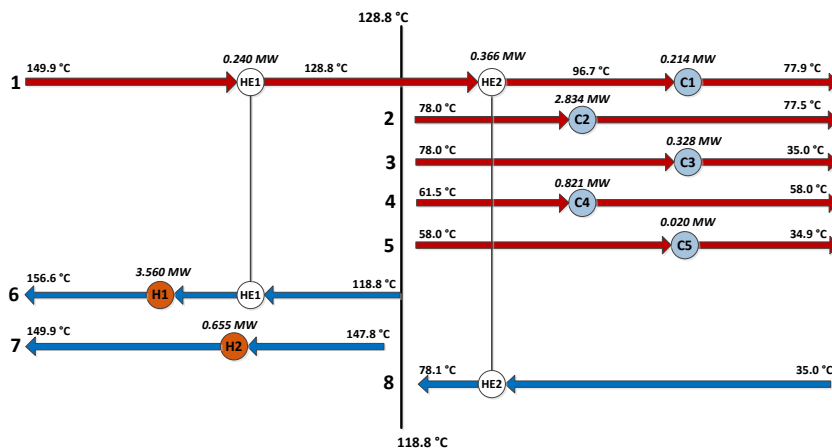


Figure 6.21: Heat exchanger network for the conventional extractive distillation process using ethylene glycol

In these figures, H, C, HE and R refer to hot utility, cold utility, process-to-process and refrigeration heat exchangers, respectively. As it can be seen in both process (Figure 6.21 and Figure 6.22), most of the recovered energy involves the cooling down of the solvent being recycled to the EDC. These streams have enough energy to heat up the feed to the EDC and even some of the energy required in the reboilers of both processes. Furthermore, for the IL process, the solvent is even able to exchange energy with two more streams. This explains why the energy savings when [EMIM][DCA] is used are higher than for the conventional solvent. In total, 9 heat exchangers are necessary in the conventional ED process and 11 in the process using [EMIM][DCA].

According to the Figure 6.21, in the conventional process the hot utility needs to provide 4.22 MW through the heat exchangers H1 and H2, the cold utility needs to remove 4.22 MW through the heat exchangers C1-C5 and there is 0.61 MW exchanged between process-to-process heat exchangers (HE1 and HE2).

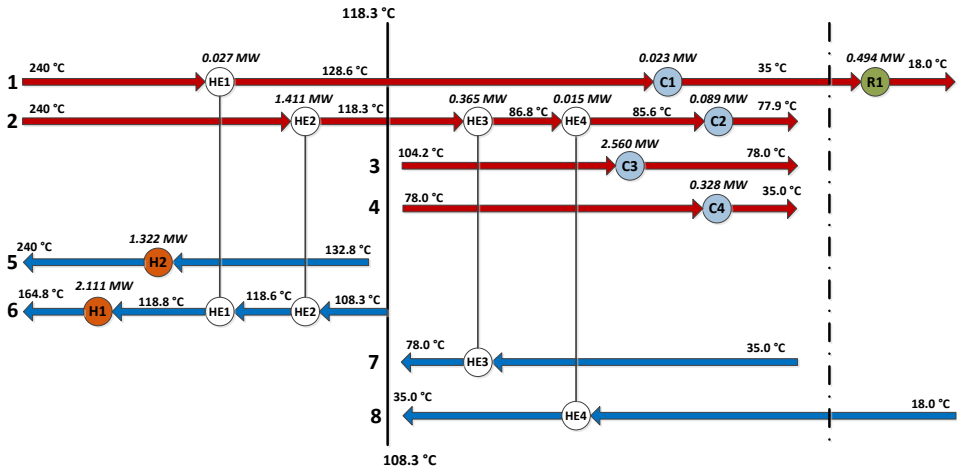


Figure 6.22: Heat exchanger network for the ED process using [EMIM][DCA]. Recovery with flash drum at 240 °C

In Figure 6.22 it can be seen that there is a recovery of 1.82 MW through the process-to-process heat exchangers HE1-HE4, the hot utility needs to provide 3.43 MW through the heat exchangers H1 and H2, and the cold utility needs to remove 3.0 MW through the heat exchangers C1-C4. Notice that a refrigerant is needed to remove 0.49 MW from stream 1 in this process through the heat exchanger R1.

The areas of the heat exchangers are obtained using the equation 6.13.

$$A = \frac{Q}{\Delta T_{LM}} \left( \frac{1}{h_c} + \frac{1}{h_h} \right) \quad 6.13$$

where  $A$  is the transfer area of the heat exchanger,  $Q$  is the duty of the heat exchanger,  $h_c$  and  $h_h$  are the film heat transfer coefficients of the cold and hot stream, respectively, and  $\Delta T_{LM}$  is the log mean temperature difference, defined in equation 6.14.

$$\Delta T_{LM} = \frac{\Delta T_H - \Delta T_C}{\ln(\Delta T_H / \Delta T_C)} \quad 6.14$$

where the subscripts  $H$  and  $C$  refers to the hot and cold side of a countercurrent heat exchanger.

The heat transfer areas for the heat exchangers in every process are shown in Table 6.12. Notice that the cooling down of the hot stream 1 (0.544 MW using 116.1 m<sup>2</sup>) and the condenser of the EDC (stream 3, 2.56 MW using 130.9 m<sup>2</sup>) requires 72% of the total heat transfer area of the process; however, the total heat duty of the stream 1 is only 1/5 of the condenser. The low pressure of stream 1 is reflected in low HTC and large areas. As a result of the low pressures involved in the recovery, the heat transfer area of the process using [EMIM][DCA] is 2 times larger than for the conventional process.

Table 6.12: Heat exchanger areas for the extractive distillation processes

EG Process			Recovering with flash @ 240 °C		
Heat exchanger	Duty (MW)	Area (m <sup>2</sup> )	Heat exchanger	Duty (MW)	Area (m <sup>2</sup> )
H1	3.560	30.47	H1	2.111	18.12
H2	0.655	8.962	H2	1.322	29.77
C1	0.214	1.894	C1	0.023	38.49
C2	2.834	61.91	C2	0.089	0.795
C3	0.328	7.400	C3	2.560	130.9
C4	0.821	47.95	C4	0.328	7.186
C5	0.020	0.545	R1	0.494	36.03
HE1	0.240	15.08	HE1	0.027	41.62
HE2	0.366	4.689	HE2	1.411	35.70
			HE3	0.365	6.003
			HE4	0.015	0.162
<b>Total</b>	<b>178.9</b>		<b>Total</b>	<b>344.8</b>	



## 7. Conclusions and recommendations for future work

The goal of this work was to investigate and analyze the performance of ionic liquids (ILs) in extractive distillation (ED) processes for three separation cases: aromatics/non-aromatics (toluene/methylcyclohexane), olefins/paraffins (1-hexene/*n*-hexane) and ethanol/water. The results of this research lead to the overall conclusion that ILs can be suitable ED solvents, depending on the whole process (especially the recovery of the ILs) and its heat integration. Energy savings are achieved when using ILs due to their unique properties (higher selectivity and non-volatility). This chapter presents the main achievements of this thesis

### 7.1 Ionic liquid selection

Conventionally, solvents giving the largest selectivity or relative volatility are considered to be the most appropriate for ED applications. Even though, ILs can drastically increase the selectivity of the mixtures, in this work (Chapter 2) it was demonstrated that not only the selectivity should be taken into account, but also the activity coefficients at (in)finite dilution of the solvents in the components, i.e.  $\gamma_{IL,i}$ . ILs can have large repelling interactions with the solutes (e.g.  $\gamma_{IL,i} > 1000$ ) which leads to the formation of two liquid phases or large attractive forces (e.g.  $\gamma_{IL,i} < 0.01$ ) which indicates difficult removal of volatiles, as in the removal of water from IL.

Experimental results for the separation of 1-hexene/*n*-hexane with the most promising ILs selected in the screening section demonstrated that none of the ILs studied in this work is a suitable replacement for the conventional solvent N-methyl-2-pyrrolidone (NMP) ( $\alpha_{NMP} = 1.55$ ). A maximum increase in the relative volatility of 6% was reached with the IL 1-hexyl-3-methyl-imidazolium tetracyanoborate [HMIM][TCB]. Furthermore, large solvent to feed mass ratios ( $S/F = 20$ ) are required to solubilize the system and avoid formation of two liquid phases.

It was found that the ILs [HMIM][TCB] and [BMIM][TCB] are suitable ED solvents for the separation of toluene/methylcyclohexane. The experimental results showed that it is possible to increase the relative volatility > 40% compared to the conventional solvent NMP ( $\alpha_{NMP} = 9.9$ ). Additionally, for the separation of ethanol/water, the experimental results revealed that the relative volatility can be increased > 27% when ethylene glycol (EG) ( $\alpha_{EG} = 2.1$ ) is replaced by [EMIM][OAc]. The IL [EMIM][DCA] has a high degradation temperature and its similar relative volatility to EG makes it an interesting IL to be studied. The aforementioned ILs were chosen for further research based on the experimental results, performance and commercial availability.

### 7.2 Extractive distillation process

Due to the higher selectivity of the ILs, the number of equilibrium stages of the ED column can be reduced by 15-25 %. However, because of their high molecular weight, these processes use 1.4 – 2.3 times more mass of solvent compared with the conventional process (more kilograms of IL are needed for the same separation).

For the cases studied in this work, the ILs yield to energy savings in the reboilers of the ED columns. However, in order to fully evaluate the feasibility of ILs in ED processes, several recovery technologies were studied and analyzed in this research. It was demonstrated that the most attractive technologies, due to their lowest energy requirements, are:

- *Recovery with a flash drum*
- *Stripping with methylcyclohexane (separation of MCH and toluene)*

After heat integration, an ED process (ED column + solvent recovery) using ILs to separate toluene and methylcyclohexane decreases the energy requirements from 21 MW (using the conventional solvent NMP) to 10 MW, saving 51% of the energy supply. It can be concluded that the IL [HMIM][TCB] is a suitable replacement of the conventional solvent (NMP) in the ED of methylcyclohexane/toluene.

In the separation of ethanol – water, the IL with the highest relative volatility ([EMIM][OAc]) was not a feasible solvent due to its high hydrophilicity. It can be concluded that besides a high solubility, an ED solvent should be easily recovered. On the other hand, it was found that, without heat integration, the ED process to separate ethanol from water using [EMIM][DCA] requires 11% more energy than the benchmark (EG). However, after heat integration, the process using this IL becomes more attractive, and the energy requirements can be decreased from 4.2 MW (using the conventional solvent EG) to 3.5 MW, yielding 16% of energy savings.

The energy savings in an ED process depends on two properties of the IL: their non-volatility and their selectivity. The non-volatility can contribute up to 6% to the energy savings in the ED column (Table 6.2). Increasing the selectivity by 40% can decrease the energy requirements of the ED column by 40% (Table 5.2), and the energy requirements of the solvent recovery process are decreased by 10%. It can be concluded that the selectivity of the ILs is a much more determining property than their non-volatility regarding the energy requirements.

As a general guideline, an IL might become interesting for its usage in ED processes when its increase in the relative volatility of the mixture is enough to yield 20% of energy savings. Nevertheless, special attention should be paid to the interactions between the ILs and the less volatile compound. Strong attractive forces (or hydrophilicity) should be avoided to facilitate the IL recovery. Besides, heat integration needs to be performed in order to make these processes and solvents economically more attractive. Heat integration is a key design step in ED processes.

### 7.3 Recommendations for future work

The software *COSMOtherm* (version C2.1 release 01.11a) has been designed to predict physical and thermodynamic properties based on quantum chemical calculations. This tool has been successfully applied for the selection of the suitable ILs. As it was shown in this research, it only can be used as a qualitative tool. Therefore, experimental data during the solvent selection was always necessary, not only to determine the relative volatility of the solvents but also to corroborate that no two liquid phases are being formed. In order to

improve the solvent selection methodology, the accuracy of the predictions should be improved.

It is known that the physical, thermodynamic, corrosive and toxicological properties of the ILs are scarce. More research needs to be done in each of these fields to determine the practical suitability of the ILs in industrial scale applications.

ILs are believed to not have any vapor pressure, and, hence, cannot be obtained in the vapor phase. However, it has been demonstrated that they can be distilled at pressures of 10 kPa and temperatures of 300 °C [1]. As it was shown in this thesis, pressures as low as 3 kPa are sometimes necessary to recover the ILs to the desired and required purity. Special attention should be paid and the actual IL loss in the processes should be studied.

In order to entirely evaluate the applicability of ILs on industrial scale, further research has to be conducted with feeds of the actual processes. The impurities could modify the performance of ILs in ED processes. Besides, pilot plant experiments are necessary to test the actual behavior and performance of ILs in extractive distillation processes.

For future work and especially for the separation of methylcyclohexane and toluene, it is recommended to estimate the capital expenditures (CAPEX), perform a detailed economic evaluation and a technical feasibility study in order to fully evaluate the application of ILs in ED processes.

#### 7.4 References

1. Earle, M.J., J.M.S.S. Esperanca, M.A. Gilea, J.N. Canongia Lopes, L.P.N. Rebelo, J.W. Magee, K.R. Seddon and J.A. Widegren, *The distillation and volatility of ionic liquids*. Nature, 2006. **439**(7078): p. 831-834.





## List of publications

---

### Publications

J.P. Gutierrez, G.W. Meindersma, A.B. de Haan. Binary and ternary (liquid + liquid) equilibrium for methylcyclohexane (1)+toluene (2)+1-hexyl-3-methylimidazolium tetracyanoborate (3)/1-butyl-3-methylimidazolium tetracyanoborate (3). *The Journal of Chemical Thermodynamics*, 43, **2011**, 1672-1677.

J.P. Gutierrez, G.W. Meindersma, A.B. de Haan. COSMO-RS-based ionic-liquid selection for extractive distillation processes. *Industrial and Engineering Chemistry Research*, August **2012** (available online) DOI: 10.1021/ie301506n.

J.P. Gutierrez, G.W. Meindersma, A.B. de Haan. Extractive distillation process for the separation of toluene + methylcyclohexane using the ionic liquid [HMIM][TCB]. *Chemical Engineering Research and Design*, Submitted July **2012**.

### Peer reviewed conference proceedings

J.P. Gutierrez, G.W. Meindersma, A.B. de Haan. Ionic liquid selection and performance evaluation for the separation of methylcyclohexane/toluene by extractive distillation. Eds A.B de Haan, H. Kooijman, A Górak. *Distillation and Absorption 2010*, **2010**, 473 – 478.

### Book chapter

Meindersma, Wytze; Quijada-Maldonado, Esteban; Aelmans, Tim; Gutierrez-Hernandez, Juan; de Haan, André. Ionic Liquids in Extractive Distillation of Ethanol/water, from Laboratory to Pilot Plant, in *Ionic Liquids: Science and Applications*. ACS Symposium Series. Accepted for publication, 2012.

### Oral presentations

J.P. Gutierrez, G.W. Meindersma, A.B. de Haan. Extractive distillation with ionic liquids – Separation of methylcyclohexane and toluene. Netherlands Process Technology Symposium 2010. NPS-10. 2010. Veldhoven – Netherlands.

### Oral presentations prior to the PhD thesis

J.P. Gutierrez, W. Osorio-Viana, J. Fontalvo, M.A. Gomez-Garcia. Hybrid process for the recovery and degradation of phenol from industrial wastewater. II International Congress of Chemical and Biotechnological processes. EAFIT University. 2006. Medellin – Colombia.

J.P. Gutierrez, W. Osorio-Viana, J. Fontalvo, M.A. Gomez-Garcia. Hybrid schemes and distillation-pervaporation integrated unit. . II International Congress of Chemical and Biotechnological processes. EAFIT University. 2006. Medellin – Colombia.

W. Osorio-Viana, J.P. Gutierrez , J. Fontalvo, M.A. Gomez-Garcia. Process intensification of methane steam reforming by mean of a catalytic membrane reactor. II International Congress of Chemical and Biotechnological processes. EAFIT University. 2006. Medellin – Colombia.

### **Poster presentations**

J.P. Gutierrez, G.W. Meindersma, A.B. de Haan. Separation of toluene/MCH by extractive distillation using ionic liquids as solvents. CHISA 2012. Prague – Czech Republic.

J.P. Gutierrez, G.W. Meindersma, A.B. de Haan. Feasibility study of an extractive distillation process using ionic liquids as solvents. ILSEPT 2011. Sitges – Spain.

J.P. Gutierrez, G.W. Meindersma, A.B. de Haan. Binary and ternary (liquid + liquid) equilibrium for methylcyclohexane + toluene + [HMIM][TCB]/[BMIM][TCB]. COIL-4 2011. Washington DC – United States of America.

J.P. Gutierrez, G.W. Meindersma, A.B. de Haan. Thermodynamic analysis in extractive distillation using ionic liquids. CAPE Forum 2010. Aachen – Germany.

J.P. Gutierrez, G.W. Meindersma, A.B. de Haan. Ionic liquid selection and performance evaluation for the separation of methylcyclohexane and toluene by extractive distillation – 2. Distillation and Absorption 2010. Eindhoven – Netherlands.

J.P. Gutierrez, G.W. Meindersma, A.B. de Haan. Ionic liquid selection and performance evaluation for the separation of methylcyclohexane and toluene by extractive distillation – 1. Netherlands Process Technology Symposium 2010. NPS-10. Veldhoven – Netherlands.

J.P. Gutierrez, G.W. Meindersma, A.B. de Haan. Extractive distillation with ionic liquids – solvent screening. Netherlands Process Technology Symposium 2009. NPS-9. Veldhoven – Netherlands.

J.P. Gutierrez, G.W. Meindersma, A.B. de Haan. Extractive distillation with ionic liquids – presenting case studies. DSTI Congress 2009. Amersfoort – Netherlands.

J.P. Gutierrez, G.W. Meindersma, A.B. de Haan. Ionic liquids in extractive distillation – process proposal. Netherlands Process Technology Symposium 2008. NPS-8. Veldhoven – Netherlands.

J.P. Gutierrez, W. Osorio-Viana, J. Fontalvo, M.A. Gomez-Garcia. Simulation studies of catalytic membrane reactor for enhanced methane steam reforming. 4<sup>th</sup> EFCATS school on catalysis. Catalyst design-From molecular to industrial level. 2006. St Petersburg – Russia.



## Acknowledgments

---

Let me start by acknowledging “you” for, at least, reading this small section of this thesis :-) I have always liked this section because here I can write what it is immediately coming into my mind, without spending several minutes/hours analysing and deciding the best way how to write it. However, I have been afraid that I will forget somebody. If you think you should be mentioned here (and you are not), then my apologies for that.

Especial thanks to my promoter, prof. André de Haan and dr. Wytze Meindersma for giving me the opportunity to join your group, tailoring this project and direct me towards the right direction, for your ideas ideas, advices and guidance.

To my family, mi hermanita, Lorena, de quien he aprendido que sin importar qué tan difícil sea una situación, siempre se debe luchar por lo que uno se ha comprometido. Mi adorada madre, Maria Nilsa, mi gran amor, mi gran soporte y confidente, siempre estaré dispuesto a hacer lo que sea necesario por tu bienestar. Mi querido padre, Saul, mi negro, a quien le debo todo lo que soy y he logrado, mi gran inspiración personal, siempre te recordaré. Mil gracias a todos ustedes por estar siempre conmigo.

I have to thank my flaca, Renate, for being with me during those moments when I really needed your support. I have loved every moment I have spent with you. Thank you very much; you are unforgettable and very special person who deserves more than you think. I should not forget her family, especially Mirian and Jan, thanks for welcome me and share the most gezellig moments I have spent in the Netherlands.

To my dear and good Colombian friends, Guapacha, Kevin, Restrepo y Andrea, sin importar el tiempo y la distancia, siempre los recordaré y tendré presentes. A Wilmar, Javier Fontalvo y Miguel Angel Gomez muchas gracias por su apoyo especialmente al inicio de mi doctorado. No podría dejar fuera de este grupo a Nestor y Valentina, el matrimonio más feliz que he conocido. Gracias a todos ustedes por los felices momentos y graciosas situaciones por las que hemos pasado. No saben cuantos buenos recuerdos tengo.

During my stay in Eindhoven I met a lot of people, but I specially remember the BBC, Miran, Edwin, Ivi and, lately, Miguel. The moments sharing a biertje with you were very special and I will remember all of them (well, sometimes remembering is not possible).

I had the opportunity to supervise several students. To Tom, Maarten, Siamak, Jens, Ben and Erhan, thanks for the time invested in this project, your ideas and discussions. However, I also met students from other PhD's: Chris, Kirill, Nick, we did not share a project, but we did have a good time during your stay.

I remember a lot all my latin friends I have met in the Netherlands, my housemate Toña, Lesly, Youse, Kathy, Tros, Armando, Pachangas, Alfredo, y muchos más que seguramente olvido mencionar, muchas gracias por hacer mi estadia en estos “países del bajo mundo” mucho más grata.

I especially thank the SPS group: André, Wytze, Boelo, Edwin, Miran, Lesly, Miguel (I am not sure if you belong here), Mayank, Esteban, Esayas, Antje, Mark, Jeroen, Maartijn, Caecilia, Ana, Bo, Wilko, Wouter, Pleunie and Caroline and the dreamteam the “SuPerStars” soccer team for the incredible matches, nice moments, discussions and situations we shared during the our PhD life, meetings, coffee breaks, etc.

Last but not least, I would like to thank the committee members, prof.dr. Geert-Jan Witkamp, prof.dr. Henk van den Berg, prof.dr. Dieter Vogt, dr. ir. Anton A. Kiss, prof.dr. Kai Leonhard, for taking your time reading and suggesting on how to improve this work.

## Curriculum Vitae

---

Juan Pablo Gutierrez Hernandez was born the 12<sup>th</sup> of April 1983 in Manizales, Colombia. After completing his high school studies at Instituto Universitario de Caldas in 1999 in Manizales, he started his studies in Chemical Engineering at the National University of Colombia, Manizales (in Spanish Universidad Nacional de Colombia). In June 2005 he graduated as a Chemical Engineer with emphasis in Chemical, Catalytic and Biotechnological Processes with his final project “Influence of heat and mass transfer in the distillation of multicomponent mixtures”, written in Spanish and under the supervision of Prof. Miguel .A. Gomez Garcia. In July 2005 he was appointed in the Master of Science (M.Sc.) program at the National University of Colombia, Manizales with emphasis in Intensification of Chemical Processes. He concluded his master studies in July 2007 with the project called “Process design for the recovery and degradation of phenol from wastewater”, written in Spanish and under the supervision of Prof. Javier Fontalvo Alzate. From January 2007 till December 2007 he worked as teaching assistant at the National University of Colombia, Manizales in the subjects Separation Processes and Thermodynamics for bachelor programs. In February 2008 he moved to The Netherlands where he started his PhD research at Eindhoven University of Technology (TU/e). He joined the Process Systems Engineering Group under the supervision of dr. ir. G.W. Meindersma and Prof. dr. André B. de Haan. His research was focused on the topic presented in this dissertation. On 1<sup>st</sup> of February 2012 he joined AkzoNobel Research, Development and Innovation as a researcher in Separation Technology.